OUTLINE OF A NEW THEORY FOR THE NATURAL CONVECTION TURBULENT BOUNDARY LAYER NEXT TO HEATED VERTICAL SURFACES

by

Martin Wosnik

A thesis submitted to the
Department of Mechanical and Aerospace Engineering
and the Faculty of the Graduate School of the
State University of New York at Buffalo
in partial fulfillment of the requirements for the degree of

Master of Science

June 1994

To Sandra

Abstract

A theory is proposed for the *Turbulent Natural Convection Boundary Layer* next to heated vertical surfaces, based on a similarity analysis of two separate reduced sets of Reynolds-averaged single-point equations describing the inner and outer parts of the flowfield. Scaling functions for mean and fluctuating quantities are found from the boundary conditions at the wall and from the matching of profiles using an Asymptotic Invariance Principle. The analysis presented here suggests that the local scaling functions are valid both in the limit of infinite Grashof number (Nusselt number) and for any position downstream well into the turbulent regime.

It is found that the boundary layer does not grow linearly for the range of Grashof numbers experiments were performed at. However, it slowly loses its streamwise inhomogeneity until asymptotically $d\delta/dx = const.$ In this limit, the proposed heat transfer relation reduces to the widely accepted form $Nu_\delta \propto H_\delta^{*1/4}$ (i.e. as $\varepsilon = {Nu_\delta}^{-1} \to 0$ and $H_\delta^* = Gr_\delta \cdot Nu_\delta \cdot Pr^2 \to \infty$). With the new theory it is possible to explain the failure of the earlier analysis of George and Capp [26] at finite Grashof number, and why experimental data plots collapse or why they do not. It is also possible to explain the "apparent collapse" of data, observed by some investigators when the variation of the improperly chosen scaling function was small and the range of the experiment limited. The theory is seen to be at least consistent with the data sets investigated.

Acknowledgements

I would like to thank, first of all, my advisor Professor Dr. William K. George for his support and guidance throughout the course of this work. This thesis would not have been possible without the many enlightening discussions with him. I would like to express my appreciation to the faculty of the Department of Mechanical and Aerospace Engineering at the University of Buffalo for providing such an international and open-minded academic environment. I would also like to thank Professor Dr. William J. Rae and Professor Dr. Dale Taulbee for being on my thesis defense committee.

On a more personal note I want to thank my fellow students in the Turbulence Research Laboratory and throughout UB for their friendship, many helpful discussions and joyful times. It has been quite an experience so far...

Financial support from the Department of Mechanical and Aerospace Engineering at the University of Buffalo, the Fulbright Commission, the UB Research Foundation and my family is gratefully acknowledged.

...my warmest and deepest gratitude goes to my friends and family for their unconditional support and understanding...

Contents

Abstract i

Acknowledgements ii

Table of Contents iii

List of Figures v

Nomenclature vii

1 Introduction 1
- 1.1 Motivation . . . 1
- 1.2 The Subject to Be Studied . . . 2
- 1.3 Thesis Outline . . . 3

2 Previous Research 6
- 2.1 General Remarks . . . 6
- 2.2 Turbulent Natural Convection . . . 7

3 The Equations of Motion 18
- 3.1 The Main Part of the Boundary Layer . . . 19
- 3.2 The Near Wall Region . . . 20
- 3.3 The Buoyant Sublayer . . . 23

4 Similarity Considerations 25
- 4.1 Dimensional Analysis . . . 25
- 4.2 Similarity Solutions and the Asymptotic Invariance Principle . . . 29
- 4.3 Similarity of the Inner Equations . . . 30
- 4.4 Similarity of the Outer Equations . . . 33

5 Matching of Inner and Outer Profiles 36

6 Scaling Functions for the Outer Layer 41

6.1 Outer Scales From Matching 41
6.2 Outer Scales From Physical Argument 43

7 A "New" Heat Transfer Law **45**

8 The Asymptotic Limit **46**
8.1 Turbulence Quantities and $d\delta/dx$ 46
8.2 Asymptotic Limit and GC79 Theory 48
8.3 Integral Boundary Layer Thickness as Outer Lengthscale 48

9 Experimental Data **50**
9.1 On the Value of Experimental Data 50
9.2 The Influence of a Stratified Environment 52
9.3 Acquisition of Experimental Data 54
9.4 Comparing the Proposed Theory to Experimental Data 55
9.4.1 Explaining Plots of Experimental Data with the New Theory . 55
9.4.2 Mean Temperature Profiles 55
9.4.3 Mean Velocity Profiles 56

10 Summary and Conclusions **58**
10.1 Thesis Summary 58
10.2 Suggestions for Future Work 59

The Figures **60**

A Derivation of the Governing Equations **81**
A.1 Continuity, Momentum and Heat Diffusion 82
A.2 Turbulence Kinetic Energy and Temperature Fluctuations Transport 90

B Scaling of the Governing Equations **94**
B.1 The "Outer" Set of Equations 94
B.2 The "Inner" Set of Equations 99

References **102**

List of Figures

1 Schematic of the turbulent natural convection boundary layer next to heated vertical surfaces. 60

2 Regimes of laminar, transitional and turbulent heat transfer (includes recompiled experimental data for water ($Pr = 4 \ldots 8$ from Fujii et al. [20]). 61

3 Comparison of theoretical and numerical local heat transfer predictions, Nu_x vs. Gr_x, for air ($Pr = 0.72$), including experimental heat transfer data from Tsuji and Nagano 1988 [64] for two different wall temperatures in the turbulent regime. 62

4 Comparison of theoretical average heat transfer predictions, Nu_L vs. Gr_L. Plotted are graphs for $Pr = 0.72$, $Pr = 100$ and $Pr = 0.01$. . . 63

5 Temperature dependence of fluid properties in air (taken from tables in ref. [33]) and water (calculated from formulas for physical properties given in ref. [20]) under atmospheric conditions. 64

6 Graphical explanation of the inner lengthscale η. 65

7 Turbulent natural convection in a vertical channel. 65

8 Mean temperature data of Smith 1972 [59] plotted in inner variables of George and Capp 1979 [26] 66

9 Mean temperature data of Smith 1972 [59] plotted in inner variables of George and Capp 1979 [26] on a log-linear plot. 67

10 Mean temperature data of Smith 1972 [59] plotted in inner variables from new theory. 68
11 Mean temperature data of Smith 1972 [59] plotted in inner variables from new theory on a log-linear plot. 69
12 Comparison of mean temperature profiles in inner variables on a linear-linear plot (replotted from Tsuji and Nagano 1988 [64]). 70
13 Comparison of mean temperature profiles in inner variables on a log-linear plot (replotted from Tsuji and Nagano 1988 [64]). 71
14 Mean velocity data of Cheesewright 1968 [11] plotted in inner variables of George and Capp 1979 [26] 72
15 Mean velocity data of Cheesewright 1968 [11] plotted in inner variables of George and Capp 1979 [26] on a log-linear plot. 73
16 Mean velocity data of Cheesewright 1968 [11] plotted in inner variables from new theory. 74
17 Mean velocity data of Cheesewright 1968 [11] plotted in inner variables from new theory on a log-linear plot. 75
18 Mean velocity data of Smith 1972 plotted in inner variables of George and Capp 1979 [26] 76
19 Mean velocity data of Smith 1972 plotted in inner variables of George and Capp 1979 [26] on a log-linear plot. 77
20 Mean velocity data of Smith 1972 [59] plotted in inner variables from new theory. 78
21 Mean velocity data of Smith 1972 [59] plotted in inner variables from new theory on a log-linear plot. 79
22 Mean velocity data from Tsuji and Nagano 1989 [65] plotted in (asymptotic) outer variables from new theory. 80

Nomenclature

a : Speed of sound (Appendix A)

a, b, c, d : Power law exponents from matching with AIP

C, D : Constants

c : Specific heat (Appendix A)

c_p : Specific heat at constant pressure

c_v : Specific heat at constant volume

e : Internal (thermal) energy

$\mathbf{f}, f_i$: Vector of bodyforces (Appendix A)

F_S : Local scale for turbulent heat flux

F_0 : $= \frac{q_w}{\rho c_p}$. Kinematic wall heat flux

f_1 : Functional form for mean streamwise velocity

f_2 : Functional form for mean temperature

g : Gravitational acceleration

g_1 : Functional form for Reynolds stress

g_2 : Functional form for turbulent heat flux

h : $= \frac{q_w}{T_w - T_\infty}$. Heat transfer coefficient

i, j, k : Indeces in index notation (Appendix A)

k : Thermal conductivity

L : Characteristic streamwise length

m, n : Integer numbers (Pi-Theorem, Dimensional analysis)

m, n : Exponents (Similarity of the outer equations)

P : Mean static pressure

P_* : Mean static pressure minus the hydrostatic pressure

P_{ij} : Deviatoric stress tensor

P_∞ : Hydrostatic pressure at infinite distance from the wall

p : fluctuating pressure (or pressure in general, Appendix A)

$\tilde{p}$: Instantaneous pressure

q_i : Heat flux vector

q_w : $= -k\left(\frac{\partial T}{\partial y}\right)_{y=0} = h(T_w - T_\infty) = h\Delta T_w$. Wall heat flux

R_S : Local scale for Reynolds' stress

r : Ratio of scales

r : Rank of a matrix (Pi-Theorem, Dimensional analysis)

$\mathcal{R}$: Individual gas constant (Appendix A)

T : Mean temperature (or temperature in general, Appendix A)

T_S : Temperature scale

T_w : Wall (surface) temperature

T_∞ : Temperature at infinite distance from the wall

ΔT : $= T - T_\infty$. Temperature difference

t : Fluctuating temperature

t_i, t_o : Scales for fluctuating temperature (Appendix B)

U : Mean streamwise velocity

U_i : Vector of mean velocity

U_M : Maximum velocity

U_S : Velocity scale

u : Streamwise fluctuating velocity

u_* : $= \sqrt{\tau_w/\rho}$. Friction velocity

u_i, u_o : Scales for fluctuating velocity (Appendix B)

V : Mean cross-stream velocity

v : Cross-stream fluctuating velocity

W : Mean cross-stream velocity (in the z-direction)

w : Cross-stream fluctuating velocity (in the z-direction)

x : Streamwise coordinate

y : Cross-stream coordinate perpendicular to wall

$\bar{y}$: $= \frac{y}{\delta}$. Outer variable, similarity variable

y^+ : $= \frac{y}{\eta}, \frac{y}{\eta_T}$. Inner variable, similarity variable

z : Cross-stream coordinate parallel to wall

Greek Symbols

α : $= \frac{k}{\rho c_p}$. Thermal diffusivity

β : $= -\frac{1}{\rho}\left(\frac{\partial \rho}{\partial T}\right)_{p=const.}$. Coefficient of thermal expansion

δ : Outer cross-stream lengthscale

δ_{ij} : Kronecker-delta

η : Inner cross-stream lengthscale

μ : Dynamic (absolute) viscosity

ν : $= \frac{\mu}{\rho}$. Kinematic viscosity

τ_{ij} : Stress tensor

τ_w : $= \mu\left(\frac{\partial U}{\partial y}\right)_{y=0}$. Wall shear stress

Φ : Dissipation function (Appendix A)

ψ : Potential of bodyforce (Appendix A)

ϵ : Dissipation of turbulent kinetic energy

Nondimensional Parameters and Characteristic Numbers

Gr_x : $= \frac{g\beta\Delta T_w x^3}{\nu^2}$. The Grashof number

Gr_x^* : $= Gr_x \cdot Nu_x = \frac{g\beta F_0 x^4}{\nu^2 \alpha}$. Modified Grashof number

H_x^* : $= \frac{g\beta F_0 x^4}{\alpha^3} = Gr_x^* \cdot Pr^2$. The "H-number"

M : $= \frac{U}{a}$. The Mach number (Appendix A)

Nu_x : $= \frac{hx}{k} = \frac{F_0\ x}{\Delta T_w \alpha}$. The Nusselt number

Pe_x : $= Re_x \cdot Pr$. The Peclet number

Pr : $= \frac{\nu}{\alpha}$. The Prandtl number

Re_x : $= \frac{U_S x}{\nu}$. The Reynolds number

Ra_x : $= Gr_x \cdot Pr$. The Raleigh number

Ra_x^* : $= Gr_x^* \cdot Pr$. Modified Raleigh number

ε : $= \frac{\eta}{\delta} = Nu_\delta{}^{-1}$. Dimensionless parameter for asymptotic matching

Subscripts

i : Quantities asssociated with the inner layer

o : Quantities associated with the outer layer

S : Scaling function

t : Quantities associated with the turbulent regime

l : Quantities associated with the laminar regime

w : Evaluated at the wall

∞ : Evaluated at infinite distance from the wall

Relation Symbols

$\propto$: "proportional to"

$\sim$: "on the order of magnitude of"

$\equiv$: "defined as" (equivalent to)

$\cong$: "approximately equal to"

Chapter 1

Introduction

1.1 Motivation

One of the principal research areas today within the field of Fluid Dynamics and Heat Transfer is concerned with the understanding of the fundamental structures of turbulent heat transfer phenomena, one of the classical problems being the *Turbulent Natural Convection Boundary Layer* (TNCBL) next to heated vertical surfaces. Although there have been numerous investigations, its characteristics have been clarified only to a moderate degree to present.

Theoretical framework on this subject had first been established in the 1950s by Eckert and Jackson [17] and Bayley [5]. Both used a profile method to determine the heat transfer law, a velocity scale and the boundary layer thickness (an outer length scale), their analyses were made to fit a limited range of experimental data.

While scaling laws have been chosen by experimenters to obtain good correlation of their data, most are arbitrary "characteristic quantities" and lack convincing physical arguments aside from elementary dimensional analysis. Not surprisingly, a great variety of scaling laws can be found in the literature and the existence of universal profiles has yet to be established experimentally.

The most successful attempt to date to derive scaling laws, profiles and heat

transfer relations (at least in describing the asymptotic behaviour) from a "local similarity" analysis of the governing equations was made by George and Capp [26] in 1979 (GC79). Unfortunately in most recent experiments and numerical calculations, researchers encountered difficulty using the GC79 theory to collapse data which continue to show a residual dependence on Grashof number based on downstream distance, Gr_x, over the range of their experiments. Therefore, divergent beliefs on scaling relations, wall functions and laws describing specific parts of the boundary layer continue to persist in the vast body of literature (e.g. Miyamoto et al. 1982 [43], Siebers et al. 1985 [58], Tsuji and Nagano 1988 [64] and 1989 [65], Tsuji et al. 1990 [66] and 1992 [67]).

This work presents a theoretical approach based on a strict similarity analysis applied separately to a reduced inner and outer set of the coupled single point boundary layer equations. The scaling laws derived retain a Grashof number dependence for finite Grashof numbers, Gr_x, but the George/Capp scaling will be recovered as the asymptotic limit for infinite Grashof number, $Gr_x \to \infty$. We will examine the consequences of the new formulations on correlating data in the TNCBL at moderate Grashof numbers Gr_x, on power-law behaviour in the buoyant sublayer as well as on the heat transfer relationship. Useful fragments of previous works are expanded and united into a single theory.

1.2 The Subject to Be Studied

We confine our attention to the natural convection boundary layer next to heated, semi-infinite vertical surfaces. The flow to be analyzed is shown in figure 1. We choose the positive x-direction to be opposite to the vector of gravitational acceleration and the y-direction to be our cross-stream coordinate perpendicular to the surface. The z-direction, by right-hand rule, is pointing into the drawing surface. The fluid bounded by the wall is assumed to be of infinite extent and reference quantities are taken at

infinite distance from the wall. The surface is assumed to be free of any obstacles which might interfere with the flow. For a given heat flux across the surface, unsteady and initially traveling wave-like motions appear at some distance downstream. These hydrodynamic instabilities arise when a balance of buoyancy, pressure, and viscous forces contribute net energy to a disturbance (c.f. Gebhardt 1973 [22]). This causes the disturbance to grow as it is convected downstream until a breakdown of the regular wave pattern into an intense mixing region with completely irregular motion occurs completing the transition to a fully developed turbulent flow. Thus turbulence develops over a given range of x under given conditions. It is the fully developed turbulent natural convection boundary layer which is the subject to be studied in this work.

Note that most natural convection flows found in nature occur on such large length and time scales that their flow mechanisms are predominantly turbulent. However, for the scales and details of the flows important in engineering and our environment, we typically find either laminar flow (becoming unstable due to ever-present disturbances), flow in transition or turbulent flow, or sometimes several of these conditions together in a single flowfield. Examples for engineering applications are the cooling of rotating turbine blades, where buoyancy forces are very large because of inevitably large centrifugal accelerations, cooling towers of power plants, airflows adjacent to burning walls, etc. Also note that in gases of low density and in liquids of high Prandtl number, the length scale for transition becomes very large.

1.3 Thesis Outline

The following is a short outline of the remainder of this thesis: Chapter 2 summarizes the history of theoretical and numerical work on the subject and reviews some of the more important analyses. Local and average heat transfer relations as well as scaling parameters are compared.

The new theory proposing two separate similarity solutions to the momentum and energy equations is outlined in chapters 3 to 8: Chapter 3 introduces the equations of motion and shows that the natural convection turbulent boundary layer has to be treated in two parts, an outer and an inner region, each governed by a seperate set of equations. In Chapter 4 functional forms of relevant flow quantities are derived from dimensional analysis and similarity concepts are discussed, leading to the introduction of the Asymptotic Invariance Principle. Scaling laws for the inner layer and constraints on the scaling laws of the outer layer will be obtained from the self-preservation condition of the equations of motion.

From the reasoning that there has to be a region of common validity of both descriptions and facing the necessity to tie the information from the inner boundary conditions to the outer layer, we match inner and outer profiles in Chapter 5. Using the previously introduced Asymptotic Invariance Principle, we derive a power-law behavior for an intermediate layer. In chapter 6, we find scaling laws for the outer layer with the information from matching and reconsidering the similarity conditions. A more physical approach to the outer scales is also given here. The analysis presented so far naturally leads to a "new" heat transfer law, which is introduced in chapter 7. In chapter 8, the turbulent kinetic energy component equations are briefly investigated to find the asymptotic growth rate of the boundary layer. This also yields the asymptotic behaviour of inner and outer scales and the heat transfer law.

Experimental data is the subject of chapter 9. After a discussion of the state of experimental data and the influence of a thermally stratified environment, some experiments are investigated in the light of the new theory. Finally, chapter 10 summarizes the main results of this work, draws conclusions and makes suggestions for future research.

No detailed derivation of the differential equations governing the fully developed turbulent natural convection boundary layer can be found in the literature. Therefore, equations for conservation of mass and momentum, diffusion of heat, turbulence

kinetic energy (Reynolds' stress) and transport of the mean square temperature fluctuations for this specific problem are derived in Appendix A. An order of magnitude analysis leading to properly reduced sets of equations is carried out in Appendix B.

Chapter 2

Previous Research

2.1 General Remarks

The early development of the subject was characterized by the publication of many papers about experiments on natural convection; theoretical work was rare. Only recently has this situation changed. Analytical work had been mainly concerned with laminar flow for a long time, no doubt because turbulence is much less tangible.

The set of differential equations governing the laminar natural convection boundary layer flow was first derived by Oberbeck in 1879 [46]. In 1881 Lorenz [41] simplified this set and was the first to give an expression for the heat transfer based on the one-fourth power of the product of Prandtl and Grashof numbers, $Nu_L = f(Gr_L \cdot Pr)^{1/4}$. A lot of the early research in natural convection is connected with the name of W. Nusselt, after whom the nondimensional parameter which is a characteristic number for the heat transfer is named. Dimensional analysis revealed that the Nusselt number $Nu_x = hx/k$ is a function of the Grashof number $Gr_x = g\beta(T_w - T_\infty)x^3/\nu^2$ and the Prandtl number $Pr = \nu/\alpha = c_p\mu/k$. For the case of a given constant wall heat flux, q_w, a modified Grashof number $Gr_x^* = Gr_x \cdot Nu_x$ is usually employed, since $q_w = h(T_w - T_\infty)$.

During the attempt to solve the laminar problem, two principal methods of analysis had been developed: Solution of the differential equations in an integral form by assuming plausible velocity and temperature distributions and a direct solution of the equations with the the aid of a similarity transformation, the latter providing an exact solution (e.g. Ostrach 1952 [47]). Both methods assume the profiles to have essentially the same shape for any value of x.

2.2 Turbulent Natural Convection

The criterion for the beginning of turbulence in forced convection is the Reynolds number Re_x, experimental findings suggest that the Grashof number Gr_x or the Rayleigh number Ra_x ($Ra_x = Gr_x \cdot Pr$) have a similar function in natural convection. For example in air ($Pr \sim 0.7$), critical values of Gr_x ranging from 3.5×10^8 to 1.5×10^{10} have been reported in literature, showing the dependence on the actual flow situation with its given disturbances. In the same manner as for the Reynolds number, we have to distinguish between two critical Grashof numbers, one at which the flow becomes unstable for the first time and the Grashof number at which the flow finally becomes turbulent. In general it is agreed upon that turbulence prevails for roughly $Gr_x > 10^{10}$ (in air).

Early approaches to turbulent natural convection were, as in the laminar case, based mostly on dimensional considerations. Jakob and Linke [34] suggested that the local heat transfer coefficient should be independent of x, leading to a heat transfer law of the form $Nu_x = Gr_x^{1/3} \cdot f(Pr)$, a theory already supported by some of the early experiments. Another line of thought involves the Prandtl number: For the fully developed turbulent boundary layer viscous effects should be very small, leading to the viscosity-free relationship $Nu_x = f(Gr_x \cdot Pr^2)$. Frank-Kamenickij [19] adds the requirement that the thermal conductivity should also be negligible, so that the equation assumes the form $Nu_x = A(Gr_x \cdot Pr^2)^{1/2}$.

In the following paragraphs some theoretical approaches will be discussed in more detail. Commonly, heat transfer laws are given in terms of a local Nusselt number, $Nu_x = hx/k$, based on the downstream position x and a local heat transfer coefficient h, or an average Nusselt number, $Nu_L = h_{avg}L/k$, based on the surface height L and an average heat transfer coefficient h_{avg}. A scientific investigation of fundamental flow structures requires the knowledge of the local heat transfer rate, while in most engineering problems — other than calculating the maximum local heat transfer rate to prevent damage of employed materials — the average heat transfer rate is of great interest, since it enables us to predict the overall heat transfer for similar problems. The average Nusselt number Nu_L is usually obtained through integration of the x-dependence of the local heat transfer coefficient, $h_{avg} = \frac{1}{L}\int_0^L h(x)dx$.

One of the first attempts to analyze the turbulent natural convection boundary layer was made in 1930 by **Colburn and Hougen** [14]. They discovered that Lorenz's equation [41], derived for the heat transfer in laminar flows, "does not agree with the data for long surfaces, since the exponent is 1/4 instead of 1/3" (c.f. figure 2). Therefore they introduced "a new conception in the mechanism of heat transmission by natural convection": They assumed the existence of a visco-conductive sublayer, within which both velocity and temperature varied linearly with the distance from the wall y. At the outer boundary of this sublayer the derivative of velocity with respect to y was zero and the Reynolds number formed from this maximum velocity and the "critical thickness" δ_1 corresponded to the critical value found in comparable experiments on forced convection. A simple balance of momentum and energy for a layer of fluid lead to the solution:

$$Nu_x = (6Re_{cr})^{-1/3} Gr_x^{1/3} \tag{2.1}$$

where Re_{cr} is the critical Reynolds number (in figure 3: $Re_{cr} = 130$). Thus, the local heat transfer rate is independent of x. For the case of a vertical surface and large

Grashof numbers they calculated a mean Nusselt number to

$$Nu_L = 0.104 Gr_L^{1/3} \quad . \tag{2.2}$$

At the same time they conducted experiments with cooling water passing through vertical pipes at low velocities. For upward flow best agreement with the data was reached for the following equation:

$$Nu_L = 0.128 (Gr_L Pr)^{1/3} \quad . \tag{2.3}$$

Note that the relations $Nu_x \propto Gr_x^{1/4}$ for the laminar part of the boundary layer and $Nu_x \propto Gr_x^{1/3}$ for the turbulent part of the boundary layer for specified wall temperature (c.f. figure 2) correspond to $Nu_x \propto Gr_x^{*1/5}$ (laminar) and $Nu_x \propto Gr_x^{*1/4}$ (turbulent) for the case of given wall heat flux, since $Gr_x^* = Gr_x Nu_x$. The heat transfer relations for laminar natural convection are found from exact solutions of the boundary layer equations (e.g. the similarity solution of Ostrach 1952 [47]). There is still a lot of dissent about the correct heat transfer law for the turbulent regime (c.f. figures 3 and 4). However, the relations given above could be labeled as "largely agreed upon".

A semiempirical, more direct solution was obtained by **Eckert and Jackson** [17] by using the integral equation method. Facing the necessity to adopt approximate expressions for velocity and temperature profiles, they took the following from forced convection theory (i.e. what the theory provided in 1950, equations are for moderate Reynolds numbers):

$$U = U_S \left(\frac{y}{\delta}\right)^{1/7} \left(1 - \left(\frac{y}{\delta}\right)\right)^4 \quad , \qquad T = T_w \left(1 - \left(\frac{y}{\delta}\right)^{1/7}\right) \quad , \tag{2.4}$$

where the velocity profile was modified to account correctly for the zero velocity outside the boundary layer in the natural convection case. The wall shear stress τ_w

and the wall heat transfer rate q_w also need to be known to be able to solve the integral equations. Accordingly, Eckert and Jackson replaced them by "wall functions" from turbulent forced convection work. Note that these adopted profiles and relations are the only "turbulence" terms, no Reynolds' stress or turbulent heat flux terms appear in the calculation. No sublayer configuration was taken into account either. Proceeding this way they were able to obtain explicit relations for the characteristic velocity U_S, $U_S \propto x^{0.5}$, and for the boundary layer thickness δ, $\delta \propto x^{0.7}$. The local heat transfer rate then followed to:

$$Nu_x = 0.0295 Gr_x^{2/5} Pr^{7/15} \left(1 + 0.494 Pr^{2/3}\right)^{-2/5} \quad . \tag{2.5}$$

This can be changed to an average value along the plate by integrating the proportionality $h \propto x^{0.2}$ from the equation above, assuming the flow is turbulent over most of the surface under consideration ($Nu_L = 5/6 Nu_x$):

$$Nu_L = 0.0246 Gr_L^{2/5} Pr^{7/15} \left(1 + 0.494 Pr^{2/3}\right)^{-2/5} \quad . \tag{2.6}$$

Examined was the experimental data of Griffiths and Davis [28], who conducted the first experiments on the turbulent natural convection boundary layer in order to apply the results to refrigerated food storage, and others. For air ($Pr = 0.72, Ra_x = 10^{10} - 10^{12}$) the equation reduces to:

$$Nu_L = 0.0210 \left(Gr_L Pr\right)^{2/5} \quad . \tag{2.7}$$

However, the 1/7-power profile is an inappropriate choice for the case of natural convection and e.g. Cheesewright [11] showed that it is seriously in error.

A few years later, **Bayley** [5] extended this integral method analysis to fluids of low Prandtl number. He used the same expressions as Eckert and Jackson for velocity and wall shear stress, arguing that the velocity profile near the wall is similar to the

one in forced convection and that the 1/7-power is characteristic for turbulent flows. He then rejected their wall function for q_w and was more careful in the selection of an approximate temperature profile: Dividing the flow into a laminar sublayer including the buffer layer and a fully turbulent region, he derived expressions for the temperature drop across each part. In the turbulent region the heat transfer was described by means of Reynolds' analogy and the eddy diffusivity $\nu_t = f(y)$ was estimated with Prandtl's mixing length model. For the calculations the constant relation $\nu_t = 7\nu$ was adopted and the eddy diffusivity for heat was taken to be the same as for momentum. With the erroneous assumption that for $Pr \ll 1$ the thermal and the hydrodynamic layers have the same thickness, the total temperature drop can be calculated and leads to the heat transfer law:

$$\frac{1}{Nu_x} = \frac{\delta_l}{x} + 0.186\frac{\delta}{x}\frac{1}{1+\frac{\epsilon}{\nu}Pr} \quad . \tag{2.8}$$

Eckert and Jackson's integral boundary layer equations are now solved for U_S and δ with an elegant substitution (Air: $U_S \propto x^{0.305}$, $\delta \propto x^{0.3475}$, mercury: $U_S \propto x^{0.5}$, $\delta \propto x^{0.25}$).

For low Prandtl numbers (mercury: $Pr \cong 0.01$ at boiling temperature) the above equation can then be rewritten as

$$Nu_x = Gr_x^{1/4}\left(37.59I^{-15/32}Gr_x^{-7/32}Pr^{-1/16} + 0.97I^{-1/4}Pr^{-1/2}\right)^{-1} \quad , \tag{2.9}$$

where $I = \int_0^\delta (T-T_\infty)dy/\delta(T_w-T_\infty)$. With $I = 0.125$ for a temperature profile of the 1/7-power form and Grashof numbers between 10^{10} and 10^{15} this can be approximated by

$$Nu_L = 0.080Gr_L^{1/4} \quad , \tag{2.10}$$

where $Nu_L = 4/3Nu_x$ was again obtained by integration. This is, of course, the familiar result for the laminar natural convection boundary layer, since the power of the laminar heat transfer relationship was found not to change in the turbulent region

for $Pr \ll 1$.

For air, the heat transfer relation becomes:

$$Nu_x = Gr_x^{0.2175} \left(26.9 Gr_x^{-0.19} Pr^{0.059} + 0.35 Pr^{-0.435}\right)^{-1} \quad . \tag{2.11}$$

Again $I = 0.125$ was used for the temperature profile and for $Gr \cdot Pr = 2 \times 10^9 - 10^{12}$ comparison with experiments by Saunders [55] gives a correct prediction for the heat transfer:

$$Nu_L = 0.10 (Gr_L Pr)^{0.33} \quad . \tag{2.12}$$

He concluded that for fluids of low Prandtl number, extrapolation of laminar flow data is possible, since even under turbulent flow conditions molecular conductivity remains the main means of transferring heat in liquid metals.

Tackling the opposite end of the regime, **Ruckenstein and Felske** [54] derived an analytical expression for the heat transfer coefficient for a high Prandtl number fluid in 1980. They used a combination of "inner and outer sets of equations" (c.f. sections 3.1,3.2) to describe the entire boundary layer flow and the concept of eddy diffusivity as a turbulence closure model. Knowing that the extent of the temperature boundary layer will be much less than the velocity layer (for $Pr \gg 1$) and even closer to the wall than the point of maximum velocity, convective transport in this thermal layer is negligible and molecular and molar ("eddy") diffusion dominate, leading to equation (3.21) for the heat flux across it. The eddy diffusivity is found through expansion in a Taylor series, $\nu_t \propto y^3$, and is the same as in forced convection, since it was assumed that the friction velocity ($u_*^2 = \tau_w/\rho$) is the appropriate scaling velocity in the near wall region. Given the eddy diffusivity, the temperature distribution can be determined. The wall shear stress τ_w can be related to the heat flux by integrating the momentum equation across the whole boundary layer neglecting the acceleration of the fluid (far from the leading edge). With these results, the heat transfer relation

is obtained as

$$Nu_L = 0.257 Pr^{1/6} {Gr_L^*}^{1/4} \tag{2.13}$$

for the case of constant wall heat flux and as

$$Nu_L = 0.163 Pr^{2/9} {Gr_L}^{1/3} \tag{2.14}$$

for the case of constant wall temperature. The last equation is seen to be in good agreement with the numerical studies of Kato et al. [37] and Noto and Matsumoto [45].

Quite different from previous theoretical work was the analysis of **George and Capp** 1979 [26]. It has been the most successful attempt so far in deriving scaling laws, profiles and heat transfer relations from a "local similarity" analysis of the governing equations. Dividing the flow into an inner and outer layer, they used "local similarity" arguments — purely dimensional, but physical — to find scaling laws for both parts in the limit of infinite Grashof number. For the inner layer, the scales are $U_{Si} = (g\beta F_0 \alpha)^{1/4}$, $T_{Si} = ({F_0}^3/g\beta\alpha)^{1/4}$ and $\eta = (\alpha^3/g\beta F_0)^{1/4}$. For the outer layer, George and Capp found $U_{So} = (g\beta F_0 \delta)^{1/3}$, $T_{So} = ({F_0}^2/g\beta\delta)^{1/3}$ in terms of the undetermined outer length scale δ. By equating the outer limit of the inner solution and the inner limit of the outer solution, expressions for velocity ($U \propto y^{1/3}$) and temperature ($T \propto y^{-1/3}$) can be found for this intermediate regime, which they called "buoyant sublayer", in direct analogy with the inertial sublayer in forced convection flows (c.f. Monin and Yaglom [44]). The matching of inner and outer temperature profiles also yielded the heat transfer law

$$Nu_x = C_H(Pr) {H_x}^{1/3} \qquad \text{and} \qquad Nu_x = C'_H(Pr) H_x^{*1/4} \tag{2.15}$$

for constant wall temperature and constant wall heat flux cases, respectively; while the matching of inner and outer velocity profiles shows that $U_{So} \propto U_M$ in the limit as $H_x^* \to \infty$. It is also shown that the temperature profile is linear near the wall, $(T - T_w) \propto -y$, and that the leading term in the velocity profile is linear (although

the inner layer was shown not to be a constant stress layer and the extent of this linear region is limited through the the contribution of the higher order terms and Reynolds' stresses). Several researchers compared the results of their experimental and numerical studies to the scaling laws and buoyant sublayer profiles derived by George and Capp (e.g. Siebers et al. 1985 [58], Tsuji and Nagano 1988 [64], Henkes and Hoogendoorn 1990 [31]). Although large parts of the proposed theory were confirmed, the lack in agreement is attributed to the finite Grashof numbers experiments were performed at. Note that it will be shown later that the theory proposed by George and Capp is valid in the limit of infinite Nusselt number, $Nu_x \to \infty$ (and only in this limit!).

Of course all **numerical investigations** involve a theoretical part, too, where **turbulence closure models** are needed to close the Reynolds-averaged governing equations. While the first theoretical studies used an approximate profile method to solve the integral equations (c.f. Eckert and Jackson [17], Bayley [5]), the first researchers to adopt an *eddy diffusivity distribution model* were Kato et al. 1968 [37]. They closed the integrated boundary layer equations by assuming distributions of wall shear stress, heat flux, eddy diffusivity (turbulent viscosity) and a turbulent Prandtl number $Pr_t = \nu_t/\alpha_t$ of unity and solved them with a trial and error method, also using results from forced convection heat transfer. For a moderate Prandtl number Pr and within the range $10^{10} < Ra_x < 10^{13}$ the heat transfer relationship becomes:

$$Nu_x = 0.149 Gr_x^{0.36} \left(Pr^{0.175} - 0.55 \right) \tag{2.16}$$

The eddy viscosity model was subsequently used by Yang and Nee 1970 [72], Mason and Seban 1974 [42], Cebeci and Khattab 1975 [10], Noto and Matsumoto [45] and Kulkarni and Chou 1989 [39]. Yang and Nee let a parabolic rate equation based on differential field theory govern their eddy viscosity and used a constant turbulent Prandtl number Pr_t. Mason and Seban calculated the turbulent viscosity from a dimensionally correct combination of an algebraically determined mixing length (c.f.

Prandtl 1961 [52]) and kinetic energy in order to avoid the contradiction brought in through the mixing length approach. The eddy diffusivity for heat was determined by setting the turbulent Prandtl number equal to a constant. Cebeci and Khattab used an algebraic eddy diffusivity formulation to model the Reynolds' stress and a turbulent Prandtl number expression given in terms of the friction velocity u_* and the Prandtl number Pr. Noto and Matsumoto chose the closure model of Kato et al., then performed a transformation with a streamfunction and dimensionless variables that were taken from laminar similarity theory to eliminate the dependence on the derivative of x. This proves advantageous for solving the transformed equations numerically and they obtain results similar to those of Mason and Seban. Kulkarni and Chou presented a complete model describing laminar, transitional and turbulent flow together to study different cases of ambient thermal stratification of a quiescent atmosphere, where an eddy viscosity model and a turbulent Prandtl number distribution were used for the transitional and turbulent regimes. They also perform a transformation involving a "laminar" similarity variable and solve the resulting set of equations numerically.

A $K-\epsilon$ *turbulence closure model* was applied to turbulent natural convection by Plumb and Kennedy 1977 [51], To and Humphrey 1986 [63], Henkes and Hoogendoorn 1990 [31] and Peeters and Henkes 1992 [49]. Plumb and Kennedy solve equations for turbulent kinetic energy, dissipation rate of turbulent kinetic energy and mean square temperature fluctuations. Prandtl [52] and Kolmogorov [38] proposed that the turbulent viscosity should be proportional to the square root of the turbulent kinetic energy (a velocity scale) times a length scale representative of the energy containing eddies. For isotropic turbulence, the loss of energy from energy containing eddies is equal to the energy dissipated at small scales (equilibrium energy spectrum) and the entire energy cascade process can be described in terms of a single length scale. In standard $K-\epsilon$ models characterized by that of Jones and Launder [35], this length scale is then taken to be the dissipation length scale, given by $L = K^{3/2}/\epsilon$

on dimensional grounds. Thus, the turbulent viscosity can be written as $\nu_t \propto K^2/\epsilon$. The crucial assumption for the validity of this expression is high Reynolds number, so that the flow tends toward isotropy. Plumb and Kennedy chose a turbulent Prandtl number distribution, so that $Pr_t = 2.5$ at the wall and $Pr_t = 0.5$ at the outer edge of the boundary layer. To and Humphrey also used a basic two equation $(K - \epsilon)$ model and modified their constants to account for the low Reynolds number effects of the wall on the inner regions of the boundary layer flow. Henkes and Hoogendoorn employ a $K - \epsilon$ model with low Reynolds number modifications to derive similarity scalings, which are compared to the GC79 scales. Peeters and Henkes used a $K - \epsilon$ model with constant turbulent Prandtl number Pr_t by analogy between turbulent transport of momentum and heat.

To and Humphrey 1986 [63] also developed an *algebraic Reynolds' stress model* (ASM) for low Reynolds number turbulent free convection. It is based on truncated algebraic expressions for $\overline{u_i u_j}$ and $\overline{u_j t}$ derived from a local equilibrium assumption. Peeters and Henkes 1992 [49] investigated the boundary layer with two types of second order models, an algebraic stress model (ASM) and a *fully differential Reynolds' stress model* (RSM), which is capable of capturing the turbulence structure of the flow. Some of the above mentioned work can be found in Henkes and Hoogendoorn 1989 [30], where the authors compare the algebraic eddy diffusivity distribution model, the standard $K - \epsilon$ model and different low Reynolds number $K - \epsilon$ models.

The theoretical heat transfer predictions introduced in this chapter are compared in figure 3 (Nu_x vs. Gr_x) and figure 4 (Nu_L vs. Gr_L).

Besides theoretical and numerical studies, numerous **experimental investigations** (c.f. [11, 12, 16, 18, 20, 32, 40, 43, 48, 50, 53, 55, 58, 59, 64, 65, 66, 67, 68, 70, 71]) have been carried out on this subject. They will be discussed in chapter 9, where they are also compared to the theory proposed in the following chapters. A comparison of scaling functions chosen by the experimentalists is given in table 2.1 (Note: All scales are expressed in the nomenclature defined in the beginning).

author(s) & year	inner/ outer	lengthscales η, δ	velocity U_S	temperature T_S	R. stress R_S	t. heat flux F_S
Cheese-wright 1968	no distinction	$x/{Gr_x}^{0.1}$	$(g\beta\Delta T_w x)^{1/2}$ "lam. buoyancy correlation"	$T_w - T_\infty$	not plotted	
Fujii et al. 1970	no distinction	$x/Nu_x = \eta$ "thermal BL thickness"	not plotted	$T_w - T_\infty$	not plotted	
Smith 1972	no distinction	$\frac{T_w - T_\infty}{-(\partial T/\partial y)_{y=0}} = \eta$ "heat transfer distance"	$(g\beta\Delta T_w x)^{1/2}$ "buoyancy velocity"	$T_w - T_\infty$	dimensional plots	
Kutate-ladze et al. 1972	no distinction	all plots dimensional				not plotted
Welty & Peinecke 1976	no distinction	$x\left(\frac{5}{Gr_x^*}\right)^{0.2}$	$\frac{5\nu}{x}\left(\frac{Gr_x^*}{5}\right)^{0.4}$	not plotted		
Cheesewright et al. 1982	no distinction	all plots dimensional		not plotted		
Miyamoto et al. 1982	no distinction	$x/Nu_x = \eta$	U_M	not plotted	${U_M}^2$	$U_M \Delta T_w$
Siebers et al. 1985	inner:	$\left(\frac{\alpha^2}{g\beta\Delta T_w}\right)^{1/3}$ w. Temp.-correction: $\left(\frac{k_w}{k_\infty}\right)\left(\frac{T_w}{T_\infty}\right)^{0.14}$	not plotted	$T_w - T_\infty$	not plotted	
	outer:	$\int_0^\infty \frac{T - T_\infty}{T_w - T_\infty} dy$ "enthalpy thickness"	not plotted	$T_w - T_\infty$	not plotted	
Tsuji & Nagano 1988	inner:	ν/u_*	u_* "friction velocity"	F_0/u_* "friction temperature"	not plotted	
	outer:	$\frac{T_w - T_\infty}{-(\partial T/\partial y)_{y=0}} = \eta$	U_M	$T_w - T_\infty$	not plotted	

Table 2.1: Scaling functions chosen by experimenters to collapse data

Chapter 3

The Equations of Motion

A set of equations governing the fully developed turbulent natural convection boundary layer flow next to a heated vertical surface is given by (see Appendix A, p.81, for derivation and approximations made):

$$\frac{\partial U}{\partial x} + \frac{\partial V}{\partial y} = 0 \tag{3.1}$$

$$U\frac{\partial U}{\partial x} + V\frac{\partial U}{\partial y} = -\frac{1}{\rho}\frac{\partial P_*}{\partial x} + \frac{\partial}{\partial x}\left(\nu\frac{\partial U}{\partial x} - \overline{u^2}\right) + \frac{\partial}{\partial y}\left(\nu\frac{\partial U}{\partial y} - \overline{uv}\right) + g\beta(T - T_\infty) \tag{3.2}$$

$$U\frac{\partial V}{\partial x} + V\frac{\partial V}{\partial y} = -\frac{1}{\rho}\frac{\partial P_*}{\partial y} + \frac{\partial}{\partial x}\left(\nu\frac{\partial V}{\partial x} - \overline{uv}\right) + \frac{\partial}{\partial y}\left(\nu\frac{\partial V}{\partial y} - \overline{v^2}\right) \tag{3.3}$$

$$U\frac{\partial T}{\partial x} + V\frac{\partial T}{\partial y} = \frac{\partial}{\partial x}\left(\alpha\frac{\partial T}{\partial x} - \overline{ut}\right) + \frac{\partial}{\partial y}\left(\alpha\frac{\partial T}{\partial y} - \overline{vt}\right) \tag{3.4}$$

Capital letters in the equations refer to mean values of velocities, pressure and temperature while lowercase letters refer to the fluctuating parts.

Turbulent flows in general are characterized by the existence of several length scales, some of them assuming very important roles in the analysis of the flow. The range of length scales is bounded between the dimensions of the flow field as the largest

scale and a finite, small length scale associated with molecular diffusion (viscosity), the latter preventing the generation of infinitely small scales of motion through dissipation of small-scale energy into heat. Turbulent boundary layer flows are constrained by viscosity in yet another way. No matter how small it is, it will always enforce a no-slip condition at the wall (i.e. under normal conditions. This is not the case in, e.g. rarefied gases, when the mean free path becomes large enough to exceed the characteristic length of the flow under consideration, i.e. the boundary layer thickness. Molecular collisions near a solid surface then become unimportant.) We will now examine how this affects further treatment of the equations of motion.

3.1 The Main Part of the Boundary Layer

We make the usual boundary layer approximation that $\partial/\partial x \sim 1/L \ll \partial/\partial y \sim 1/\delta$, where L is a streamwise length scale and δ is a length scale perpendicular to the surface. We define characteristic scale quantities for mean streamwise velocity and temperature as U_{S_o} and T_{S_o}, and for fluctuating velocities and temperature as u_o and t_o, respectively. Using a standard order of magnitude analysis (c.f. Prandtl 1961 [52], Tennekes and Lumley 1972 [62]) it is easily shown that the equations of motion within a Bousinesq approximation can be reduced to (c.f. Appendix B, p.94):

$$U\frac{\partial U}{\partial x} + V\frac{\partial U}{\partial y} \cong \frac{\partial}{\partial y}(-\overline{uv}) + g\beta(T - T_\infty) \tag{3.5}$$

$$U\frac{\partial T}{\partial x} + V\frac{\partial T}{\partial y} \cong \frac{\partial}{\partial y}(-\overline{vt}) \tag{3.6}$$

subject to the boundary conditions:

$$U = 0 \qquad \text{as} \qquad y \to \infty \tag{3.7}$$

$$T = T_\infty \qquad \text{as} \qquad y \to \infty \tag{3.8}$$

and

$$-\overline{uv} = 0 \qquad \text{as} \qquad y \to \infty \tag{3.9}$$

$$-\overline{vt} = 0 \qquad \text{as} \qquad y \to \infty \tag{3.10}$$

The continuity equation (3.1) remains unchanged and the y-momentum equation (3.3) has been used to eliminate the pressure term in the x-momentum equation (3.2). The leading neglected term in the y-momentum equation is the streamwise gradient of the turbulent stress, $\partial(-\overline{uv})/\partial x$. The leading neglected term in equation (3.5) is the streamwise gradient of the turbulent normal stress difference, $\partial(\overline{u^2} - \overline{v^2})/\partial x$, which includes the pressure gradient, while the leading neglected term in equation (3.6) is the streamwise gradient of the turbulent heat flux in the x-direction, $\partial(-\overline{ut})/\partial x$. All these terms are of one order of magnitude less than the terms that were kept. With the above scaling, no viscous and conduction terms remain in the equations of motion, therefore they cannot be valid close to the wall and fail to describe the complete flowfield. Equations (3.1), (3.5) and (3.6) are referred to as the "outer" set of equations.

However, these equations are strictly valid only at infinite Reynolds and Péclét numbers, $Re_\delta, Pe_\delta \to \infty$. This is of considerable importance in the analysis presented below, since the properly scaled profiles will reduce to similarity solutions only in this limit. It is equally important to realize that all constraints on the flow are imposed at the wall. A solution for the "outer" part of the boundary layer is only possible, if the "inner" or wall problem has been solved!

3.2 The Near Wall Region

To account correctly for the phenomenon of natural convection, we have to find a set of equations which includes the crucial information given at the wall. The equations of motion have to be rescaled so that at least one viscous and one conduction term

are retained. Defining characteristic scale quantities of mean streamwise velocity and temperature as U_{Si} and T_{Si}, and for fluctuating velocities and temperature as u_i and t_i, respectively, it can be shown that a viscous term can only be retained in the x-momentum equation (3.2) if an inner length scale is defined by

$$\eta \sim \frac{\nu}{U_{Si}} \tag{3.11}$$

and a conduction term can only be retained in the energy equation (3.4) if an inner length scale is given by

$$\eta_T \sim \frac{\alpha}{U_{Si}} \quad , \tag{3.12}$$

where η, η_T have to be sufficiently small relative to δ. Rescaling the equations of motion this way leads to (c.f. Appendix B, p.99):

$$0 \cong \frac{\partial}{\partial y}\left(\nu\frac{\partial U}{\partial y} - \overline{uv}\right) + g\beta(T - T_\infty) \tag{3.13}$$

$$0 \cong \frac{\partial}{\partial y}\left(\alpha\frac{\partial T}{\partial y} - \overline{vt}\right) \tag{3.14}$$

subject to the boundary conditions:

$$U = 0 \quad \text{at} \quad y = 0 \tag{3.15}$$

$$-k\frac{\partial T}{\partial y} = q_w \quad \text{at} \quad y = 0 \tag{3.16}$$

$$\text{or} \quad T = T_w \quad \text{at} \quad y = 0 \tag{3.17}$$

and

$$-\overline{uv} = 0 \quad \text{at} \quad y = 0 \tag{3.18}$$

$$-\overline{vt} = 0 \quad \text{at} \quad y = 0 \tag{3.19}$$

The continuity equation (3.1) remains unchanged. The largest neglected terms in the y-momentum equation now are the streamwise gradient of the turbulent stress, $\partial(-\overline{uv})/\partial x$ and the cross-stream gradient of the viscous stress, $\partial(\nu\partial V/\partial y)/\partial y$. The largest neglected terms in equation (3.13) are the mean convection terms, $U\partial U/\partial x$ and $V\partial U/\partial y$ and the streamwise gradient of the turbulent normal stress difference, $\partial(\overline{u^2}-\overline{v^2})/\partial x$. In equation (3.14), the leading neglected terms are the mean convection terms, $U\partial T/\partial x$ and $V\partial T/\partial y$, and the streamwise gradient of the turbulent heat flux in the x-direction, $\partial(-\overline{ut})/\partial x$. Again, the neglected terms are of one order of magnitude less than the remaining terms. Clearly, these equations (eqns. (3.1),(3.13) and (3.14)) are capable of capturing the wall effects and describe the inner layer and are referred to as the "inner" set of equations. They are also exact only in the limit of infinite Reynolds and Péclét numbers.

Following an idea from the integral equation method, which was originally developed by Von Kármán [36] and others to solve the classical problem of the laminar forced convection boundary layer, we integrate equations (3.13) and (3.14) with respect to y. The x-momentum equation becomes

$$\nu\frac{\partial U}{\partial y} - \overline{uv} + \int_0^y g\beta(T-T_\infty)d\hat{y} \cong \nu\left(\frac{\partial U}{\partial y}\right)_{y=0} \equiv \frac{\tau_w}{\rho} \equiv u_*^2 \quad , \tag{3.20}$$

where τ_w is the wall shear stress and u_* is the friction velocity defined by this equation. Because of the presence of the integral of the buoyancy force, it is obvious that the inner layer cannot be a constant stress layer. This is one of the substantial differences between the natural convection boundary layer and the forced convection boundary layer. For the forced convection boundary layer, it was shown by George et al. [27] and others that in the limit of infinite Reynolds number the total stress is constant across the inner layer. Thus the wall shear stress provides the inner boundary condition for the outer layer, and viscosity effects enter the inviscid outer equations only through this boundary condition. Clearly, in our problem the wall shear stress

cannot be a fundamental parameter of the flow (see George et al. [27] for discussion of forced convection problem) and has to be treated as a dependent parameter! Most importantly (as noted by George and Capp [26]), since the shear stress varies across the inner layer, u_* cannot enter the outer layer analysis.

Integration of the energy equation leads to

$$\alpha \frac{\partial T}{\partial y} - \overline{vt} \cong \alpha \left(\frac{\partial T}{\partial y} \right)_{y=0} \equiv -\frac{q_w}{\rho c_p} \equiv -F_0 \quad , \tag{3.21}$$

where q_w is the wall heat flux, the thermal diffusivity α is defined by $\alpha \equiv k/\rho c_p$ and F_0 is the "kinematic" wall heat flux defined by this equation. F_0 can at most be a function of x. We conclude that the total heat flux across the inner layer is independent of the distance y from the wall and therefore, the inner layer is a constant heat flux layer. In this sense, the wall heat flux F_0, unlike u_*, is a fundamental parameter of the turbulent natural convection boundary layer, since it provides an inner boundary condition for the outer layer. It directly measures the forcing of the flow in the inner layer by the imposed conditions at the wall and it also measures the forcing of the outer flow through the boundary conditions provided by the inner layer. This will be the basis for the matching of inner and outer profiles (see chapter 5).

3.3 The Buoyant Sublayer

We note the existence of a flow region at the outside of the inner layer where viscous and conduction terms are losing their importance. This region can also be viewed as the inside of the outer layer, where the mean convection terms are not yet important. We are thus considering both inner and outer sets of equations and keep only the common terms. The governing equations for this intermediate region, referred to as the "buoyant sublayer" by George and Capp (by analogy to the inertial sublayer in

forced convection flows, c.f. Monin and Yaglom 1975 [44]), reduce to

$$0 \cong \frac{\partial}{\partial y}(-\overline{uv}) + g\beta(T - T_\infty) \tag{3.22}$$

$$0 \cong \frac{\partial}{\partial y}(-\overline{vt}) \quad . \tag{3.23}$$

Clearly, the heat flux across this layer is also nearly constant and dominated by the turbulent heat flux $\overline{vt} \cong F_0$, to first order. The Reynolds' stress, on the other hand, is continously modified by the buoyancy term, a clear distinction from the forced convection boundary layer.

Chapter 4

Similarity Considerations

4.1 Dimensional Analysis

Classical dimensional analysis stems from the famous Buckingham Pi Theorem, which states (c.f. [29, 57, 61]): "Suppose that a physical occurrence is governed by n independent parameters and each of these parameters can be expressed in terms of certain fundamental dimensions (e.g. mass $[M]$, length $[L]$, time $[T]$, temperature $[\theta]$), which are m in total number. Then the occurence can be described in terms of $n - r$ independent nondimensional quantities, called the Π-variables, where r is the rank of the $m \times n$ matrix formed from the m dimensions of the n quantities." Definite units of mass , length, time and temperature are chosen, e.g. kilograms [kg], meters [m], seconds [s] and Kelvin [K], respectively; these are agreed-upon standards which are either carefully preserved or reproducible. The fundamental dimensions $[M]$, $[L]$, $[T]$ and $[\theta]$ are abstract positive numbers, related to the fundamental units simply by a multiplication factor. Thus, the dimensionless Π-variables are invariant under a change of fundamental units. Dimensional analysis applied to problems typically encountered in mechanics or fluid dynamics can be found in e.g. Sedov 1959 [57] and Spurk 1992 [61], while a more fundamental treatment of dimensional analysis and similarity emphasizing the mathematical aspect of it is given in Barenblatt 1987 [2].

For the turbulent natural convection boundary layer, the only parameters which can govern the evolution of the flow are either those occurring in the equations of motion or the boundary conditions. Parameters occuring in the equations of motion are ν, $g\beta$ and α. The ambient fluid temperature T_∞ provides the only nontrivial boundary condition as $y \to \infty$. Typically, either heat flux F_0 or temperature T_w are specified at the wall. It is important to realize that only *one* of these boundary conditions can be chosen as an independent parameter, i.e. for given x a given local wall heat flux F_0 automatically defines the local temperature drop across the boundary layer ΔT_w, and vice versa (The asymptotic behaviour of $\Delta T_w = f(F_0)$ will be deduced from the GC79 theory).

Also entering the problem are the independent variables, which are the distance from the leading edge x and the cross-stream position y. Instead of x we could also employ the local cross-stream length-scale δ, which of course is a function of the downstream position, $\delta = \delta(x)$. Here we will seek solutions to the governing equations which depend on the streamwise coordinate x only through the local cross-stream length-scale $\delta(x)$. This is , in fact, the "local similarity" hypothesis which represents a considerable "leap of faith" on the part of the researchers. Unlike earlier analyses, however, it will be shown later to be consistent with similarity of the governing equations (which are the ultimate arbiter).

The theory presented here will consider the case where the wall heat flux F_0 is specified. Data from constant wall temperature experiments can easily be transformed into a constant wall heat flux form, since F_0 and ΔT_w are dependent on each other. Also, it is straightforward to reproduce the succeeding analysis for the constant wall temperature case.

Every flow quantity at any position within the flowfield of the boundary layer can then be described with this basic set of six independent parameters. The powers of the dimensions of the parameters are arranged in matrix form (c.f. table 4.1). The rank r of this matrix is three, therefore every quantity in the flowfield can be

described by $n - r = 6 - 3 = 3$ independent nondimensional ratios. The application

	α	ν	$g\beta$	F_0	$\delta(x)$	y
L	2	2	1	1	1	1
T	-1	-1	-2	-1	0	0
θ	0	0	-1	1	0	0

Table 4.1: The Π-Theorem: Dimensions of fundamental parameters

of the Buckingham Pi Theorem yields a number of possibilities, the significance of its results being easily overestimated, at least when the number of Π-variables is greater than two (as is the case here). All it can do in such a situation is suggest a variety of nondimensional parameters, from which the proper functional forms have to be selected with care. We choose the following Π-variables for consideration:

$$\Pi_1 = \frac{\nu}{\alpha} = Pr \tag{4.1}$$

$$\Pi_2 = \frac{g\beta F_0 \delta(x)^4}{\alpha^3} \equiv H^*_\delta \tag{4.2}$$

$$\Pi_3 = \frac{F_0\ \delta}{\Delta T_w \alpha} = Nu_\delta \tag{4.3}$$

$$\Pi_4 = \frac{y}{\delta(x)} \tag{4.4}$$

Π_1 is recognized as the Prandtl number, while equation (4.2) defines the local "H-number", as introduced by George and Capp [26]. Of course, H^*_δ serves an analogous purpose as the Grashof or Rayleigh numbers, Gr^*_x and Ra^*_x, did in previous analytical work and plays a similar role as the Reynolds number in forced convection (c.f. Monin and Yaglom [44]). This new characteristic dimensionless ratio only uses thermal diffusivity instead of kinematic viscosity (both have the same dimensions). A look at the property tables for fluids of technical interest tells us that the latter shows a stronger dependence on temperature in liquids, whereas they both show approximately the same temperature dependence in gases (c.f. figure 5). Therefore, thermal diffusivity α was employed instead of kinematic viscosity ν for its more desirable temperature dependence in liquids for the temperature differences to be expected.

Π_3 defines the local Nusselt number. The Pi-Theorem immediately leads to the relationship $Nu_\delta = f(H^*_\delta, Pr)$, which is the local heat transfer law. Thus only two of the first three are independent, and either H^*_δ or Nu_δ can be eliminated in any subsequent analysis. It will be shown below that Nu_δ is in fact the ratio of outer to inner length scales. This is a significant departure from the earlier GC79 theory, where the ratio of length scales was $H^{*1/4}_\delta$, and will be seen to be a key feature of retaining the x-dependence for finite values of H^*_δ (or H_δ). Π_4 defines a relative cross-stream position based on a cross-stream lengthscale and provides the third independent variable.

Now profiles are sought which scale only with the local length scale. Therefore functional forms (scaling laws) of ratios of flow quantities and local scale factors can be expressed as:

$$\frac{U}{U_S(x)} = f_1\left(\frac{y}{\delta}, H^*_\delta, Pr\right) \tag{4.5}$$

$$\frac{T}{T_S(x)} = f_2\left(\frac{y}{\delta}, H^*_\delta, Pr\right) \tag{4.6}$$

$$\frac{-\overline{uv}}{R_S(x)} = g_1\left(\frac{y}{\delta}, H^*_\delta, Pr\right) \tag{4.7}$$

$$\frac{-\overline{vt}}{F_S(x)} = g_2\left(\frac{y}{\delta}, H^*_\delta, Pr\right) \tag{4.8}$$

for the mean velocity, mean temperature,turbulent transport of momentum (Reynolds' stress) and heat (turbulent heat flux), respectively. Scaling laws can be obtained from the functional forms (4.5)–(4.8), since they have to become asymptotically independent of H^*_δ in the limit as $H^*_\delta \to \infty$ in order to be well-behaved. Thus separation of the x-dependence from f_1, f_2, g_1 and g_2 seems possible. The scale factors U_S, T_S, R_S and F_S are not specified (nor could they be), but must be determined from the governing equations using the Asymptotic Invariance Principle as set forth below.

4.2 Similarity Solutions and the Asymptotic Invariance Principle

Similar profiles of U, $T - T_\infty$, $-\overline{uv}$ and $-\overline{vt}$ are observed at different downstream locations. "Similarity" (or self-preservation) is said to occur when one can bring these profiles into congruence by simply scaling them with scale factors which depend only on one of the variables. An immediate consequence would be that the governing equations become independent of this variable. The functional dependence of the equations is then reduced by one variable, which is extremely helpful when dealing with a two-dimensional or axisymmetrical flowfield. If such a "similarity" actually exists, a mathematical transformation of variables can be performed to reflect this fact, separating the dependence of the flow quantities on the new variables, called the "similarity variables". The governing equations for a two-dimensional flow are thus reduced from nonlinear partial differential equations to nonlinear ordinary differential equations.

An alternative definition is given by George 1989 [23]: "A flow is said to be self-preserving if solutions to its governing equations and boundary conditions exist, for which all quantities of dynamical significance have the same relative value at the same relative location. The flow then has reached some kind of equilibrium where all of its dynamical influences evolve together. Thus self-preservation is an asymptotic state attained by a flow once its internal readjustments are complete."

A set of Reynolds-averaged equations governing turbulent flow is always unsolvable as it is, some form of turbulence modeling is needed to close the equations. Using similarity theory can provide further insight without addressing the turbulence closure problem.

Similarity solutions had first been introduced to fluid dynamics by Blasius in 1908 [7], who applied them in laminar boundary layer theory leading to the well-known "Blasius-equation".

Analytical approaches to any turbulent convection problem usually abandon full similarity solutions at the outset and *hypothesize* the existence of "local similarity" solutions. The word "local similarity" is somewhat misleading, since scaling laws are actually found on purely dimensional grounds. In the analysis presented below, however, full similarity solutions will be sought for inner and outer sets of equations separately. (This relatively new idea was introduced by George et al. 1994 [27] in considering the forced convection boundary layer) Since both sets of equations are exact only in the limit of infinite Reynolds and Péclét numbers — or infinite H-number — their full similarity solutions will also be exact only in this limit. The neglected terms vanish only in the limit of infinite H-number, thus the governing equations will be H-number dependent for finite H-numbers and lose this dependence only in the limit. This knowledge will be used to determine the functional forms in a region of common validity, the procedure is referred to as the *Asymptotic Invariance Principle* (AIP). Similar arguments are usually made for free turbulent shear flows, the difference for boundary layer flows is that we are seeking two sets of solutions, which reduce to full similarity solutions in the limit of infinite H-number (or, equivalently, infinite Nusselt number). A very important aspect of the theory presented here is that no scaling laws are defined *a priori*; they will be determined from the conditions for similarity.

4.3 Similarity of the Inner Equations

The inner local cross-stream length-scale is given by $\eta(x)$, which remains to be determined. As indicated by dimensional analysis, we choose one similarity variable to be y/η, and leave the variable x unchanged. We seek similarity solutions to the inner equations of the form:

$$U(x, y^+) \;=\; U_{Si}(x) f_{1i}\left(y^+, Pr\right) \tag{4.9}$$

$$T(x,y^+) - T_w(x) = T_{Si}(x) f_{2i}\left(y^+, Pr\right) \tag{4.10}$$

$$-\overline{uv}(x,y^+) = R_{Si}(x) g_{1i}\left(y^+, Pr\right) \tag{4.11}$$

$$-\overline{vt}(x,y^+) = F_{Si}(x) g_{2i}\left(y^+, Pr\right) \tag{4.12}$$

where the "inner" variable y^+ is defined by:

$$y^+ = \frac{y}{\eta} \quad . \tag{4.13}$$

Substituting these functional forms into equations (3.20) and(3.21), nondimensionalizing and clearing terms leads to

$$\begin{aligned}\left[\frac{u_*^2}{{U_{Si}}^2}\right] &= \left[\frac{\nu}{\eta U_{Si}}\right] {f_{1i}}' + \left[\frac{R_{Si}}{{U_{Si}}^2}\right] g_{1i} + \\ &+ \left[\frac{\eta g \beta T_{Si}}{{U_{Si}}^2}\right] \int_0^{y^+} f_{2i}(\hat{y}^+, Pr) d\hat{y}^+ + \left[\frac{\eta g \beta \Delta T_w}{{U_{Si}}^2}\right] y^+ \end{aligned} \tag{4.14}$$

and

$$-\left[\frac{F_0}{U_{Si} T_{Si}}\right] = \left[\frac{\alpha}{\eta U_{Si}}\right] {f_{2i}}' + \left[\frac{F_{Si}}{U_{Si} T_{Si}}\right] g_{2i} \quad . \tag{4.15}$$

To this point only a transformation of variables was performed. Full similarity is only possible if all the terms in brackets have the same x-dependence which leads to the conditions

$$\frac{u_*^2}{{U_{Si}}^2} \propto \frac{\nu}{\eta U_{Si}} \propto \frac{R_{Si}}{{U_{Si}}^2} \propto \frac{\eta g \beta T_{Si}}{{U_{Si}}^2} \propto \frac{\eta g \beta \Delta T_w}{{U_{Si}}^2} \tag{4.16}$$

and

$$\frac{F_0}{U_{Si} T_{Si}} \propto \frac{\alpha}{\eta U_{Si}} \propto \frac{F_{Si}}{U_{Si} T_{Si}} \quad . \tag{4.17}$$

Solving this system of six relations for the six unknowns T_{si}, F_{Si}, η, U_{Si}, R_{Si} and u_* gives scales of the form:

$$T_{Si} \propto T_w - T_\infty = \Delta T_w \tag{4.18}$$

$$F_{Si} \propto F_0 \tag{4.19}$$

$$\eta \propto \frac{\alpha \Delta T_w}{F_0} \tag{4.20}$$

$$U_{Si} \propto \frac{\alpha}{Pr} g\beta \frac{\Delta T_w^3}{F_0^2} \tag{4.21}$$

$$R_{Si} \propto \alpha g\beta \frac{\Delta T_w^2}{F_0} \propto u_*^2 \tag{4.22}$$

The proportionalities can be transformed into exact equations by introducing constants of proportionality. These constants can in any case be absorbed into the functions f_{1i}, f_{2i}, g_{1i} and g_{2i}, which determines our inner scales as

$$T_{Si} = T_w - T_\infty = \Delta T_w \tag{4.23}$$

$$F_{Si} = F_0 \tag{4.24}$$

$$\eta = \frac{\alpha \Delta T_w}{F_0} \tag{4.25}$$

$$U_{Si} = \frac{\alpha}{Pr} g\beta \frac{{\Delta T_w}^3}{{F_0}^2} \tag{4.26}$$

$$R_{Si} = \alpha g\beta \frac{{\Delta T_w}^2}{F_0} \propto {u_*}^2 \tag{4.27}$$

The inner length scale, $\eta = \Delta T_w \alpha / F_0$ was originally used by Fujii et al. 1970 [20] as "thermal boundary layer thickness" and was adopted by Smith 1972 [59], who termed it "heat transfer distance". A graphical explanation of η is given in figure 6. It is a natural choice since it is the heat flux ($(\partial T/\partial y)_{y=0}$) which ultimately drives the flow. Note that the local Nusselt number, Nu_δ, is the ratio of outer and inner lengthscales, which has to be large for the scaling to be valid since it is based on reduced inner and outer equations.

The value of u_* has been determined to within a constant by the similarity constraint (the exact value of u_* cannot be determined this way since it would overspecify the problem). Note that the occurence of both ΔT_w and F_0 will permit the x-dependence which was missing in the GC79 analysis.

The inner equations (3.20,3.21) can now be written as:

$$1 = {f_{1i}}' + g_{1i} + \int_0^{y^+} f_{2i}(\hat{y}^+)d\hat{y}^+ + y^+ \tag{4.28}$$

and

$$-1 = {f_{2i}}' + g_{2i} \quad , \tag{4.29}$$

The Prandtl number dependence has been incorporated into the inner scales and is thus taken out of the functional formulation, as opposed to the GC79 theory.

4.4 Similarity of the Outer Equations

Note that the outer set of equations is independent of the Prandtl number, since both viscosity and thermal diffusivity do not occur in equations (3.5) and (3.6). We now choose the similarity variable to be y/δ, and seek similarity solutions to the outer equations of the form:

$$U(x,\bar{y}) = U_{So}(x) f_{1o}(\bar{y}) \tag{4.30}$$

$$T(x,\bar{y}) - T_\infty(x) = T_{So}(x) f_{2o}(\bar{y}) \tag{4.31}$$

$$-\overline{uv}(x,\bar{y}) = R_{So}(x) g_{1o}(\bar{y}) \tag{4.32}$$

$$-\overline{vt}(x,\bar{y}) = F_{So}(x) g_{2o}(\bar{y}) \tag{4.33}$$

where the "outer" variable $\bar{y}$ is defined by:

$$\bar{y} = \frac{y}{\delta} \quad . \tag{4.34}$$

Note that the derivative of the outer variable $\bar{y}$ with respect to x does not vanish, since $\delta = \delta(x)$. The cross-stream component of the mean velocity V can be written in a similarity form (in terms of U_{So}, eqn. (4.30)) with the help of the continuity

equation (3.1) and integration by parts:

$$V = -\left[\frac{dU_{So}}{dx}\delta + U_{So}\frac{d\delta}{dx}\right]\int_0^{\bar{y}} f_{1o}(\hat{\bar{y}})d\hat{\bar{y}} - \left[\frac{dU_M}{dx}\delta\right]\bar{y} + \left[U_{So}\frac{d\delta}{dx}\right]\bar{y}f_{1o}(\bar{y}) \quad . \tag{4.35}$$

Upon substituting and clearing terms the x-momentum equation (3.5) assumes the following nondimensionalized form:

$$\begin{aligned}\left[\frac{\delta}{U_{So}}\frac{dU_{So}}{dx}\right]\left({f_{1o}}^2 - {f_{1o}}'\int_0^{\bar{y}} f_{1o}(\hat{\bar{y}})d\hat{\bar{y}}\right) \quad &- \quad \left[\frac{d\delta}{dx}\right]{f_{1o}}'\int_0^{\bar{y}} f_{1o}(\hat{\bar{y}})d\hat{\bar{y}} \\ = \quad \left[\frac{R_{So}}{{U_{So}}^2}\right]{g_{1o}}' \quad &+ \quad \left[\frac{\delta g\beta T_{So}}{{U_{So}}^2}\right]f_{2o} \quad .\end{aligned} \tag{4.36}$$

Similarly, substitution into the energy equation (3.6) and clearing terms leads to

$$\begin{aligned}\left[\frac{\delta}{T_{So}}\frac{dT_{So}}{dx}\right](f_{1o}f_{2o} + f_{1o}) \quad &- \quad \left[\frac{\delta}{U_{So}}\frac{dU_{So}}{dx}\right]{f_{2o}}'\int_0^{\bar{y}} f_{1o}(\hat{\bar{y}})d\hat{\bar{y}} \\ - \left[\frac{d\delta}{dx}\right]{f_{2o}}'\int_0^{\bar{y}} f_{1o}(\hat{\bar{y}})d\hat{\bar{y}} \quad &= \quad \left[\frac{F_{So}}{U_{So}T_{So}}\right]{g_{2o}}' \quad .\end{aligned} \tag{4.37}$$

As before, only a change of variables was performed to this point (i.e. a similarity transformation, and the transformed equations only reduce to ordinary nonlinear differential equations, if the terms in brackets have the same x-dependence). From the self-preservation condition, we obtain the relations

$$\frac{\delta}{U_{So}}\frac{dU_{So}}{dx} \propto \frac{\delta}{T_{So}}\frac{dT_{So}}{dx} \propto \frac{d\delta}{dx} \propto \frac{R_{So}}{{U_{So}}^2} \propto \frac{g\beta T_{So}\delta}{{U_{So}}^2} \propto \frac{F_{So}}{U_{So}T_{So}} \tag{4.38}$$

From the first three terms we find

$$T_{So} \propto \delta^m \qquad \text{and} \qquad U_{So} \propto \delta^n \quad . \tag{4.39}$$

Substituting this into the fourth and fifth term gives

$$R_{S_o} \propto T_{S_o}\delta \propto \delta^{m+1} \quad . \tag{4.40}$$

From equation (4.38) it is clear that there must be two different velocity scales in the outer layer, as opposed to traditional boundary layer analysis. The scale for the Reynolds' stress is not just the square of the velocity scale, as usually assumed (c.f. Tennekes and Lumley [62]), but it also depends on the growth rate of the boundary layer, $R_{S_o} \sim {U_{S_o}}^2 d\delta/dx$. The requirement $R_{S_o} = {U_{S_o}}^2$ seems too restrictive, experimental findings suggest that the growth rate $d\delta/dx$, for the range of finite Grashof numbers experiments were performed at, is not constant. Note that we cannot determine the outer scales yet, since only homogenous boundary conditions are given at the outside of the outer layer. The missing piece of information must be acquired from matching to the inner layer.

Chapter 5

Matching of Inner and Outer Profiles

Both inner and outer functional forms describe the entire flowfield as long as the dependence on the nondimensional ratios (as in eqns. (4.5)-(4.8)) is retained. Since $Nu_\delta = f(H_\delta^*)$ and $Nu_\delta \to \infty$ as $H_\delta^* \to \infty$, we can conveniently use the ratio of lengthscales as a parameter instead of H_δ^*, defining

$$\varepsilon = \frac{\eta}{\delta} = \frac{\Delta T_w \alpha}{F_0\ \delta} = {Nu_\delta}^{-1} \tag{5.1}$$

as our dimensionless matching parameter (similar to a perturbation parameter), therefore $\varepsilon \to 0$ as $H_\delta^* \to \infty$. The solutions to each set of governing equations reduce to similarity solutions (inner: eqns. (4.9)–(4.12), outer: eqns. (4.30)–(4.33)) only in the limit as $\varepsilon \to 0$. The outer forms then fail to describe the behaviour close to the wall while the inner fail to describe the outer part of the boundary layer. The solutions thus degenerate in different ways at infinite Nusselt number, we will investigate whether they possess a common region in this limit.

Considering mean velocity first and with the argument made above, we can equate

the inner and outer profiles at finite ε

$$f_{10}\left(\bar{y},\varepsilon\right) = \frac{U_{Si}}{U_{So}} f_{1i}\left(y^+,\varepsilon\right) = r_U(\varepsilon) f_{1i}\left(y^+,\varepsilon\right) \quad . \tag{5.2}$$

The ratio $r_U(\varepsilon) = U_{Si}/U_{So}$ (unknown so far, U_{So} remains to be determined) is not constant and is a function of ε only.

The velocity derivative must also be the same for both forms, which can be written as:

$$\frac{\bar{y}}{f_{1o}} \frac{\partial(f_{1o})}{\partial \bar{y}} = \frac{y^+}{f_{1i}} \frac{\partial f_{1i}}{\partial y^+} \tag{5.3}$$

According to the AIP, both $f_{1o}(\bar{y},\varepsilon)$ and $f_{1i}(y^+,\varepsilon)$ must become asymptotically independent of ε in the limit as $\varepsilon \to 0$, otherwise the velocity scales would have been improperly chosen.

As the limit $\varepsilon \to 0$ is approached, the question is: Does an overlap region exist, for which equation (5.2) is still valid? Since both lengthscales η and δ are increasing with downstream position, this overlap layer will move further away from the wall in physical variables. Therefore it is necessary to introduce an intermediate variable $\tilde{y}$ which remains fixed in the overlap region for any x, regardless of what is happening in physical space (c.f. Cole [15]). (Note: This is not necessary for turbulent natural convection between two vertical plates (c.f. Elder [18]) since the matched layer will remain at fixed distance from the wall because of the streamwise homogeneity, c.f. 7.) This can be accomplished by a variable defined as:

$$\tilde{y} = y^+ \varepsilon^n \tag{5.4}$$

or, for inner and outer variables with $\varepsilon = \bar{y}/y^+$:

$$y^+ = \tilde{y}\varepsilon^{-n} \quad \text{and} \quad \bar{y} = \tilde{y}\varepsilon^{1-n} \quad . \tag{5.5}$$

For $0 < n < 1$, the variable $\tilde{y}$ can stay fixed in the overlap region as $\varepsilon \to 0$ while

$\bar{y} \to 0$ and $y^+ \to \infty$. Rewriting equation (5.2) with $\tilde{y}$:

$$f_{1o}\left(\bar{y},\varepsilon\right) = r_U(\varepsilon) f_{1i}\left(\tilde{y}\varepsilon^{-n},\varepsilon\right) \tag{5.6}$$

Note that taking the derivative with respect to $\tilde{y}$ of equation (5.6) also results in equation (5.3). Differentiating equation (5.6) with respect to ε, multiplying by ε/f_{1o} and with equation (5.3) we obtain:

$$\begin{aligned} \left.\frac{\bar{y}}{f_{1o}}\frac{\partial f_{1o}}{\partial \bar{y}}\right|_\varepsilon &= \frac{\varepsilon}{r_U}\frac{\partial r_U}{\partial \varepsilon} + \left\{ \left.\frac{\varepsilon}{f_{1i}}\frac{\partial f_{1i}}{\partial \varepsilon}\right|_{y^+} - \left.\frac{\varepsilon}{f_{1o}}\frac{\partial f_{1o}}{\partial \varepsilon}\right|_{\bar{y}} \right\} \\ &= a(\varepsilon) + \left\{ \quad a_2(\varepsilon, y^+, \bar{y}) \quad \right\} \end{aligned} \tag{5.7}$$

The first term on the right-hand side is only a function of ε while the second term (in braces) contains all the residual y-dependence. Since $f_{1o}(\bar{y},\varepsilon)$ and $f_{1i}(y^+,\varepsilon)$ are asymptotically independent of ε (as determined by the AIP) and since their derivatives with respect to $\tilde{y}$ vanish for the same reason, the first term dominates and the expression in braces represents the contribution from higher order terms. To leading order in ε equation (5.7) can thus be written as (with eqn.(5.3)):

$$\left.\frac{\bar{y}}{f_{1o}}\frac{\partial f_{1o}}{\partial \bar{y}}\right|_\varepsilon = a(\varepsilon) = \left.\frac{y^+}{f_{1i}}\frac{\partial f_{1i}}{\partial y^+}\right|_\varepsilon \quad . \tag{5.8}$$

The functional forms can now be integrated to yield to first order:

$$f_{1o} = C_{1o}(\varepsilon)\bar{y}^{a(\varepsilon)} \tag{5.9}$$

$$f_{1i} = C_{1i}(\varepsilon) y^{+\,a(\varepsilon)} \tag{5.10}$$

Substituting these solutions back into the matching condition (5.2) leads to

$$r_U = \frac{U_{Si}}{U_{So}} = \frac{C_{1o}(\varepsilon)}{C_{1i}(\varepsilon)}\left(\frac{\eta}{\delta}\right)^{a(\varepsilon)} = \frac{C_{1o}(\varepsilon)}{C_{1i}(\varepsilon)}\varepsilon^{a(\varepsilon)} \quad . \tag{5.11}$$

When writing equation (5.7) with (5.11) we can find an equation constraining C_{1i}, C_{1o} and a:

$$\ln \varepsilon \frac{d}{d\varepsilon}\, a(\varepsilon) = \frac{d}{d\varepsilon}\left[\ln\left(\frac{C_{1i}(\varepsilon)}{C_{1o}(\varepsilon)}\right)\right] \quad . \tag{5.12}$$

This is, of course, the criterion for the vanishing of the neglected higher order terms in equation (5.7) since it came from solutions that were obtained by neglecting these terms. The velocity profile in the matched layer — the "buoyant sublayer" — is thus seen to be a power law (to first order) with Nusselt number (H-number) dependent exponent and coefficients. Again, since $f_{1o}(\bar{y}, \varepsilon)$ and $f_{1i}(y^+, \varepsilon)$ must be asymptotically independent of the Nusselt number (or H-number), so must C_{1i}, C_{1o} and a. Therefore as $\varepsilon \to 0$,

$$C_{1i}(\varepsilon) \to C_{1i\infty}, \;\; C_{1o}(\varepsilon) \to C_{1o\infty} \;\; \text{and} \;\; a(\varepsilon) \to a_\infty \tag{5.13}$$

We will discuss their asymptotic values later.

For the mean temperature, we can equate the inner and outer profiles at finite ε, i.e.,

$$f_{20}\left(\bar{y}, \varepsilon\right) = \frac{T_{Si}}{T_{So}}\left(1 + f_{2i}\left(y^+, \varepsilon\right)\right) = r_T(\varepsilon)\left(1 + f_{2i}\left(y^+, \varepsilon\right)\right) \quad . \tag{5.14}$$

Proceeding in the same way as before, we find solutions to first order for the functional forms:

$$f_{2o} = C_{2o}(\varepsilon)\bar{y}^{b(\varepsilon)} \tag{5.15}$$

$$1 + f_{2i} = C_{2i}(\varepsilon) y^{+\, b(\varepsilon)} \tag{5.16}$$

Substituting into the matching condition (5.14) yields

$$r_T = \frac{T_{Si}}{T_{So}} = \frac{C_{2o}(\varepsilon)}{C_{2i}(\varepsilon)}\left(\frac{\eta}{\delta}\right)^{b(\varepsilon)} = \frac{C_{2o}(\varepsilon)}{C_{2i}(\varepsilon)}\varepsilon^{b(\varepsilon)} \quad . \tag{5.17}$$

In the same manner, we find for the Reynolds' stress:

$$g_{1o} = D_{1o}(\varepsilon)\bar{y}^{c(\varepsilon)} \tag{5.18}$$

$$g_{1i} = D_{1i}(\varepsilon) y^{+c(\varepsilon)} \tag{5.19}$$

and

$$r_R = \frac{R_{Si}}{R_{So}} = \frac{D_{1o}(\varepsilon)}{D_{1i}(\varepsilon)} \left(\frac{\eta}{\delta}\right)^{c(\varepsilon)} = \frac{D_{1o}(\varepsilon)}{D_{1i}(\varepsilon)} \varepsilon^{c(\varepsilon)} \quad . \tag{5.20}$$

For the turbulent heat flux:

$$g_{2o} = D_{2o}(\varepsilon) \bar{y}^{d(\varepsilon)} \tag{5.21}$$

$$g_{2i} = D_{2i}(\varepsilon) y^{+d(\varepsilon)} \tag{5.22}$$

and

$$r_F = \frac{F_{Si}}{F_{So}} = \frac{D_{2o}(\varepsilon)}{D_{2i}(\varepsilon)} \left(\frac{\eta}{\delta}\right)^{d(\varepsilon)} = \frac{D_{2o}(\varepsilon)}{D_{2i}(\varepsilon)} \varepsilon^{d(\varepsilon)} \quad . \tag{5.23}$$

Chapter 6

Scaling Functions for the Outer Layer

6.1 Outer Scales From Matching

We will now attempt to find the outer scaling laws of eqns.(4.30)–(4.33) from knowing the inner scales and the matching of the profiles, which links information about the inner scales to the outer scales. This is reasonable physically since this is a boundary layer flow driven exclusively by the heat transferred at the wall. Whatever happens there has a direct influence on the outer part of the flowfield. From equation (5.11) we know

$$U_{So} = U_{Si}\frac{C_{1i}}{C_{1o}}\left(\frac{\eta}{\delta}\right)^{-a} = U_{Si}\frac{C_{1i}}{C_{1o}}\ {Nu_\delta}^a \tag{6.1}$$

With the inner velocity scale found from similarity (eqn.(4.26)) we can obtain the outer velocity scale as:

$$\begin{aligned} U_{So} &= \frac{\alpha}{Pr} g\beta \frac{{\Delta T_w}^3}{{F_0}^2}\frac{C_{1i}}{C_{1o}}\left(\frac{F_0\ \delta}{\Delta T_w \alpha}\right)^a = \\ &= \left(\frac{1}{Pr}\frac{C_{1i}}{C_{1o}}\right)\frac{g\beta\ \delta}{F_0}\ {Nu_\delta}^{a-1}\ {\Delta T_w}^2 \quad . \end{aligned} \tag{6.2}$$

From the matched layer equation (3.23), we know that

$$F_{So} \propto F_{Si} = F_0 \tag{6.3}$$

to first order. From the fifth and sixth term of the self preservation condition of the outer equations (4.38) we find the outer temperature scale

$$T_{So} \propto \left(\frac{F_0}{g\beta\ \delta} U_{So}\right)^{1/2} = \left(\frac{1}{Pr}\frac{C_{1i}}{C_{1o}}\right)^{1/2}\ Nu_\delta{}^{(a-1)/2}\ \Delta T_w \quad . \tag{6.4}$$

The fourth and fifth term of (4.38) yield the outer Reynolds' stress scale

$$R_{So} \propto \left(\frac{1}{Pr}\frac{C_{1i}}{C_{1o}}\right)^{1/2} g\beta\ \delta\ Nu_\delta{}^{(a-1)/2}\ \Delta T_w \quad . \tag{6.5}$$

The ratio of constants, C_{1i}/C_{1o}, is a function of the ratio of lengthscales, η/δ, but can be eliminated using constraint (5.12). We now have determined all the outer scales in terms of the exponent $a(\varepsilon)$ and an outer lengthscale δ. The exponent $a(\varepsilon)$ can be determined by curve-fitting in the buoyant sublayer region. The actual boundary layer thickness δ is difficult to measure because of low mean velocity and temperature difference and high turbulence intensities in the outer layer. Possible choices for δ could be either displacement, momentum or enthalpy thickness. The limiting value of $a(\varepsilon)$ and the physical significance of the integral boundary layer thicknesses in terms of δ is discussed in chapter 8.

From equation (5.17) we know

$$T_{So} = T_{Si}\frac{C_{2i}}{C_{2o}}\ Nu_\delta{}^b \quad , \tag{6.6}$$

with the outer similarity condition (4.38) we can write

$$U_{So} \propto \left(\frac{C_{2i}}{C_{2o}}\right)^2 \frac{g\beta\ \delta}{F_0}\ Nu_\delta{}^{2b}\ \Delta T_w{}^2 \quad . \tag{6.7}$$

Comparing eqns.(6.2) and (6.7) shows that a and b are constrained by:

$$2b = a - 1 \quad . \tag{6.8}$$

From equation (5.20) with eqns.(4.38) and (4.27) we find

$$U_{So} \propto \left(\frac{D_{1i}}{D_{1o}}\right)^2 \frac{g\beta\ \delta}{F_0}\ Nu_\delta{}^{2c-2}\ \Delta T_w{}^2 \tag{6.9}$$

and a constraint for a and c :

$$2c = a + 1 \quad . \tag{6.10}$$

From eqns.(3.23) and (5.21), (5.22) it is clear that $d = 0$ to first order.

6.2 Outer Scales From Physical Argument

When comparing the inner and outer scales of George and Capp [26], it is found that $U_{Si}/U_{So} = (\eta/\delta)^{1/3}$ and $T_{Si}/T_{So} = (\eta/\delta)^{-1/3}$. The George/Capp scaling can be interpreted as a special, more restrictive case of the new (inner) scales, since it includes the additional requirement $T_{Si} \propto F_{Si}^{3/4}$ and $Re_\eta = \eta U_{Si}/\nu = const.$ (and therefore $R_{Si} \propto U_{Si}{}^2$). In the limit as the ratio of lengthscales vanishes we have:

$$\frac{U_{Si}}{U_{So}} \to 0, \qquad \frac{T_{Si}}{T_{So}} \to \infty \qquad \text{as} \quad \frac{\eta}{\delta} \to 0. \tag{6.11}$$

This behaviour makes sense physically: The boundary layer is trying to lose its streamwise inhomogeneity and become a channel flow. In a fully developed turbulent natural convection channel flow $U_{Si} \ll U_{So}$ and $T_{So} \ll T_{Si}$ (c.f. Elder 1965 [18] and figure 7). It will now be attempted to find ratios of inner and outer scales which satisfy

$$\frac{U_{Si}}{U_{So}} \propto \left(\frac{\eta}{\delta}\right)^a, \qquad a > 0, \tag{6.12}$$

and

$$\frac{T_{Si}}{T_{So}} \propto \left(\frac{\eta}{\delta}\right)^{b}, \qquad b < 0, \tag{6.13}$$

which is a "more general" form of the George Capp scaling. Knowing that

$$\frac{\eta}{\delta} = \frac{\alpha \Delta T_w}{\delta F_0} = {Nu_\delta}^{-1} \qquad , \tag{6.14}$$

we find e.g. an outer velocity scale to be

$$U_{So} \propto \frac{1}{Pr} \frac{g\beta\ \delta}{F_0}\ {Nu_\delta}^{a-1}\ {\Delta T_w}^2 \qquad . \tag{6.15}$$

This leads, of course, to the same scales as were found by using the matching with the Asymptotic Invariance Principle AIP, since the physical argument made above in equations (6.12) and (6.13) is also the result from the matching! The outer scales and an additional constraint on the power laws ($a > 0, b < 0$) in the buoyant sublayer can thus be found from purely physical arguments.

Chapter 7

A "New" Heat Transfer Law

The heat transfer relationship can be obtained from the remaining similarity conditions of the outer equations (4.38). The outer scales now contain information from the inner layer and therefore from the wall boundary conditions, since they were derived from the matching with the AIP. From equation (6.3) and the first three terms of equation (4.38) it follows that

$$F_0 \propto U_{So} T_{So} \frac{d\delta}{dx} \quad . \tag{7.1}$$

Substituting from equations (6.2) and (6.4) immediately yields the local heat transfer law

$$Nu_\delta \propto \left(H_\delta^* \frac{d\delta}{dx} \right)^{2/(9-3a)} \quad . \tag{7.2}$$

The appearence of $d\delta/dx$ may at first glance seem surprising. However, it directly measures the evolution of the boundary layer. It will be shown below to be related to the local turbulent Reynolds number and to be asymptotically constant.

Chapter 8

The Asymptotic Limit

8.1 Turbulence Quantities and $d\delta/dx$

An analogous similarity approach can be applied to equations governing any statistical quantity. Note that this will not be discussed further in this thesis, but is one of the main points of interest for future work. Here, we will only take a quick look at some terms of the component equations of turbulent kinetic energy and use traditional dissipation scaling arguments to find the asymptotic behaviour of the boundary layer growth rate, $d\delta/dx$. The transport equation for the streamwise component of the kinetic energy, i.e. the $\overline{u_1 u_1}$-component of the Reynolds' stress equation (A.52), in the outer layer reduces to

$$U\frac{\partial}{\partial x}\frac{1}{2}\overline{u^2} + V\frac{\partial}{\partial y}\frac{1}{2}\overline{u^2} \cong \ldots - \overline{uv}\frac{\partial U}{\partial y} + g\beta\overline{ut} - \epsilon_u \tag{8.1}$$

where "..." represent the pressure strain rate and transport terms, which are not important for the argument below. If K_{Suo} and D_{Suo} represent scale quantities for the streamwise kinetic energy and dissipation, respectively, and G_{So} is a scale for the

vertical turbulent heat flux, then similarity is possible only if

$$\frac{d\delta}{dx} \propto \frac{\delta}{K_{Suo}} \frac{dK_{Suo}}{dx} \propto \ldots \propto \frac{R_{So}}{K_{Suo}} \propto \frac{g\beta G_{So}\delta}{U_{So}K_{Suo}} \propto \frac{D_{Suo}\delta}{U_{So}K_{Suo}} \tag{8.2}$$

Using eqn.(4.38)), it follows that $K_{Suo} \propto U_{So}^2$, so that

$$D_{Suo} \propto \frac{U_{So}^3}{\delta} \frac{d\delta}{dx} \qquad \text{etc.} \tag{8.3}$$

(Outlook: By comparing the scaling of the three component equations of turbulent kinetic energy, it can be shown that similarity of the Reynolds' stress equation is only possible if $d\delta/dx = const.$ (c.f. George 1994 [25]). For the lower order moments though, $d\delta/dx \neq const.$ does not contradict similarity! Thus, the similarity solution for lower order moments (in momentum and energy equations, as outlined here) will be like a first order approximation for finite H_δ^*.)

George 1994 [25] (following George (1992) [24]) uses the traditional energy spectrum arguments of Batchelor 1953 [3] to argue that $D_{Suo} \propto U_{So}^3/\delta$ in the limit of infinite *turbulence* Reynolds number, $Re_\delta = u\delta/\nu$. Thus, in this limit (and only in this limit!), $d\delta/dx = const.$ and the asymptotic boundary layer grows linearly. In practice, a turbulent Reynolds number of appproximately 10^3 to 10^4 is required to reach this limit. The physical reason for this is that at finite turbulent Reynolds number, dissipation occurs over the entire energy spectrum, since energy-containing and dissipation wave number ranges are not separated. For all finite turbulence Reynolds numbers, $d\delta/dx$ will depend on the local Reynolds number.

Similar relations can be derived for all other turbulence quantities of interest. Their implications on similarity solutions of the type described in section 4.2 have to be investigated subsequently.

8.2 Asymptotic Limit and GC79 Theory

It is clear from the above that in the limit as the turbulent Reynolds number increases without bound ($H^*_\delta, Nu_\delta \to \infty$) the TNCBL asymptotically grows linearly, since $d\delta/dx = const.$ It follows immediately from the outer similarity conditions (4.38) that $g\beta T_{So}\delta \propto U^2_{So}$ and $U_{So}T_{So} \propto F_0$. Thus $U_{So} \propto (g\beta F_0\delta)^{1/3}$ and $T_{so} \propto F_0^{2/3}/(g\beta\delta)^{1/3}$, regardless of the x-dependence of F_0. These are exactly the outer scales of GC79 found from local similarity arguments at infinite Reynolds number.

Now that the outer scales are determined in the limit, the ratios of inner and outer scales can be used together with the heat transfer law to obtain the limiting values for a, b, c and d. The results are $a_\infty = +1/3$, $b_\infty = -1/3$, $c_\infty = 2/3$ and $d_\infty = 0$ (Note: $n = a$, $m = b$ in eqns. (4.39,4.40)) . It follows immmediately that $Nu_\delta \propto H^{*1/4}_\delta$, which is again the GC79 result and known to be the most widely accepted heat transfer relationship for the turbulent natural convection boundary layer. Thus, the new inner and outer scales are proportional to the GC79 inner and outer scales in the limit as $H^*_\delta \to \infty$ (and can be reduced to them using the asymptotic heat transfer law, $Nu_\delta \propto H^{*1/4}_\delta$).

8.3 Integral Boundary Layer Thickness as Outer Lengthscale

We can write mean temperature and velocity in a composite profile form which is valid over the entire boundary layer. This can be accomplished by e.g. writing the inner profile in outer variables, adding the outer profile and subtracting the common part. With the overlap region providing the common part, the composite temperature profile in outer variables is given by

$$T - T_\infty = T_{So} f_{2o}(\bar{y}, \varepsilon) + T_{Si}\left[(1 + f_{2i}(\bar{y}/\varepsilon, \varepsilon)) - C_{2i}(\bar{y}/\varepsilon)^b\right] \tag{8.4}$$

and the composite velocity profile in outer variables is given by

$$U = U_{So} f_{1o}(\bar{y}, \varepsilon) + U_{Si} \left[(1 + f_{1i}(\bar{y}/\varepsilon, \varepsilon)) - C_{1i} (\bar{y}/\varepsilon)^a \right] \quad . \tag{8.5}$$

Using these composite profile forms, we can further state about the integral thicknesses: The "enthalpy" thickness, defined as

$$\delta_T \equiv \int_0^\infty \frac{T - T_\infty}{T_w - T_\infty} dy \quad , \tag{8.6}$$

is not a promising candidate for an outer length scale, since $\delta_T/\delta \to 0$ as $Nu_\delta \to \infty$. Although, with $\delta_T/\delta \propto H_\delta^{*-1/9}$, we will not see much variation over a limited range of Grashof numbers (c.f. the experiments of Siebers et al. 1985 [58]). The momentum thickness, defined as

$$\delta_U \equiv \int_0^\infty \frac{U}{U_M} dy \quad , \tag{8.7}$$

is a possible outer lengthscale, since $\delta_U/\delta = const.$ as $Nu_\delta \to \infty$, if we require $U_M \propto U_{So}$. Matching their velocity profiles for the inner and outer layers and letting $\eta/\delta \to 0$, George and Capp [26] were able to show that $U_M/U_{So} = const.$ in this limit.

Chapter 9

Experimental Data

9.1 On the Value of Experimental Data

Discrepancies in the turbulent regime exist not only between the expressions derived in theoretical work (as shown in chapter 2 and in figures 3 and 4), but also among a variety of correlations given by experimentalists. Possible sources of these discrepancies which occur over relatively narrow ranges of Grashof number among various data sets or even within a single data set, are:

- The influences of property variations with temperature (i.e. those other than the essential density difference which gives rise to free convection flows). This implies a departure from constant fluid property description at moderate and high temperature differences. Clausing 1983 [13] was able to reduce the scatter in the heat transfer data with a variable property correlation. Carey and Mollendorf 1980 [9] showed that in common liquids the major temperature variation is in the absolute viscosity μ (c.f. figure 5). Property variation is most commonly accounted for by the reference temperature method. The property ratio method was introduced by Fujii et al. 1970 [20]), Clausing 1983 [13] suggested using an additional dimensionless group of the form T_w/T_∞. Siebers et al. 1985 [58] used a combination of both to modify their inner length scale (c.f.

table 2.1).

- The thermophysical properties which were used to reduce the dimensional experimental data to dimensionless variables. Even data given in recent books on heat transfer differ at high temperatures (e.g. for thermal conductivity of air). Interpolation errors contribute to discrepancies, too.

- Errors due to radiative heat transfer: The estimate of radiative heat transfer is quite often on the order of magnitude of convective heat transfer, in the experiment by Griffiths and Davis [28] it even exceeded the convective heat transfer. Warner 1966 [69] used a correction for radiation losses inferred from laminar theory and his relatively scattered laminar range heat flow data.

- Drafts or currents due to extraneous sources. Warner states: "...ambient turbulence caused by workday laboratory operations had a large effect upon the air in the test space." " ...to eliminate this, the apparatus was isolated (...) to minimize the effects of ambient room disturbances." "...test were conducted (...) while convective disturbances in the room were minimal."

- A stratified environment: Even small changes of the temperature gradient in the direction of the bodyforce can cause significant differences in the results. This is discussed in more detail in the next section.

- Three-dimensionality of the mean flow. Accurate two-dimensionality may not be obtained in flat plate experiments owing to side wall or edge effects. Fujii et al. [20] were familiar with this difficulty from own previous experiments and met it by using vertical cylinders, which introduces effects of curvature.

- Conductive heat transfer: Conduction terms are usually neglected in the main part of the boundary layer when drawing up an energy balance.

Commonly, only relatively small differences arise from the sources of errors listed above except for the thermal stratification of the environment. Experimental data

should in general be viewed critically, since experimenters will always encounter difficulties in performing the wanted experiment (Did they really measure what they thought they were measuring?). The value of dimensionless data can also be greatly reduced when given without detailed information on property evaluation.

Measuring turbulent natural convection flows has always been a difficult task: Hot wire anemometer velocity measurements lose their accuracy as the turbulence intensity $\sqrt{\overline{u^2}}/U_S$ gets higher. Especially in the outer part of the TNCBL we encounter low mean velocities and violent fluctuations. (Moving hot-wires can solve this problem, but were not utilized in any of the referenced experiments.) Laser Doppler Anemometers can also be adjusted to very low mean velocities by creating moving fringes in the measuring control volume, but suffer from refractive index variation within the field.

The state of the published experimental data is such that one could argue for (and against) a lot of things from it. With the data available for the turbulent flow regime, it can at least be shown to be consistent with the proposed theory.

9.2 The Influence of a Stratified Environment

Ambient stratification is often neglected and can easily be shown to lead to discrepancies between theoretical and experimental results. The importance of the ambient stratification can be understood from the energy equation (3.4), rearranged with help of continuity (3.1) and integrated from 0 to ∞ with respect to y:

$$\frac{d}{dx}\int_0^\infty [U(T-T_\infty)+\overline{ut}]\,dy = F_0 - \frac{dT_\infty}{dx}\int_0^\infty U\,dy \tag{9.1}$$

Clearly, positive ambient stratification acts like an "energy sink", since the volume flux per unit depth is positive for a heated wall. The energy flux (left-hand side) will be less than in an unstratified environment, the second term on the right-hand side

"consumes" buoyancy.

Let us take a look at an example: Hoogendoorn and Euser 1978 [32] reexamined the data of Cheesewright 1968 [11] and found up to a 60% difference between the local Nusselt number calculated from his mean temperature and velocity profiles and his relation for the Nusselt number, concluding that his velocity measurements were seriously in error. They noted that the heat balance across the boundary layer would fit the Nusselt number relation, if the higher velocities found by Mason and Seban [42] (with constant ambient temperature) were used. Cheesewright used the temperature gradient at the wall to calculate the Nusselt number, which is therefore representative of the total heat flux. Of course, the Nusselt number calculated from U and T profiles will be lower in the presence of an ambient temperature gradient $\Delta T_\infty/dx$. Cheesewright and Ierokiopitis 1982 [12] then remeasured the velocity profiles, this time accounting for ambient stratification (The energy equation given by them can be obtained from equation (3.4) through integration by parts and is equivalent to the formulation used in eqn. (9.1)). An estimate for the influence of temperature stratification at $y = \infty$ can be obtained from data supplied by Smith 1972 [59], who performed experiments on the same apparatus at "very stable laboratory conditions" (according to Cheesewright). Smith reported a vertical ambient temperature gradient of approximately 1.1K/m and thus, the second term on the right-hand side of equation (9.1), $\frac{dT_\infty}{dx}\int_0^\infty U dy$, amounts to $15\ldots23\%$ of the wall heat flux F_0 for Grashof numbers ranging from $2.82\text{x}10^{10}$ to $6.81\text{x}10^{10}$! Therefore, the hot-wire data of Cheesewright [11] (and in general) may still be of doubtful accuracy for the high levels of turbulence towards the outer edge, but should be fairly accurate in higher velocity regions. Hoogendoorn and Euser would have found much less discrepancy, had they allowed for thermal stratification (which they did in their own experiment for a variation of ambient temperature of "only" 2K over 1.8m !). Cheesewright 1968 [11] did not provide any information on stratification while the variation in the experiment by Cheesewright and Ierokiopitis 1982 [12] was 8K over a height of 3.5m. Note

that equation (9.1) neglects the entrainment velocity at infinity, V_∞ ($V_\infty \approx 0.03\ U_M$ calculated from Smith's data).

The importance of local conditions is evident from the above, i.e. the necessity of including ambient stratification to satisfy the governing equations. Even when thermal stratification is accounted for, large ambient temperature gradients will probably cause the flow to be quite different from its unstratified counterpart (e.g. turbulent buoyant plume experiments by Beuther [6]).

9.3 Acquisition of Experimental Data

Data utilized in this chapter was acquired from enlarged plots, taken from publications of experimental studies using a digitizer setup. Reliability of this setup and reproducabilty of the digitized data were tested (and found to be satisfactory) by measuring several graphs by hand and by digitizing single graphs up to five times and comparing the results (single sets and averages). The combined accuracy of the digitizing pen and pad (minimum stepsize) and the procedure of reading data points from graphs was, of course, limited. Therefore, possible translation errors (and also the state of the experimental data itself. c.f. section 9.1) will allow only qualitativestatements regarding the validity of a theory. A prerequisite to meaningful comparisons with dimensionless data is the knowledge of the local conditions (T_w, T_∞, F_0, x, etc.) at each point as well as the temperature physical properties were evaluated at. For some data sets, missing information had to be acquired by iteration until the data set was consistent in itself.

The experimental data were then transformed to a nondimensional form using the proposed scaling functions.

9.4 Comparing the Proposed Theory to Experimental Data

9.4.1 Explaining Plots of Experimental Data with the New Theory

Before taking on the enormous task to reinvestigate experimental data, it was somewhat reassuring to be able to explain virtually every plot published in literature. To name a few:

Tsuji and Nagano's 1988 [64] "outer" variable plots for mean velocity and temperature are seen not to work very well on the outside of the boundary layer but collapse the data perfectly over the inner layer. This was to be expected, since they used the inner lengthscale η introduced here.

The same applies for the mean velocity plot of Miyamoto et al. 1982 [43]. Their plots of Reynolds' stress $\overline{uv}$ and turbulent heat flux $\overline{vt}$ in mixed outer and inner variables do not collapse either. They chose scales ($R_S = {U_S}^2$, $F_S = U_S T_S$) which were shown to be valid only in the limit as $Nu_\delta \to 0$ by this theory. Both plots show noncongruence clearly due to downstream development, which was not accounted for by their only asymptotically valid scaling functions.

In a subsequent publication, Tsuji and Nagano 1989 [65] successfully used the momentum thickness $\delta_U = \int_0^\infty U/U_M dy$ to collapse velocity data in the outer layer. The thermal boundary layer thickness $\delta_T = \int_0^\infty \Delta T/\Delta T_w dy$ achieves good collapse of temperature profiles over a range of $Gr_x = 1.55\text{x}10^{10}$ to $1.80\text{x}10^{11}$ for reasons given in section 8.2.

9.4.2 Mean Temperature Profiles

Mean temperature profiles were plotted in the inner variables found from the theory introduced here (and in inner variables of George and Capp [26] where noted).

Plotting near-wall data of Smith 1972 [59] we cannot see much difference on a linear plot (c.f. figures 8 and 10), both the GC79-scales and the new scales give reasonable collapse. When stretching out the near wall region by using a semi-logarithmic plot, the new scaling laws are seen to collapse the data better for a region up to $y^+ = 2...3$ (in new variables. Multiply by $4.1...4.5$ to obtain y^+ in GC79-variables), as seen in figures 9 and 11.

Data from different experiments, i.e. Tsuji and Nagano 1988 [64], Miyamoto et al. 1982 [43], Smith 1972 [59] and Cheesewright 1968 [11], which were plotted in inner variables are compared in figures 12 and 13, where the excellent collapse over the inner part of the boundary layer becomes apparent. In figure 13 the buoyant sublayer power law region can clearly be detected.

9.4.3 Mean Velocity Profiles

Mean velocity data of Cheesewright [11] is plotted in figures 14-17. The flow was suspected to be not fully turbulent at the lowest H-number plotted (also noted by other researchers). The new scales pull the data closer together to a point further away from the wall.

While the collapse obtained with the velocity data of Cheesewright was not very satisfactory (due to high ambient temperature stratification?), the effect of the new scaling laws explains itself fully with the plots of near-wall velocity data from Smith [59] in figures 18-21. Very good collapse over the inner part of the boundary layer is obtained (Note that the plots are stretched out laterally, the boundary layer ends at approximately $y^+ = 40$).

Another plot showing excellent collapse of the mean velocity data of Tsuji and Nagano 1989 [65] in outer variables is presented in figure 18. Here the asymptotically valid outer velocity scale $U_M \propto U_{S_o}$ and the momentum thickness δ_U were utilized to nondimensionalize the data.

Concluding this section, it can be said that the need for tabulated experimental

data became more and more obvious the more this project advanced. Exact dimensional data and more downstream profiles than available in any published experiment are necessary to determine the downstream development of the proposed scaling laws.

Chapter 10

Summary and Conclusions

10.1 Thesis Summary

A new theory has been proposed for the turbulent natural convection boundary layer next to a heated, vertical surface. The scaling laws have been derived by insisting that properly scaled profiles reduce to similarity solutions of the reduced inner and outer equations in the limit of infinite local Nusselt or H-number. The outer scaling functions could only be determined in terms of the inner by matching the inner and outer profiles at finite Nusselt numbers.

It was possible to establish limits on the similarity solution and its asymptotic behavior by considering how the turbulence energy dissipation varies with turbulence Reynolds number. The earlier local similarity theory of George and Capp was recovered as the infinite H-number (or Nusselt number) limit. For finite values of the turbulence Reynolds number, the equations — and thus the local inner and outer scales — retain the x-dependence characteristic of laboratory experiments.

It is concluded: The proposed scaling laws for the inner and outer part of the turbulent natural convection boundary layer should collapse any profiles within the fully turbulent regime. Researchers are encouraged to re-examine their TNCBL data under the aspect of this new theory.

10.2 Suggestions for Future Work

With the introduction of this new theory for the natural convection turbulent boundary layer, an immense scope could open up for future work. Possibilities for experimental, numerical and further analytical investigation along the lines of the proposed similarity analysis exist.

First of all, the theory should be extended to higher order moments (Reynolds' stress equation, turbulence kinetic energy, mean square temperature fluctuations, third order moments, etc.). The consistency with existing experimental data should be explored to its full extent, which can only be done with tabulated data provided by experimentalists. Its implications on the statistical description of turbulence, two-point equations and related buoyant or boundary layer flows await investigation.

Judging from the state of the published experimental results, there definitely is a need for data on the downstream development of characteristical quantities (scaling laws) up to a high range of Grashof numbers without having to account for variable property effects. This calls for larger experimental setups.

The transformed governing equations could be solved numerically (closure model?) to learn more about the validity of this theory. Since they contain an implicit x-dependence, the proposed scaling laws may be helpful in turbulence modeling, where they could provide more accurate wall functions.

The Figures

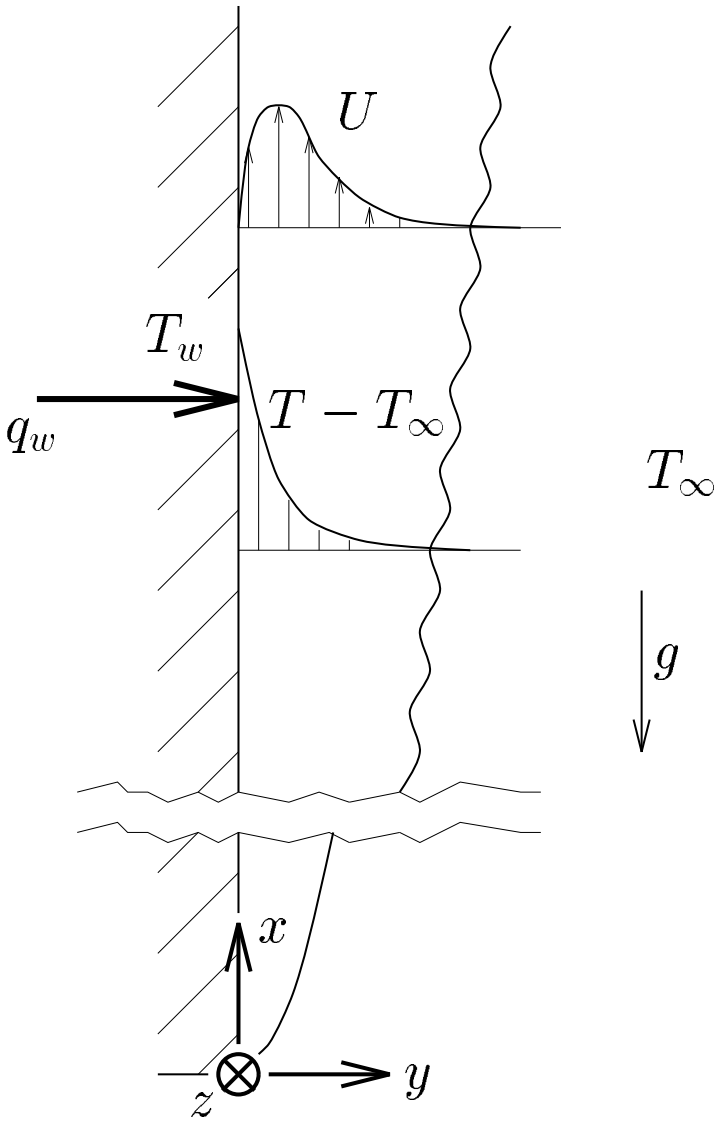

Figure 1: Schematic of the turbulent natural convection boundary layer next to heated vertical surfaces.

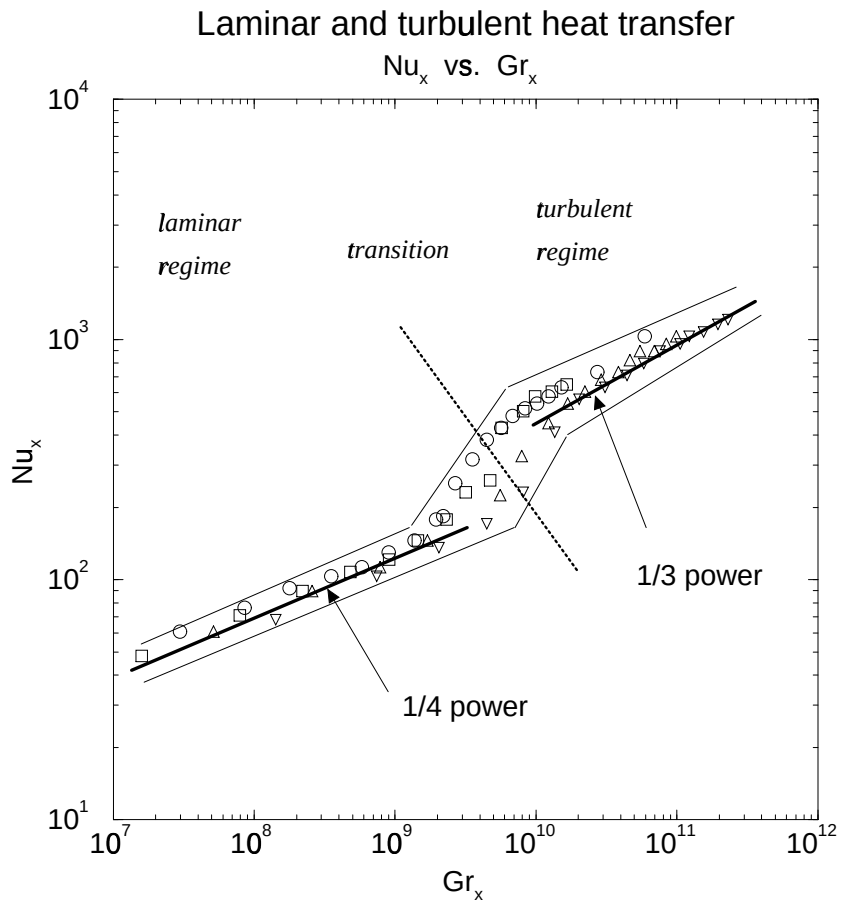

Figure 2: Regimes of laminar, transitional and turbulent heat transfer (includes recompiled experimental data for water ($Pr = 4 \ldots 8$ from Fujii et al. [20]).

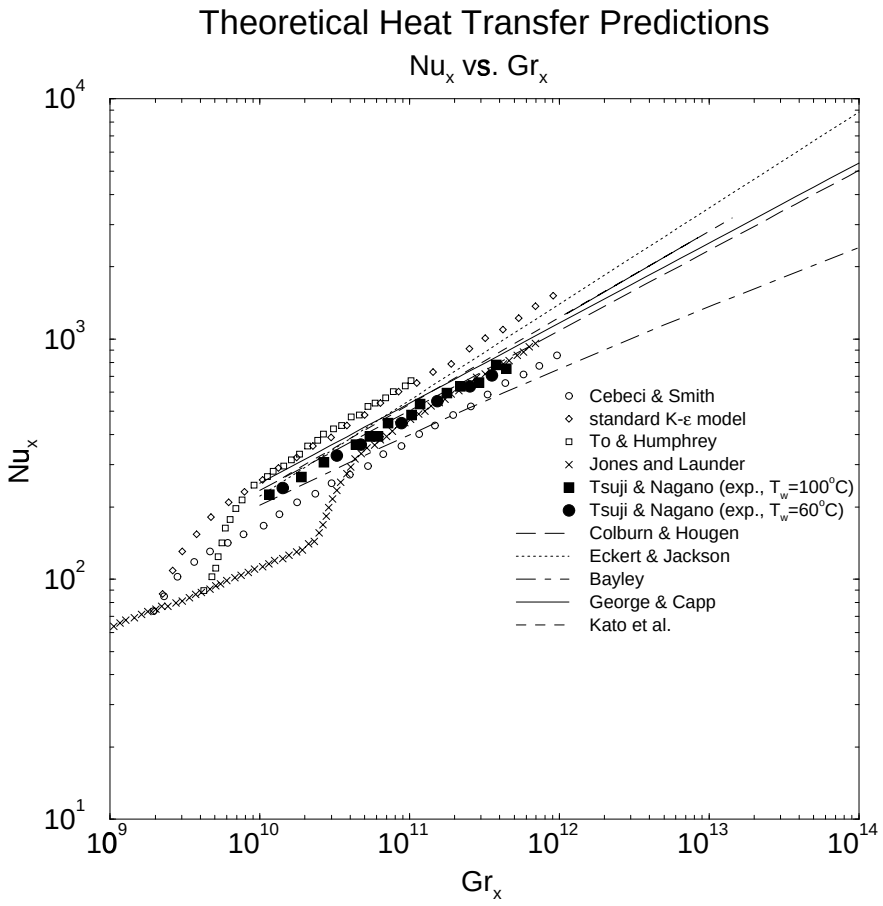

Figure 3: Comparison of theoretical and numerical local heat transfer predictions, Nu_x vs. Gr_x, for air ($Pr = 0.72$), including experimental heat transfer data from Tsuji and Nagano 1988 [64] for two different wall temperatures in the turbulent regime.

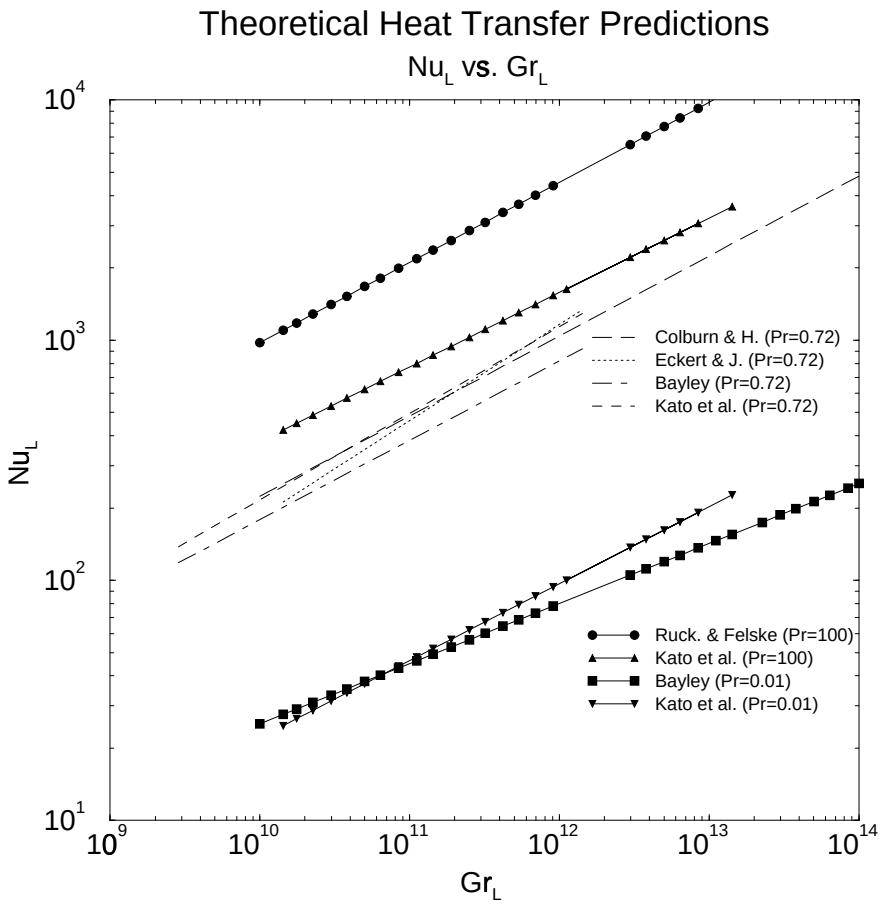

Figure 4: Comparison of theoretical average heat transfer predictions, Nu_L vs. Gr_L. Plotted are graphs for $Pr = 0.72$, $Pr = 100$ and $Pr = 0.01$.

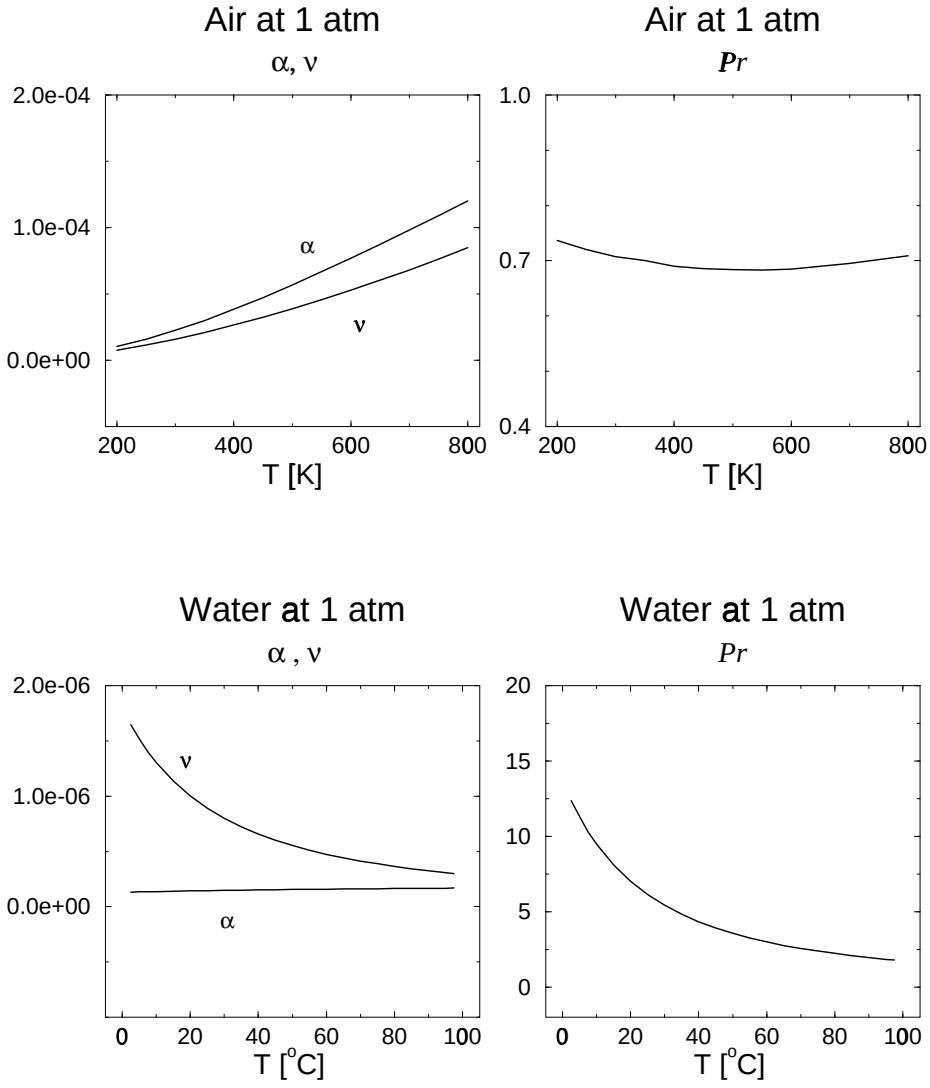

Figure 5: Temperature dependence of fluid properties in air (taken from tables in ref. [33]) and water (calculated from formulas for physical properties given in ref. [20]) under atmospheric conditions.

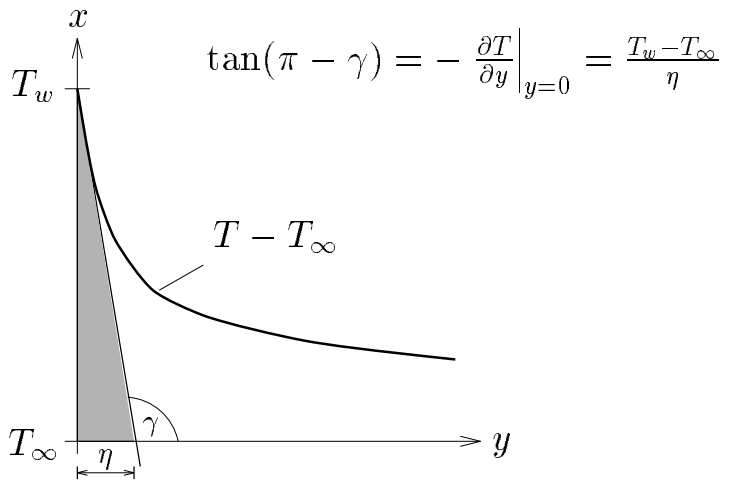

Figure 6: Graphical explanation of the inner lengthscale η.

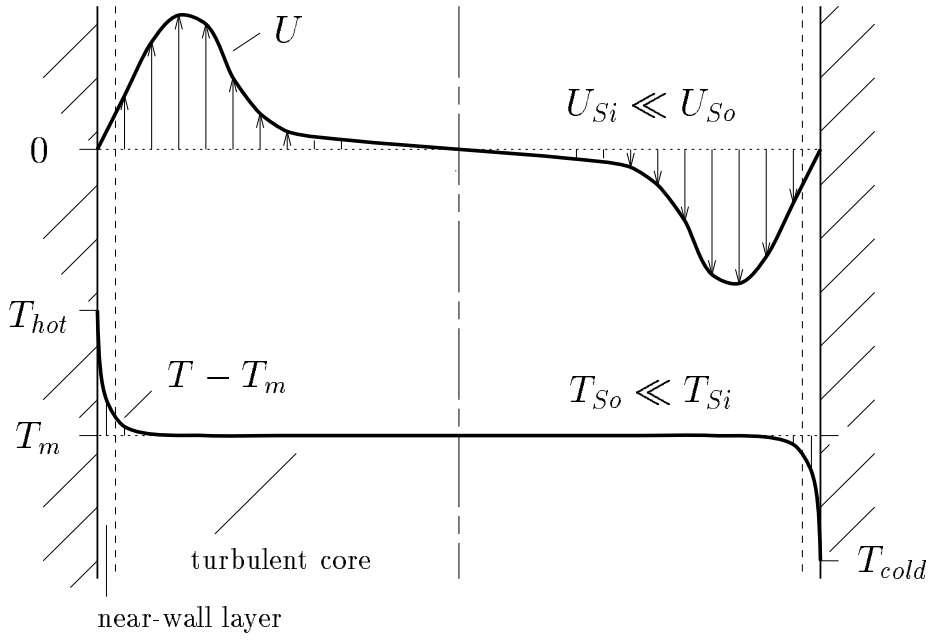

Figure 7: Turbulent natural convection in a vertical channel.

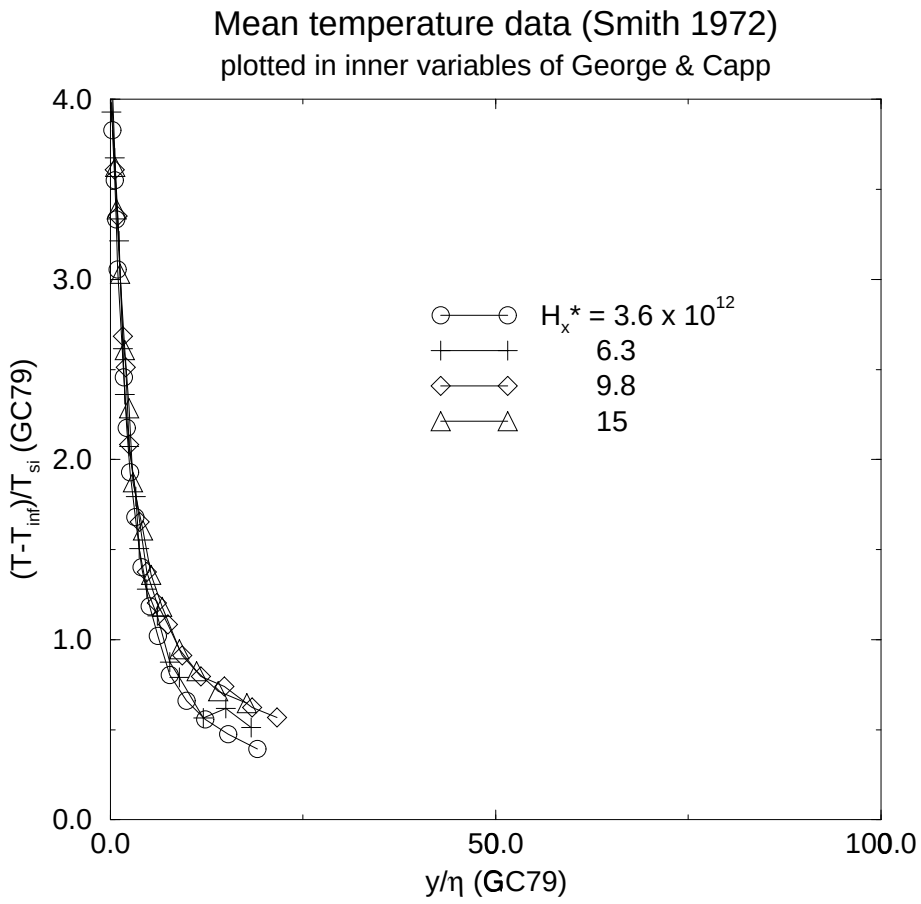

Figure 8: Mean temperature data of Smith 1972 [59] plotted in inner variables of George and Capp 1979 [26].

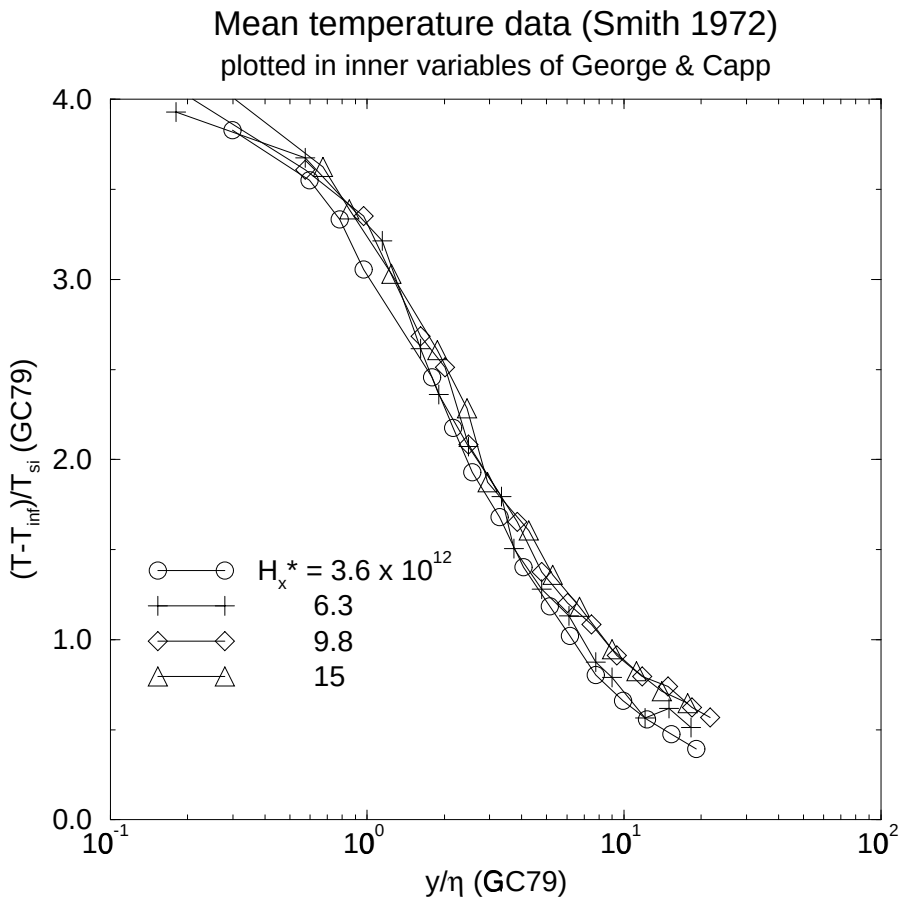

Figure 9: Mean temperature data of Smith 1972 [59] plotted in inner variables of George and Capp 1979 [26] on a log-linear plot.

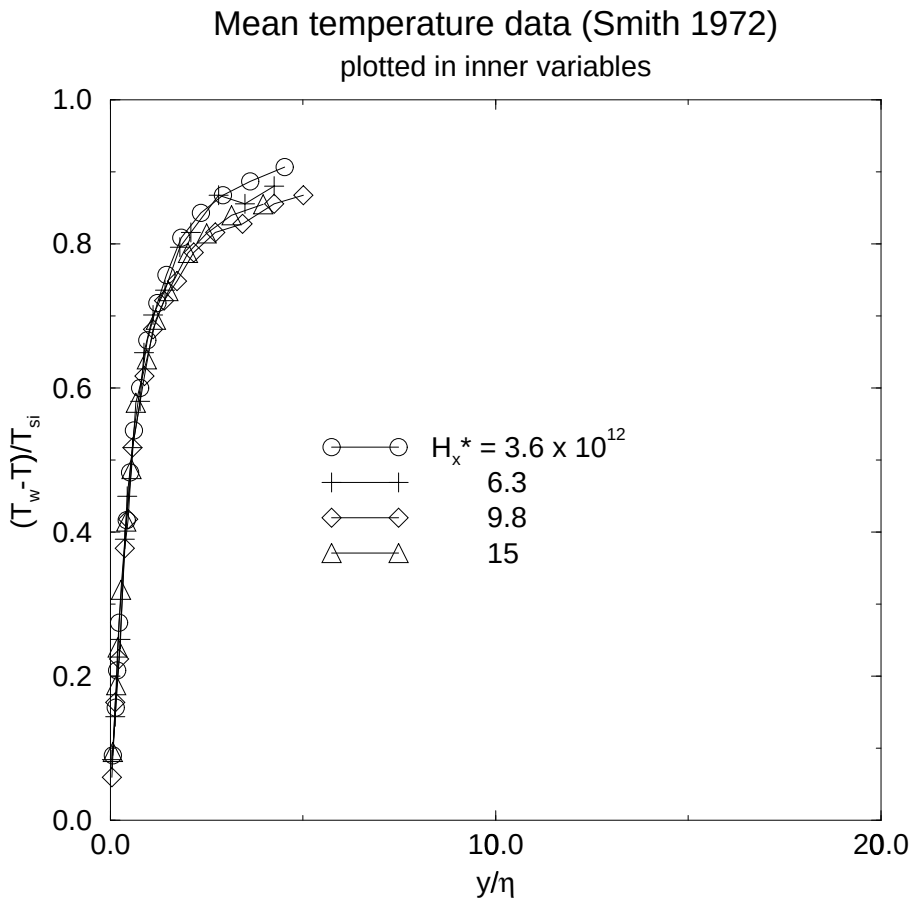

Figure 10: Mean temperature data of Smith 1972 [59] plotted in inner variables from new theory.

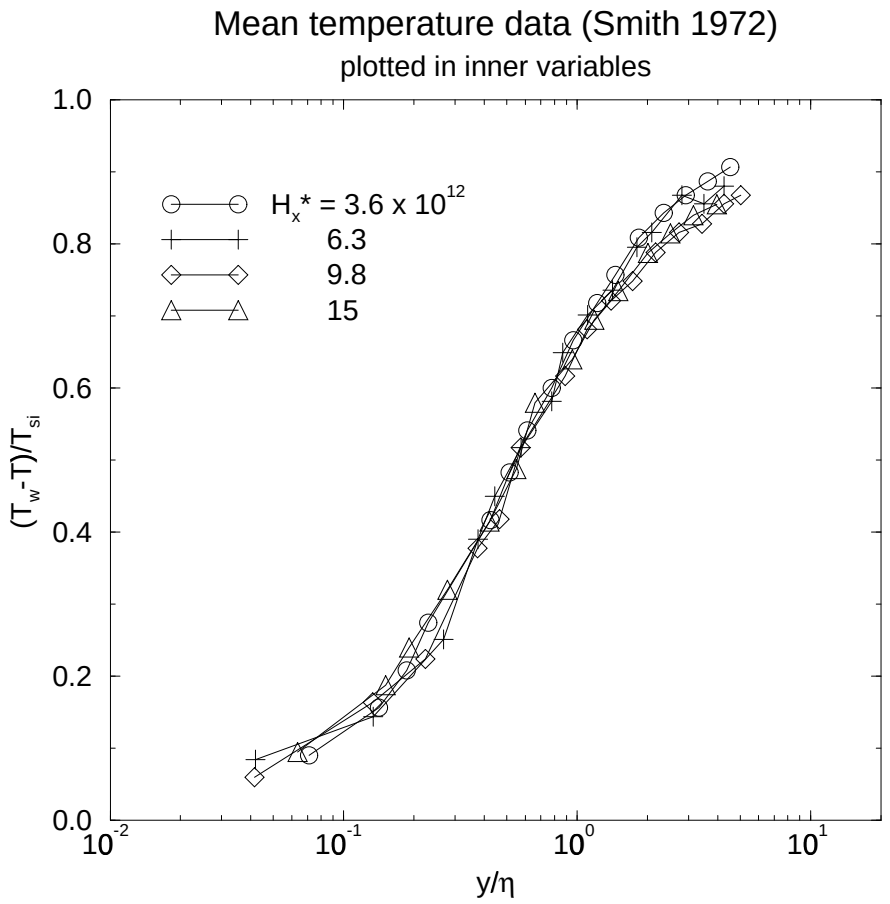

Figure 11: Mean temperature data of Smith 1972 [59] plotted in inner variables from new theory on a log-linear plot.

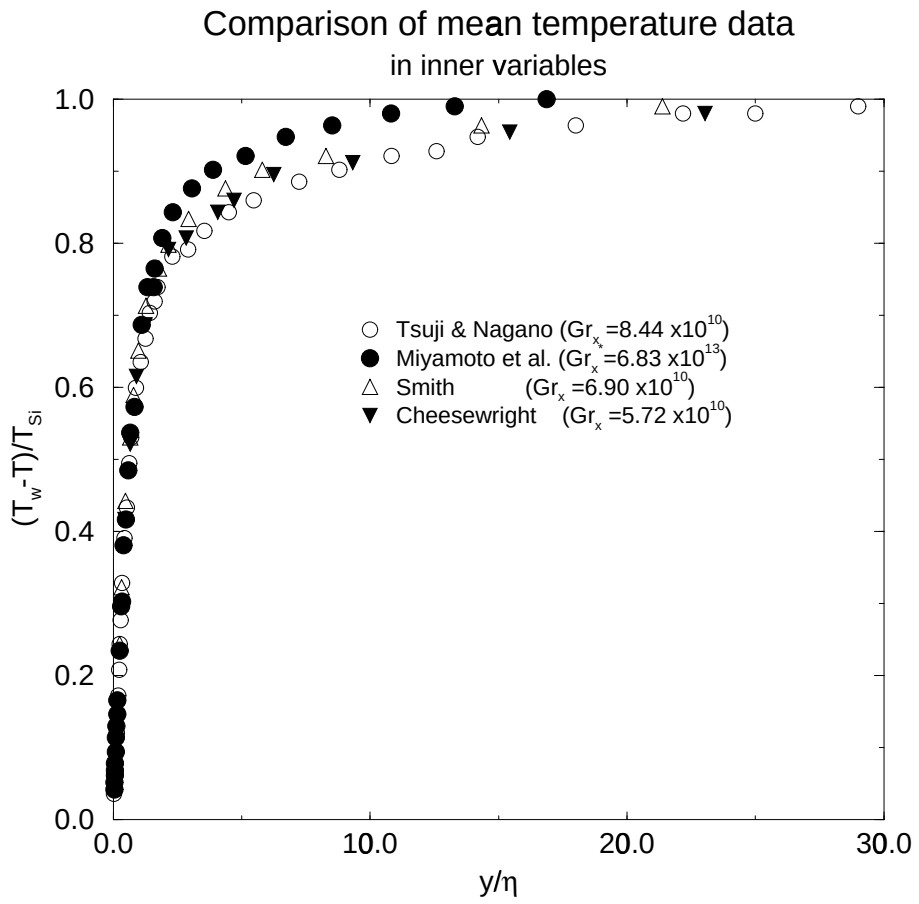

Figure 12: Comparison of mean temperature profiles in inner variables on a linear-linear plot (replotted from Tsuji and Nagano 1988 [64]).

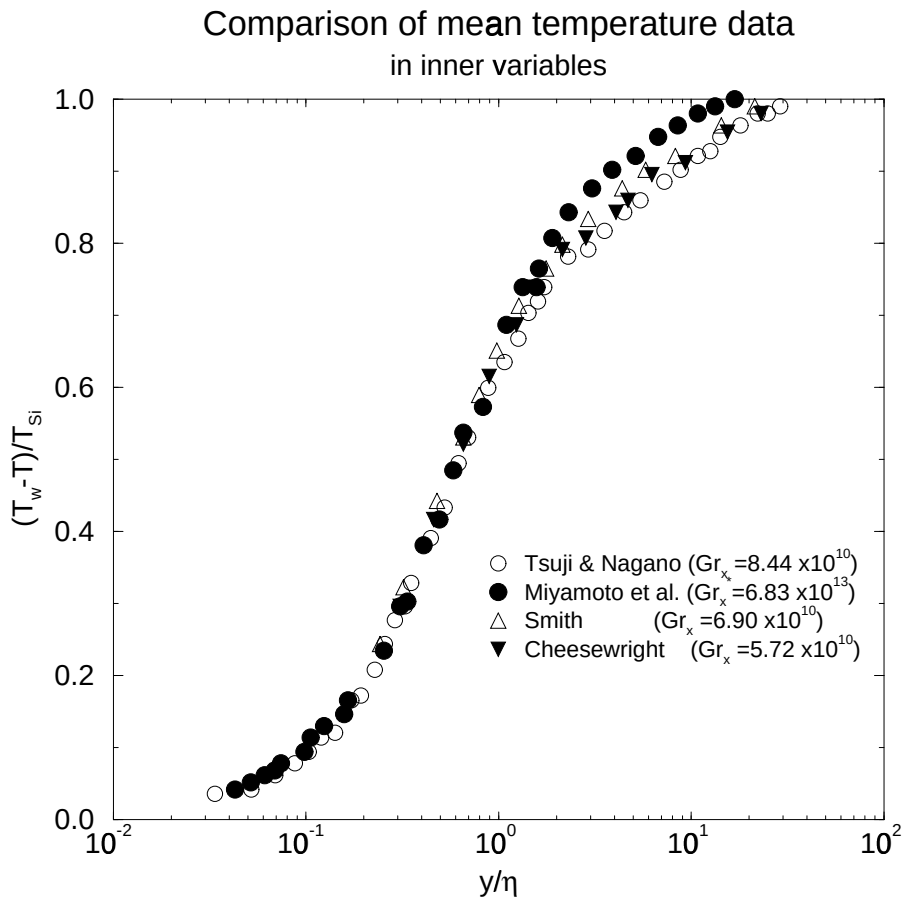

Figure 13: Comparison of mean temperature profiles in inner variables on a log-linear plot (replotted from Tsuji and Nagano 1988 [64]).

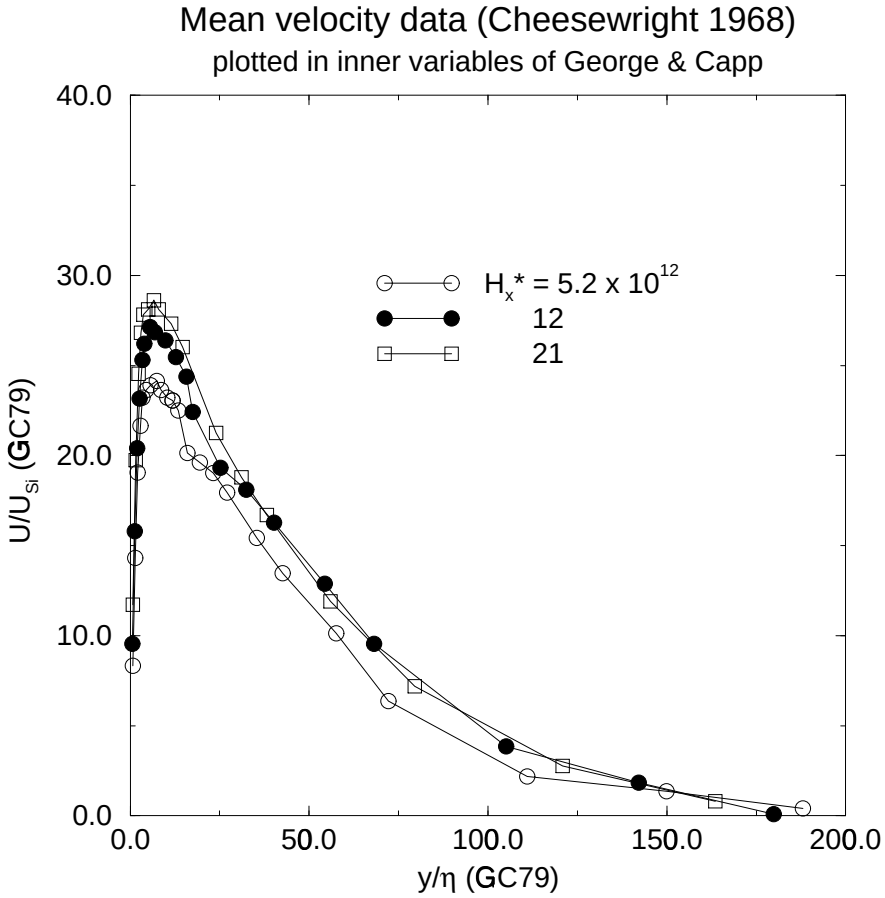

Figure 14: Mean velocity data of Cheesewright 1968 [11] plotted in inner variables of George and Capp 1979 [26].

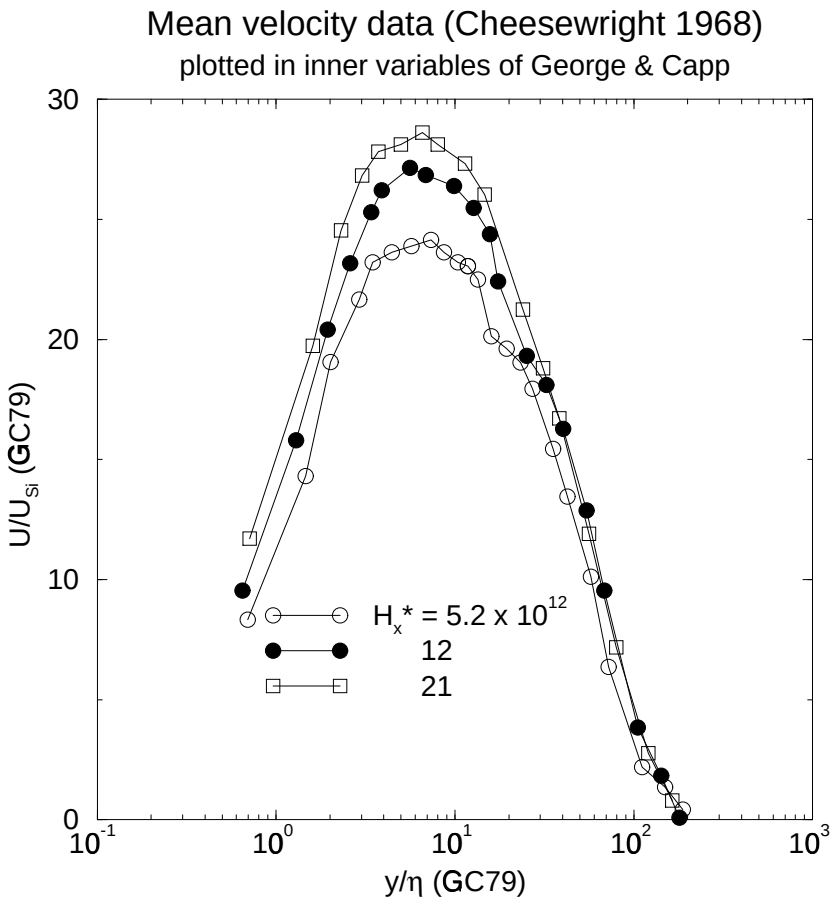

Figure 15: Mean velocity data of Cheesewright 1968 [11] plotted in inner variables of George and Capp 1979 [26] on a log-linear plot.

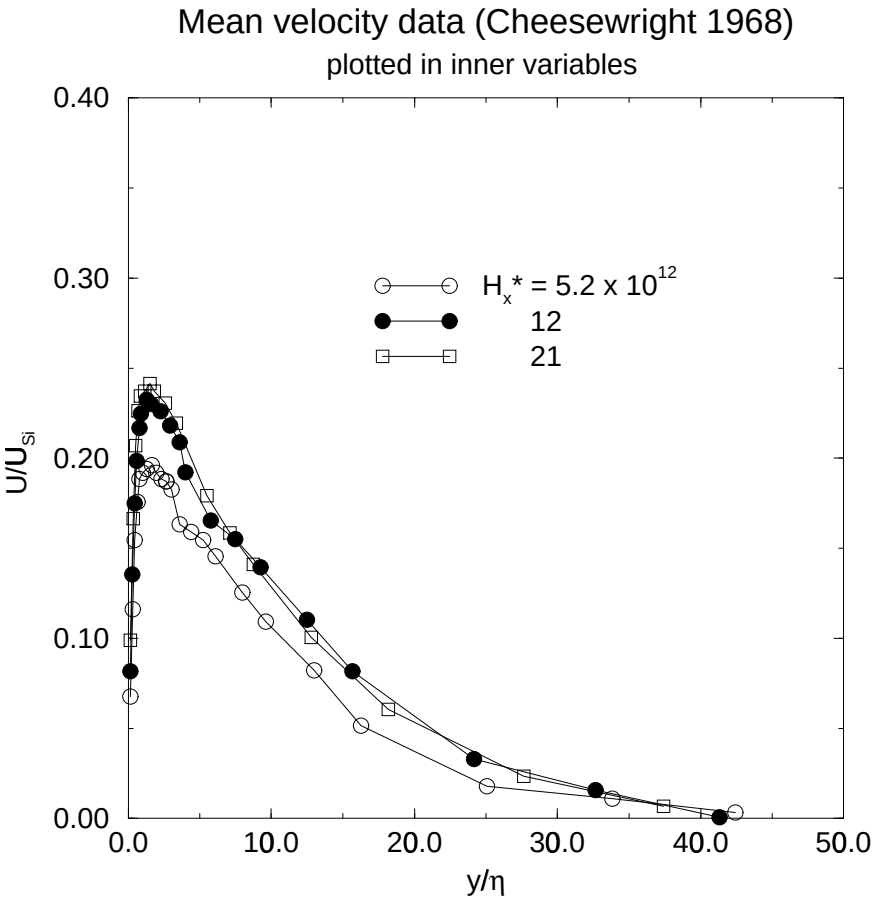

Figure 16: Mean velocity data of Cheesewright 1968 [11] plotted in inner variables from new theory.

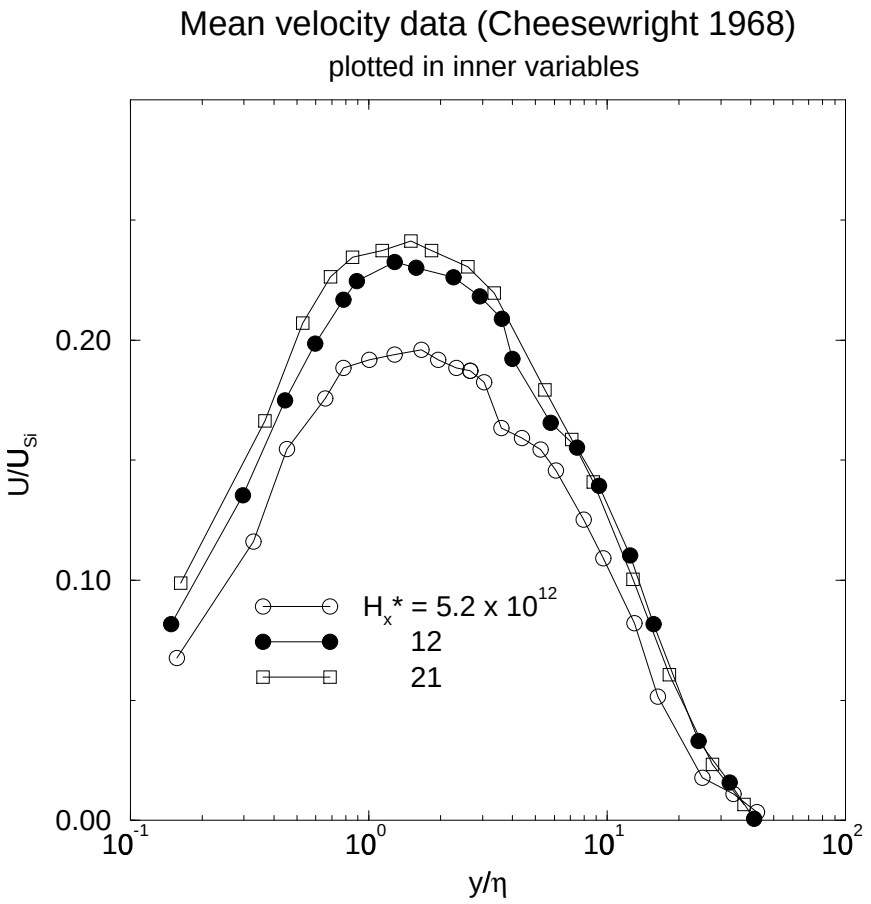

Figure 17: Mean velocity data of Cheesewright 1968 [11] plotted in inner variables from new theory on a log-linear plot.

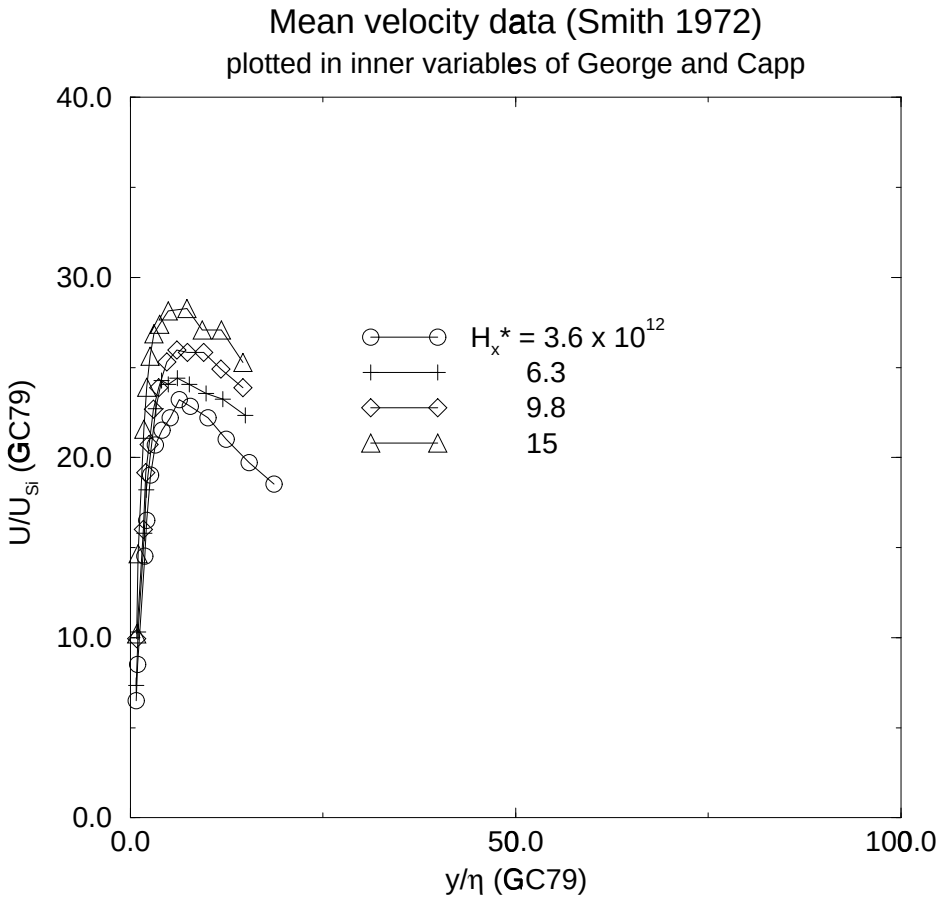

Figure 18: Mean velocity data of Smith 1972 plotted in inner variables of George and Capp 1979 [26].

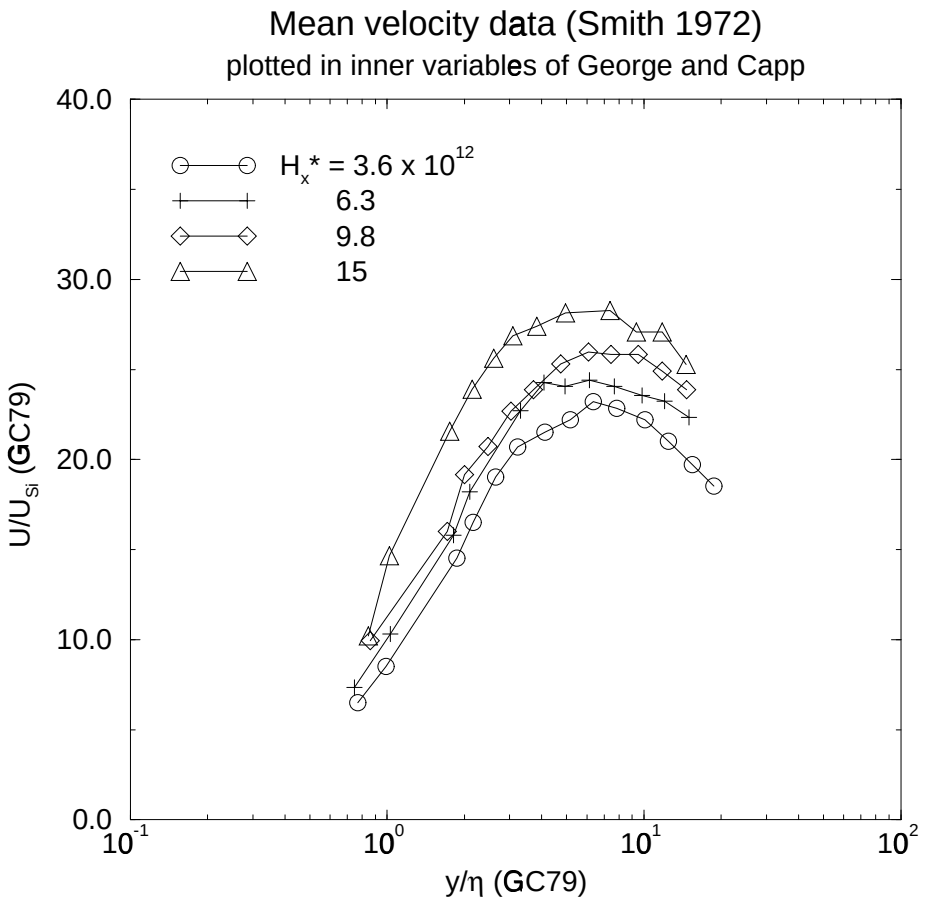

Figure 19: Mean velocity data of Smith 1972 plotted in inner variables of George and Capp 1979 [26] on a log-linear plot.

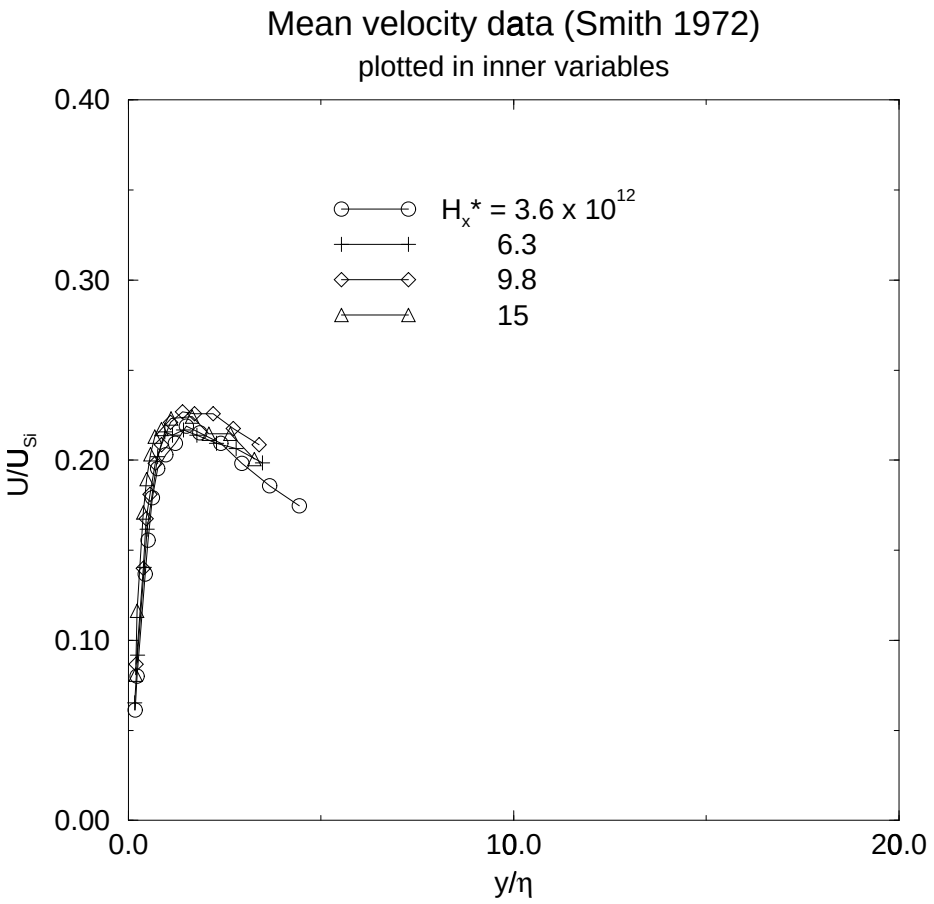

Figure 20: Mean velocity data of Smith 1972 [59] plotted in inner variables from new theory.

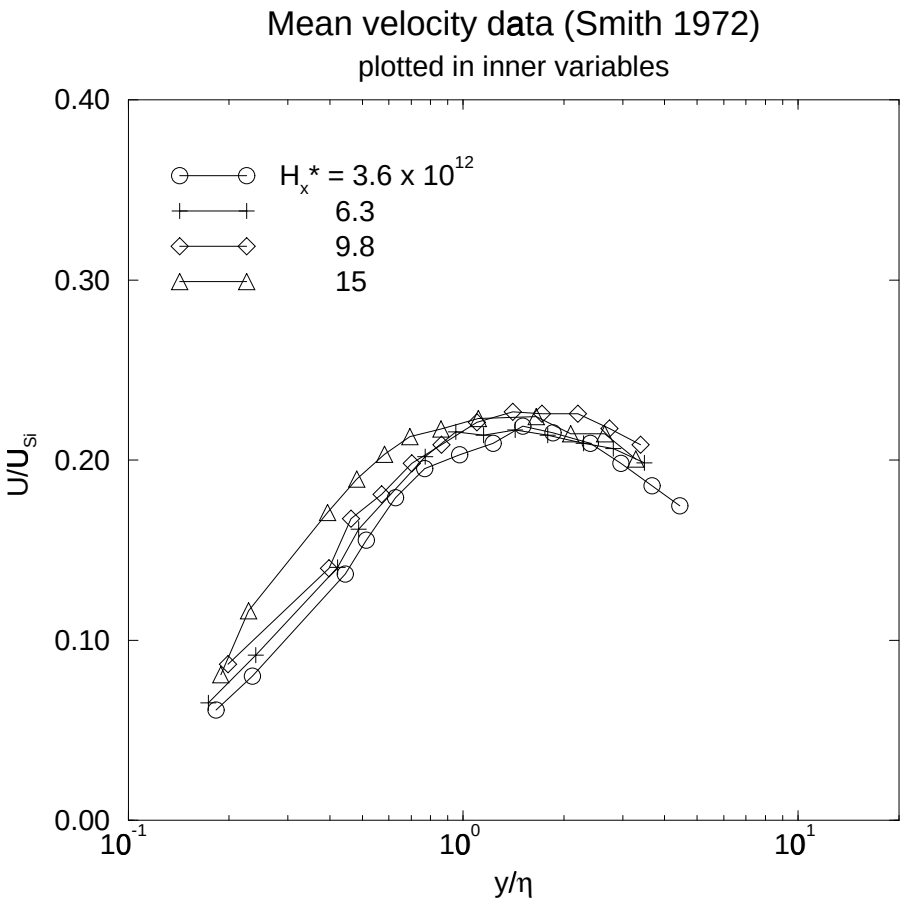

Figure 21: Mean velocity data of Smith 1972 [59] plotted in inner variables from new theory on a log-linear plot.

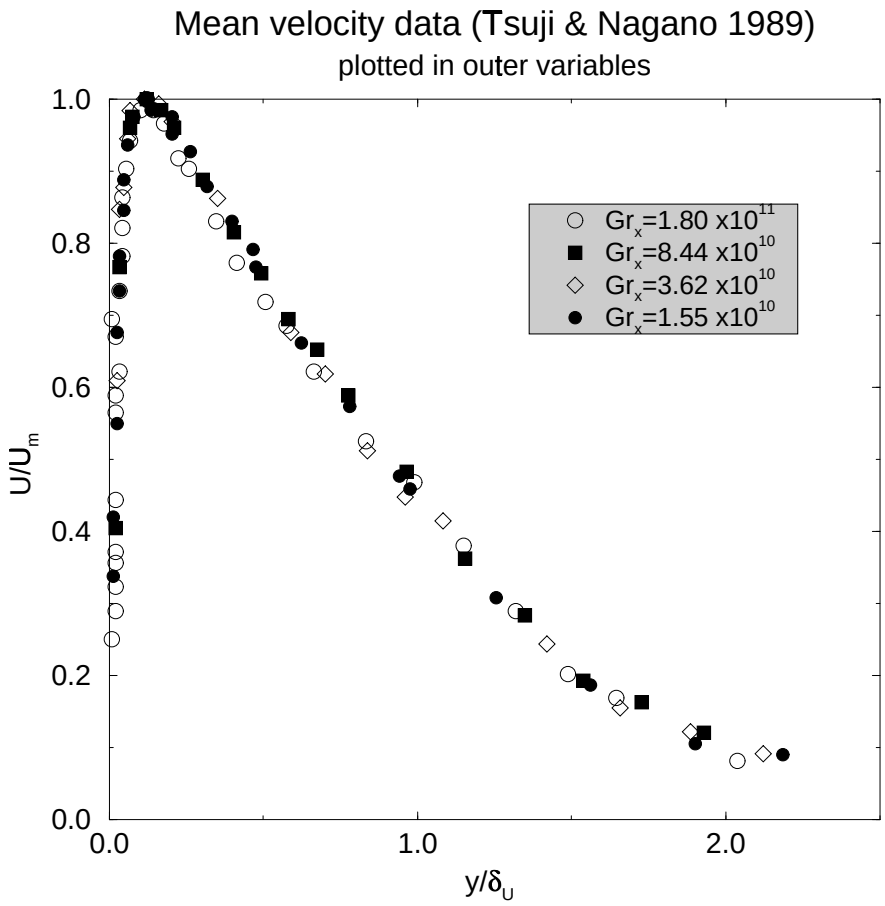

Figure 22: Mean velocity data from Tsuji and Nagano 1989 [65] plotted in (asymptotic) outer variables from new theory.

Appendix A

Derivation of the Governing Equations

A brief derivation of the differential equations governing the fully developed turbulent natural convection boundary layer is given in this section. A more general approach to the physical phenomenon natural convection is considered and the approximations and simplifications necessary in order to obtain this set of equations are examined.

We know that the density of gases and liquids depends on temperature, $\rho = \rho(T)$, generally decreasing with increasing temperature due to fluid expansion ($\partial\rho/\partial T < 0$). The necessary condition for equilibrium of a fluid is well known to be $\rho\mathbf{f} = \nabla p$. Taking the curl of both sides leads to

$$\nabla \times (\rho\mathbf{f}) = \nabla\rho \times \mathbf{f} + \rho\nabla \times \mathbf{f} = 0 \quad , \tag{A.1}$$

where the body force per unit mass $\mathbf{f}$ has to represent a conservative field (i.e. it has a potential ψ and can be written as $\mathbf{f} = -\nabla\psi$) and the gradient of the density $\nabla\rho$ has to be parallel to the vector of body forces $\mathbf{f}$ (or zero) to satisfy this equation. For a semi-infinite vertical surface with a surface temperature T_w immersed in a fluid of

infinite extent and temperature T_∞ (with $T_w \neq T_\infty$) the fluid adjacent to the wall is heated (or cooled) through conduction heat transfer. The temperature gradient and the density gradient at the wall are now perpendicular to the surface. With the bodyforce per unit mass being the acceleration of gravity, clearly, the first condition for mechanical equilibrium in equation (A.1) is violated and there has to be fluid movement, i.e. the *Natural Convection Boundary Layer Flow* develops! (Note that the first condition is always satisfied for the case of a heated (or cooled) horizontal plate, therefore thermal stability considerations come into play. Note also that a stratified temperature at infinite distance from the plate ($T_\infty = T_\infty(x)$) has not been ruled out.)

A.1 Continuity, Momentum and Heat Diffusion

A basic set of equations governing the motion of a fluid (c.f. e.g. [1], [4], [60]) is given by the continuity equation

$$\frac{D\rho}{Dt} + \rho \frac{\partial u_i}{\partial x_i} = 0 \quad , \tag{A.2}$$

Cauchy's equation of motion

$$\rho \frac{Du_i}{Dt} = \rho f_i + \frac{\partial}{\partial x_j} \tau_{ji} \quad , \tag{A.3}$$

and a form of the energy equation

$$\rho \frac{De}{Dt} = \tau_{ji} \frac{\partial u_i}{\partial x_j} - \frac{\partial q_i}{\partial x_i} \quad , \tag{A.4}$$

representing continuum mechanics' analogon of the first law of thermodynamics. Decomposing the stress tensor τ_{ij} into hydrostatic and deviatoric parts $-p\delta_{ij}$ and P_{ij} and with equation (A.2) we can rewrite the energy equation as

$$\rho \frac{De}{Dt} = \frac{p}{\rho} \frac{D\rho}{Dt} + \Phi - \frac{\partial q_i}{\partial x_i} \quad , \tag{A.5}$$

where the dissipation is defined as

$$\Phi = \frac{\partial u_i}{\partial x_j} P_{ij} \quad . \tag{A.6}$$

Employing a linear relation between deviatoric stress and rate of strain (e.g. **Newtonian Fluid**, certain non-Newtonian fluids show linear behaviour, too) and between heat flux and change in temperature (**Fourier's law**) the stress tensor within Stokes' hypothesis becomes

$$\tau_{ij} = -p\delta_{ij} + P_{ij} = -p\delta_{ij} + \mu \left(-\frac{2}{3}\frac{\partial u_k}{\partial x_k}\delta_{ij} + \left(\frac{\partial u_i}{\partial x_j} + \frac{\partial u_j}{\partial x_i} \right) \right) \quad , \tag{A.7}$$

and the heat flux vector becomes

$$q_i = -k\frac{\partial T}{\partial x_i} \quad . \tag{A.8}$$

Equations (A.2), (A.3) and (A.5), together with the definitions of the stress tensor and the heat flux vector and the two equations of state $p = p(\rho, T)$ and $e = e(\rho, T)$ provide a closed basic set of equations to solve for unknown quantities in a laminar flowfield (u_i, ρ, p, e, T).

We further assume that there are **no sources of heat within the fluid** (which could arise e.g. from chemical reactions) and **neglect heating through viscous dissipation** Φ, since the expected velocities are small and temperature differences are not (c.f. Gebhardt [21]). Note that the loss of momentum through viscous dissipation plays an important role in turbulent flow and cannot be ignored in the equations of motion!

We will now turn to the question whether the natural convection boundary layer flow can be treated as being incompressible, meaning that the continuity equation (A.2) can be reduced to the statement that the velocity field is solenoidal $(\nabla \cdot \vec{u} = 0)$. We choose the density ρ and the entropy per unit mass s as the two

independent parameters of state and write for the rate of change of pressure experienced by a material element

$$\frac{Dp}{Dt} = \left(\frac{\partial p}{\partial \rho}\right)_s \frac{D\rho}{Dt} + \left(\frac{\partial p}{\partial s}\right)_\rho \frac{Ds}{Dt} \quad . \tag{A.9}$$

With the definition of the speed of sound

$$a^2 \equiv \left(\frac{\partial p}{\partial \rho}\right)_s \tag{A.10}$$

the change in density of a material element is

$$\frac{D\rho}{Dt} = \frac{1}{a^2}\frac{Dp}{Dt} - \frac{1}{a^2}\left(\frac{\partial p}{\partial s}\right)_\rho \frac{Ds}{Dt} \quad . \tag{A.11}$$

The fluid behaves as if it were incompressible, if the righthand side vanishes, so that $D\rho/Dt = 0$. The second term on the righthand side can be decomposed into entropy transfer and irreversible entropy production. The variation of density due to internal dissipative heating is small (c.f. Gebhardt [21]), but for very large temperature differences $(T_w - T_\infty)$, the entropy transfer part may not be negligible. In this case, the boundary layer flow cannot be treated as incompressible. In estimating Dp/Dt of the first term on the righthand side we lose little generality by assuming the flow to be isentropic. Rewriting it with the aid of equation (A.3) without the viscous terms (equivalent to Euler's equation) and applying a simple order of magnitude analysis (c.f. Batchelor [4], Spurk [60]) leads to the following three conditions for the vanishing of the first term in equation (A.11)

$$M^2 = \frac{{U_S}^2}{a^2} \ll 1 \quad , \tag{A.12}$$

$$\frac{gL}{a^2} \ll 1 \tag{A.13}$$

and

$$\frac{n^2 L^2}{a^2} \ll 1 \quad , \tag{A.14}$$

where M is the Mach number, U_S is a characteristic velocity, n is a measure of the dominant frequency, L is a characteristic length and g is the acceleration of gravity. All three conditions are satisfied in the case of the natural convection boundary layer flow and the changes in density of a material element due to pressure variations can be neglected. The fluid will thus behave as if it were **incompressible**, provided the entropy transfer is small. Condition (A.13) is not satisfied for large lengthscales $L \sim a^2/g$ as they might occur in the atmosphere, e.g. natural convection flow phenomena exceeding a few hundred meters in depth cannot be treated incompressible.

With the above simplifications, the continuity equation and the Navier-Stokes equations (= Cauchy's equation (A.3) with constitutive law (A.7)) can be written as

$$\frac{\partial u_i}{\partial x_i} = 0 \tag{A.15}$$

and

$$\rho \frac{Du_i}{Dt} = \rho f_i - \frac{\partial p}{\partial x_i} + \frac{\partial}{\partial x_j}\left(\mu \frac{\partial u_i}{\partial x_j}\right) \quad . \tag{A.16}$$

In the case of external heating , the approximation $D\rho/Dt = 0$ is still good for liquids and with $de = c\ dT$ the energy equation (A.5) reduces to

$$\rho c \frac{DT}{Dt} = \frac{\partial}{\partial x_j}\left(k \frac{\partial T}{\partial x_j}\right) \quad . \tag{A.17}$$

This is not always true for gases in the presence of external heating and the energy equation has to be treated differently. Differentiating the thermal equation of state $\rho = \rho(p, T)$ for an ideal gas leads to

$$\frac{D\rho}{Dt} = -\frac{p}{\mathcal{R}T^2}\frac{DT}{Dt} \quad , \tag{A.18}$$

since we neglect density changes due to pressure changes and therefore have an isobaric process. With $de = c_v\ dT$ and $c_p = \mathcal{R} + c_v$, the energy equation (A.5) then assumes the form

$$\rho c_p \frac{DT}{Dt} = \frac{\partial}{\partial x_j}\left(k\frac{\partial T}{\partial x_j}\right) \quad . \tag{A.19}$$

The latter will be used from now on, valid for both gases and liquids. Equations (A.15), (A.16) and (A.19) are a reduced set describing both laminar and turbulent flow, since no specification has been made so far.

We are from now on considering turbulent flow and decompose the instantaneous flow quantities, denoted by a tilde, into a mean and a fluctuating part:

$$\tilde{u}_i = U_i + u_i = \left\{ \begin{array}{c} U+u \\ V+v \\ W+w \end{array} \right\} \tag{A.20}$$

$$\tilde{T} = T + t \tag{A.21}$$

$$\tilde{p} = P + p = P_\infty + P_* + p \tag{A.22}$$

$$\tilde{\rho} = \bar{\rho} + \rho \tag{A.23}$$

P_* is the local static pressure minus the hydrostatic pressure. The hydrostatic pressure distribution P_∞ will appear implicitly in the buoyancy term, as shown below. Assuming the flow to be **stationary in the mean**, i.e. the average values of flow quantities such as velocity and temperature are independent of time, the set of governing equations becomes:

$$\frac{\partial \tilde{u}_i}{\partial x_i} = 0 \tag{A.24}$$

$$\tilde{\rho}\tilde{u}_j\frac{\partial \tilde{u}_i}{\partial x_j} = \tilde{\rho}f_i - \frac{\partial \tilde{p}}{\partial x_i} + \frac{\partial}{\partial x_j}\left(\mu\frac{\partial \tilde{u}_i}{\partial x_j}\right) \tag{A.25}$$

$$\tilde{\rho}c_p\tilde{u}_j\frac{\partial \tilde{T}}{\partial x_j} = \frac{\partial}{\partial x_j}\left(k\frac{\partial \tilde{T}}{\partial x_j}\right) \tag{A.26}$$

We are left with the question of how to account for the temperature dependence of density. Knowing that $\tilde{u}_i \equiv 0$ outside the boundary layer, we find the gradient of the hydrostatic pressure distribution from equation (A.25)

$$\left(\frac{\partial \tilde{p}}{\partial x_i}\right)_{y\to\infty} = \frac{\partial P_\infty}{\partial x_i} = \rho_\infty f_i \quad . \tag{A.27}$$

With g being the acceleration of gravity and pointing in the negative x-direction, the vector of bodyforces becomes

$$f_i = \left\{ \begin{array}{c} -g \\ 0 \\ 0 \end{array} \right\} \quad . \tag{A.28}$$

We can now substitute expression (A.27) in equation (A.25) to get

$$\tilde{\rho}\tilde{u}_j \frac{\partial \tilde{u}_i}{\partial x_j} = -\frac{\partial}{\partial x_i}(P_* + p) + \frac{\partial}{\partial x_j}\left(\mu \frac{\partial \tilde{u}_i}{\partial x_j}\right) + (\tilde{\rho} - \rho_\infty) f_i \quad . \tag{A.29}$$

Within the **Boussinesq approximation** (c.f. [8], [33]) the density is assumed to be constant everywhere except in the bodyforce term, also referred to as the "buoyancy term". The Navier-Stokes equations can then be written as

$$\tilde{u}_j \frac{\partial \tilde{u}_i}{\partial x_j} = -\frac{1}{\rho_\infty}\frac{\partial}{\partial x_i}(P_* + p) + \frac{\partial}{\partial x_j}\left(\nu \frac{\partial \tilde{u}_i}{\partial x_j}\right) + \frac{\tilde{\rho} - \rho_\infty}{\rho_\infty} f_i \quad . \tag{A.30}$$

Note: The Boussinesq approximation includes incompressibility, i.e. it is more restrictive. Nevertheless it was thought to be important to show that the simplifications of incompressibility are valid even without such an assumption.
Expanding $\tilde{\rho} = \tilde{\rho}(\tilde{T})$ in a Taylor series

$$\tilde{\rho} \;=\; \sum_{m=1}^{n} \left(\frac{\partial^m \tilde{\rho}}{\partial \tilde{T}^m}\right)_{T_\infty} \frac{\left(\tilde{T} - T_\infty\right)^m}{m!} + R_m(\tilde{T})$$

$$
\begin{aligned}
&= \rho_\infty + \frac{\partial\tilde{\rho}}{\partial\tilde{T}}\left(\tilde{T}-T_\infty\right) + \frac{1}{2}\frac{\partial^2\tilde{\rho}}{\partial\tilde{T}^2}\left(\tilde{T}-T_\infty\right)^2 + \dots \\
\Rightarrow \tilde{\rho}-\rho_\infty &= \frac{\partial\tilde{\rho}}{\partial\tilde{T}}\left(\tilde{T}-T_\infty\right) + \frac{1}{2}\frac{\partial^2\tilde{\rho}}{\partial\tilde{T}^2}\left(\tilde{T}-T_\infty\right)^2 + \dots \qquad \text{(A.31)}
\end{aligned}
$$

and with the definition of the volumetric coefficient of thermal expansion

$$
\beta \equiv \left[-\frac{1}{\tilde{\rho}}\left(\frac{\partial\tilde{\rho}}{\partial\tilde{T}}\right)_{p=const.}\right]_\infty \quad , \qquad \text{(A.32)}
$$

we find the density difference in the above buoyancy term to be

$$
\tilde{\rho}-\rho_\infty \approx -\rho_\infty\beta(\tilde{T}-T_\infty) \quad , \qquad \text{(A.33)}
$$

where the higher order terms have been neglected. This **linearization** is not a good approximation for large temperature differences $\Delta T = (T - T_\infty)$, because the higher order terms become more important with higher ΔT. The Navier-Stokes equations (A.25) now read

$$
\tilde{u}_j\frac{\partial\tilde{u}_i}{\partial x_j} = -\frac{1}{\rho_\infty}\frac{\partial}{\partial x_i}(P_* + p) + \frac{\partial}{\partial x_j}\left(\nu\frac{\partial\tilde{u}_i}{\partial x_j}\right) - f_i\beta(\tilde{T}-T_\infty) \quad . \qquad \text{(A.34)}
$$

Applying all the above simplifications, substituting the vector of bodyforces and the decompositions for the instantaneous values and **averaging** (time, space or ensemble average, the operations of differentiation and averaging commute) yields

$$
\begin{aligned}
\frac{\partial U_i}{\partial x_i} &= 0 \qquad \left(\text{i.e.} \quad \frac{\partial u_i}{\partial x_i} = 0\right) && \text{(A.35)} \\
U_j\frac{\partial U_i}{\partial x_j} &= -\frac{1}{\rho_\infty}\frac{\partial P_*}{\partial x_i} + \frac{\partial}{\partial x_j}\left(\nu\frac{\partial U_i}{\partial x_j} - \overline{u_i u_j}\right) + g\beta(T-T_\infty)\delta_{i1} && \text{(A.36)} \\
U_j\frac{\partial T}{\partial x_j} &= \frac{\partial}{\partial x_j}\left(\alpha\frac{\partial T}{\partial x_j} - \overline{u_j t}\right) && \text{(A.37)}
\end{aligned}
$$

Using the summation convention for the silent index j, simplifying with $W = 0$ and **homogeneity in the z-direction** ($\partial/\partial z = 0$, as in centerline measurements

in experiments, provided the aspect ratio plate width vs. boundary layer thickness is large enough), we finally obtain the governing equations for the fully developed turbulent natural convection boundary layer:

$$\frac{\partial U}{\partial x} + \frac{\partial V}{\partial y} = 0 \tag{A.38}$$

$$U\frac{\partial U}{\partial x} + V\frac{\partial U}{\partial y} = -\frac{1}{\rho}\frac{\partial P_*}{\partial x} + \frac{\partial}{\partial x}\left(\nu\frac{\partial U}{\partial x} - \overline{u^2}\right) + \frac{\partial}{\partial y}\left(\nu\frac{\partial U}{\partial y} - \overline{uv}\right) + g\beta(T - T_\infty) \tag{A.39}$$

$$U\frac{\partial V}{\partial x} + V\frac{\partial V}{\partial y} = -\frac{1}{\rho}\frac{\partial P_*}{\partial y} + \frac{\partial}{\partial x}\left(\nu\frac{\partial V}{\partial x} - \overline{uv}\right) + \frac{\partial}{\partial y}\left(\nu\frac{\partial V}{\partial y} - \overline{v^2}\right) \tag{A.40}$$

$$0 = \frac{\partial}{\partial x}\left(-\overline{wu}\right) + \frac{\partial}{\partial y}\left(-\overline{wv}\right) \tag{A.41}$$

$$U\frac{\partial T}{\partial x} + V\frac{\partial T}{\partial y} = \frac{\partial}{\partial x}\left(\alpha\frac{\partial T}{\partial x} - \overline{ut}\right) + \frac{\partial}{\partial y}\left(\alpha\frac{\partial T}{\partial y} - \overline{vt}\right) \tag{A.42}$$

The density ρ_∞ is denoted just as ρ for convenience. An overbar is used to denote the average of the two corresponding fluctuating quantities. It is obvious that the equations of momentum and energy are coupled, as opposed to the forced convection boundary layer. Motion is present only because of the heat transfer from the surface and has therefore no independent existence. As a consequence of this peculiarity, e.g. the principle of superposition cannot be utilized to develop analytical solutions. Equation (A.41) only describes how the correlations of $\overline{wu}$ and $\overline{wv}$ are related and can be omitted.

A.2 Turbulence Kinetic Energy and Temperature Fluctuations Transport

Turbulence extracts energy from the mean flow at large scales, but this gain is approximately balanced by the loss of energy through viscous dissipation at very small scales. One way of deriving a transport equation for the turbulent kinetic energy is subtracting the kinetic energy of the mean flow from the instantaneous kinetic energy. The kinetic energy of the mean flow can be obtained by multiplying the equation governing mean momentum (A.36) by U_i

$$U_i U_j \frac{\partial U_i}{\partial x_j} = U_i \frac{\partial}{\partial x_j}\left(\frac{T_{ij}}{\rho}\right) + U_i g\beta(T - T_\infty)\delta_{i1} \quad , \tag{A.43}$$

where the stress tensor T_{ij} is defined as

$$T_{ij} = -P_*\delta_{ij} + 2\mu E_{ij} - \rho\overline{u_i u_j} = -P_*\delta_{ij} + \mu\left(\frac{\partial U_i}{\partial x_j} + \frac{\partial U_j}{\partial x_i}\right) - \rho\overline{u_i u_j} \quad . \tag{A.44}$$

By splitting the stress term in two parts with the chain rule and using symmetry, this can be rewritten as:

$$U_j \frac{\partial}{\partial x_j}\left(\frac{1}{2}U_i U_i\right) = \frac{\partial}{\partial x_j}\left(\frac{T_{ij}}{\rho}U_i\right) - \frac{T_{ij}}{\rho}E_{ij} + U_i g\beta(T - T_\infty)\delta_{i1} \quad . \tag{A.45}$$

Substituting the stress tensor into equation (A.45) yields an equation for the energy of the mean flow

$$\begin{aligned} U_j \frac{\partial}{\partial x_j}\left(\frac{1}{2}U_i U_i\right) &= \frac{\partial}{\partial x_j}\left[-\frac{P_*}{\rho}U_j + 2\nu U_i E_{ij} - U_i\overline{u_i u_j}\right] \\ &\quad - 2\nu E_{ij}E_{ij} + \overline{u_i u_j}E_{ij} + U_i g\beta(T - T_\infty)\delta_{i1} \quad , \end{aligned} \tag{A.46}$$

where the term on the left-hand side is the rate of change of mean kinetic energy due to convection, the first three terms on the right-hand side are transport terms, pressure

work, transport of mean flow energy by viscous stresses and turbulent motion, respectively. The fourth term is the viscous dissipation, the fifth is the turbulent energy production and the last a buoyancy source term (generation of mean kinetic energy by buoyancy), while the deformation work by pressure ($P_* E_{ii}$) vanishes because of incompressibility. However, this equation does not contain any new information, since it was found through mere manipulation of the momentum equation. Multiplying the Navier–Stokes equations (governing the instantaneous motion, (A.34)) by $\tilde{u}_i$ yields

$$\tilde{u}_j \frac{\partial}{\partial x_j}\left(\frac{1}{2}\tilde{u}_i\tilde{u}_i\right) = -\tilde{u}_i \frac{1}{\rho}\frac{\partial}{\partial x_i}(P_* + p) + \tilde{u}_i \frac{\partial}{\partial x_j}(2\nu\tilde{e}_{ij}) + \tilde{u}_i g\beta(\tilde{T} - T_\infty)\delta_{i1} \quad , \quad \text{(A.47)}$$

where the strain rate tensor is defined as

$$\tilde{e}_{ij} = \frac{1}{2}\left(\frac{\partial\tilde{u}_i}{\partial x_j} + \frac{\partial\tilde{u}_j}{\partial x_i}\right) = \frac{1}{2}\left(\frac{\partial U_i}{\partial x_j} + \frac{\partial U_j}{\partial x_i}\right) + \frac{1}{2}\left(\frac{\partial u_i}{\partial x_j} + \frac{\partial u_j}{\partial x_i}\right) = E_{ij} + e_{ij} \quad . \quad \text{(A.48)}$$

Averaging equation (A.47) and subtracting equation (A.46) we finally obtain the equation governing the mean kinetic energy of the velocity fluctuations $\overline{u_i u_i}$:

$$\begin{aligned} U_j \frac{\partial}{\partial x_j}\left(\frac{1}{2}\overline{u_i u_i}\right) &= \frac{\partial}{\partial x_j}\left[-\frac{1}{\rho}\overline{u_j p} + 2\nu\overline{u_i e_{ij}} - \frac{1}{2}\overline{u_i u_i u_j}\right] \\ &- 2\nu\overline{e_{ij}e_{ij}} - \overline{u_i u_j}E_{ij} + g\beta\overline{u_i t}\delta_{i1} \quad . \end{aligned} \quad \text{(A.49)}$$

On the left-hand side we have convection of the turbulent kinetic energy (the rate of change following the mean motion), the three transport terms on the right-hand side are pressure-gradient work, transport of turbulent kinetic energy by viscous stresses and by velocity fluctuations, the fourth term is the viscous disspation of turbulent kinetic energy. The fifth term is the turbulence production and the sixth term is the buoyant production. The pressure strain-rate is zero in incompressible flow. Note that the turbulence production occurs in both equations (A.46) and (A.49), but with different signs. Since $\overline{u_i u_j}$ is almost always negative if $\partial U_i/\partial x_j > 0$, this term serves to exchange kinetic energy between the mean flow and the turbulence, adding to

the latter. Temperature is obviously not a passive scalar in turbulent natural convection, but an active contaminent. Temperature fluctuations cause density fluctuations, which give rise to a fluctuating body force $-f_i\beta t\delta_{i1}$ that contributes to the turbulence kinetic energy.

Another way to derive the turbulence kinetic energy equation is via the Reynolds' stress equation: An equation governing the fluctuating velocities can be obtained by subtracting the momentum equation governing the mean motion (eqn. (A.36)) from the Navier-Stokes equation governing the instantaneous motion (eqn. (A.34))

$$U_j\frac{\partial u_i}{\partial x_j} = -\frac{1}{\rho}\frac{\partial p}{\partial x_i} + \frac{\partial}{\partial x_j}\left(2\nu e_{ij}\right) - \left(u_j\frac{\partial u_i}{\partial x_j} - \overline{u_j\frac{\partial u_i}{\partial x_j}}\right) - u_j\frac{\partial U_i}{\partial x_j} + g\beta t\delta_{i1} \quad , \qquad \text{(A.50)}$$

where the viscous terms were written with the strain rate tensor e_{ij} defined in equation (A.48). Multiplying by u_k and averaging leads to

$$U_j\overline{u_k\frac{\partial u_i}{\partial x_j}} = -\frac{1}{\rho}\overline{u_k\frac{\partial p}{\partial x_i}} + \overline{u_k\frac{\partial}{\partial x_j}\left(2\nu e_{ij}\right)} - \overline{u_k u_j\frac{\partial u_i}{\partial x_j}} - \overline{u_k u_j}\frac{\partial U_i}{\partial x_j} + g\beta\overline{u_k t}\delta_{i1} \quad . \qquad \text{(A.51)}$$

Rewriting this equation with reversed indeces i and k, adding both equations and rearranging the resulting pressure and viscous terms leads to an equation governing $\overline{u_i u_j}$:

$$\begin{aligned} U_j\frac{\partial}{\partial x_j}\left(\overline{u_k u_i}\right) &= \frac{\partial}{\partial x_j}\left[\frac{1}{\rho}\left(\overline{u_i p}\delta_{kj} + \overline{u_k p}\delta_{ij}\right) - \overline{u_i u_k u_j} + 2\nu\left(\overline{u_k e_{ij}} + \overline{u_i e_{kj}}\right)\right] \\ &+ \overline{\frac{p}{\rho}\left(\frac{\partial u_i}{\partial x_k} + \frac{\partial u_k}{\partial x_i}\right)} - \left(\overline{u_i u_j}\frac{\partial U_k}{\partial x_j} + \overline{u_k u_j}\frac{\partial U_i}{\partial x_j}\right) \\ &- 4\nu\overline{e_{ij}e_{kj}} + g\beta\left(\overline{u_k t}\delta_{i1} + \overline{u_i t}\delta_{k1}\right) \quad . \end{aligned} \qquad \text{(A.52)}$$

This is the so-called "Reynolds' stress equation". Contracting the free indeces i and k again yields the turbulent kinetic energy equation (A.49).

An equation governing the transport of the mean square temperature fluctuations can be derived in a very similar fashion, either by subtracting the mean energy equa-

tion (A.37) times the mean temperature T from the averaged product of instantaneous energy equation (A.26) and instantaneous temperature $\tilde{T}$ or by subtracting the mean energy equation (A.37) from the instantaneous energy equation (A.26), multiplying with the fluctuating temperature t and averaging. The result in both cases will be

$$U_j \frac{\partial}{\partial x_j}\left(\frac{1}{2}\overline{t^2}\right) = \frac{\partial}{\partial x_j}\left[-\frac{1}{2}\overline{u_j t^2} + \alpha \frac{\partial}{\partial x_j}\left(\frac{1}{2}\overline{t^2}\right)\right] - \overline{u_j t}\frac{\partial T}{\partial x_j} - \alpha \overline{\frac{\partial t}{\partial x_j}\frac{\partial t}{\partial x_j}} \quad . \qquad \text{(A.53)}$$

The terms occurring in the temperature fluctuations equations can be interpreted in a similar fashion as for the turbulent kinetic energy or Reynolds' stress equation: We can identify a convection term on the left-hand side, transport terms, production and dissipation on the right-hand side.

Appendix B

Scaling of the Governing Equations

A standard order of magnitude analysis (c.f. e.g. [62, 52, 44, 60, 56]) is applied to the governing equations in order to obtain properly reduced sets of equations describing the inner and outer flow regions of the turbulent natural convection boundary layer.

B.1 The "Outer" Set of Equations

We assume that the effects of natural convection are confined to a thin layer of fluid adjacent to the heated surface, so that Prandtl's boundary layer approximations (c.f. Prandtl [52] , Schlichting [56]) apply. Changes of relevant quantities in the streamwise direction are small compared to changes in the cross-stream direction, since the wall-bounded turbulent shear flow considered here evolves slowly in the x-direction. This can be written as

$$\frac{\partial}{\partial x} \sim \frac{1}{L} \ll \frac{\partial}{\partial y} \sim \frac{1}{\delta} \quad . \tag{B.1}$$

L and δ are a streamwise and a cross-stream length scale which are not defined further at this point. The mean streamwise velocity, the mean temperature, the fluctuating

velocities and the fluctuating temperature are scaled with

$$U \sim U_{So} \quad , \tag{B.2}$$

$$T \sim T_{So} \quad , \tag{B.3}$$

$$-\overline{u^2}, -\overline{v^2}, -\overline{uv} \sim {u_o}^2 \quad , \tag{B.4}$$

$$-\overline{ut}, -\overline{vt} \sim u_o t_o \quad , \tag{B.5}$$

respectively. (Note: Different symbols are used to scale the Reynolds' stress $-\overline{uv}$ and the turbulent heat flux $-\overline{vt}$ in the main part of this work. u_o and t_o and later u_i and t_i are only used in this appendix for *all* the turbulence quantities for convenience.) From the continuity equation (3.1) it is then found:

$$V \sim U_{So} \frac{\delta}{L} \tag{B.6}$$

We will now first look at equation (3.3), which governs the mean momentum in the cross-stream direction:

$$U\frac{\partial V}{\partial x} + V\frac{\partial V}{\partial y} = -\frac{1}{\rho}\frac{\partial P_*}{\partial y} + \frac{\partial}{\partial x}\left(\nu\frac{\partial V}{\partial x} - \overline{uv}\right) + \frac{\partial}{\partial y}\left(\nu\frac{\partial V}{\partial y} - \overline{v^2}\right) \tag{B.7}$$

Expressing each term in the scales defined above, we can identify their orders of magnitude as follows:

$${U_{So}}^2\frac{\delta}{L^2} + {U_{So}}^2\frac{\delta}{L^2} \quad \sim \quad ? \; + \nu U_{So}\frac{\delta}{L^3} + \frac{{u_o}^2}{L} + \nu U_{So}\frac{1}{\delta L} + \frac{{u_o}^2}{\delta} \tag{B.8}$$

The order of magnitude of the pressure term is unknown so far, we will now focus on evaluating it. Multiplying equation (B.8) by $\delta/{U_{So}}^2$ leads to a more practical, nondimensionalized form

$$\left(\frac{\delta}{L}\right)^2 + \left(\frac{\delta}{L}\right)^2 \quad \sim \quad ? + \frac{1}{Re_\delta}\left(\frac{\delta}{L}\right)^3 + \left(\frac{u_o}{U_{So}}\right)^2\left(\frac{\delta}{L}\right) + \frac{1}{Re_\delta}\left(\frac{\delta}{L}\right) + \left(\frac{u_o}{U_{So}}\right)^2 \quad , \tag{B.9}$$

where Re_δ is defined by

$$Re_\delta = \frac{U_{So}\delta}{\nu} \quad . \tag{B.10}$$

The second term on the right-hand side in equation (B.9) — which is representing equation (B.7) — is small compared to the fourth (by two orders of magnitude), the third term is small compared to the fifth (by one order of magnitude). As long as $(\delta/L)^2 \to 0$ faster than $(u_o/U_{So})^2$, both terms on the left-hand side are also negligible compared to $\partial(-\overline{v^2})/\partial y$. If the Reynolds number Re_δ is large enough, the remaining viscous term is also negligible relative to $\partial(-\overline{v^2})/\partial y$. We are thus imposing the conditions

$$\left(\frac{\delta}{L}\right)^2 \left(\frac{U_{So}}{u_o}\right)^2 \to 0 \tag{B.11}$$

and

$$\frac{1}{Re_\delta}\left(\frac{\delta}{L}\right) \left(\frac{U_{So}}{u_o}\right)^2 \to 0 \tag{B.12}$$

in the limit as $\delta/L \to 0$ (or $\delta \ll L$). In order to balance the equation, there must be another term of the order of magnitude of $\partial(-\overline{v^2})/\partial y$: Inspection of equations (B.7) and (B.9) leads to the conclusion that this has to be the pressure term. The simplified y-momentum equation — to first order — then reads:

$$0 = \frac{1}{\rho_\infty}\frac{\partial P_*}{\partial y} + \frac{\partial}{\partial y}\left(\overline{v^2}\right) \quad . \tag{B.13}$$

Let us briefly consider the more general case where the gradient of the hydrostatic part of the mean pressure, $\partial P_\infty/\partial x_i$, was not written as a bodyforce. For any distribution of static pressure, equation (B.13) — now simply with $P = P_* + P_\infty$ instead of P_* — can easily be integrated from ∞ to y to yield:

$$P = P_\infty - \rho_\infty \overline{v^2} \quad . \tag{B.14}$$

For turbulent shear flows, this expression is justifiable as follows: It is assumed that the pressure inside the thin shear shear layer is largely accounted for by the pressure

field outside of it (to first order). Because of the presence of the fluctuating term, the pressure inside the boundary layer is seen to be less than outside. This slight cross-stream pressure gradient is responsible for the entrainment of ambient fluid. Note that in the case of forced convection, the mean square of the cross-stream velocity fluctuation at infinite distance from the wall, $\overline{v_\infty^2}$, has to be included if the free stream is turbulent!

Returning to our specific problem (eqns.(B.7,B.13)), the pressure distribution (B.14) reduces to $P_* = -\rho_\infty \overline{v^2}$ and its derivative with respect to x can be written as:

$$\frac{1}{\rho_\infty}\frac{\partial P_*}{\partial x} = -\frac{\partial}{\partial x}\left(\overline{v^2}\right) \quad . \tag{B.15}$$

We will now scale the equation for the streamwise mean momentum, equation (3.2), written with (B.15) for the pressure term:

$$U\frac{\partial U}{\partial x} + V\frac{\partial U}{\partial y} = \frac{\partial}{\partial x}\left(\nu\frac{\partial U}{\partial x} - \left(\overline{u^2} - \overline{v^2}\right)\right) + \frac{\partial}{\partial y}\left(\nu\frac{\partial U}{\partial y} - \overline{uv}\right) + g\beta(T - T_\infty) \quad . \tag{B.16}$$

Expressing each term in the defined scales and nondimensionalizing the equation by multiplying by $L/{U_{So}}^2$, we obtain:

$$1 + 1 \quad \sim \quad \frac{1}{Re_\delta}\left(\frac{\delta}{L}\right) + \left(\frac{u_o}{U_{So}}\right)^2 + \frac{1}{Re_\delta}\left(\frac{L}{\delta}\right) + \left(\frac{u_o}{U_{So}}\right)^2\left(\frac{L}{\delta}\right) + ? \quad . \tag{B.17}$$

The magnitude of the buoyancy term (denoted by "?") cannot be determined at this stage. The first term on the right-hand side is small compared to the third, the second term is small compared to the fourth. With Re_δ being sufficiently large, we can make the viscous terms as small as required. In order to have "turbulence", a fluctuating term must stay in the equation. We are requiring

$$\left(\frac{u_o}{U_{So}}\right)^2\left(\frac{L}{\delta}\right) \sim 1 \quad , \tag{B.18}$$

i.e. this nondimensional group must remain bounded as $\delta/L \to 0$. The reduced

x-momentum equation — to first order — can now be written as:

$$U\frac{\partial U}{\partial x}+V\frac{\partial U}{\partial y}=\frac{\partial}{\partial y}\left(-\overline{uv}\right)+g\beta(T-T_\infty) \quad . \tag{B.19}$$

Eventually we consider the scaling of the energy equation (3.4):

$$U\frac{\partial T}{\partial x}+V\frac{\partial T}{\partial y}=\frac{\partial}{\partial x}\left(\alpha\frac{\partial T}{\partial x}-\overline{ut}\right)+\frac{\partial}{\partial y}\left(\alpha\frac{\partial T}{\partial y}-\overline{vt}\right) \quad . \tag{B.20}$$

Substituting the scaling quantities and multiplying by $L/U_{So}T_{So}$ we get the following orders of magnitude:

$$1+1 \quad \sim \quad \frac{1}{Pe_\delta}\left(\frac{\delta}{L}\right)+\left(\frac{u_o}{U_{So}}\right)\left(\frac{t_o}{T_{So}}\right)+\frac{1}{Pe_\delta}\left(\frac{L}{\delta}\right)+\left(\frac{u_o}{U_{So}}\right)\left(\frac{t_o}{T_{So}}\right)\left(\frac{L}{\delta}\right) \quad , \tag{B.21}$$

where Pe_δ is the Péclét number defined as:

$$Pe_\delta=\frac{U_{So}\delta}{\alpha} \quad . \tag{B.22}$$

Again, the first term on the right-hand side in equation (B.21) is small compared to the third, the second term is small compared to the fourth. Assuming Pe_δ is large enough, we can make the conduction terms as small as desired. For a fluctuating term to stay in the energy equation, we require

$$\left(\frac{u_o}{U_{So}}\right)\left(\frac{t_o}{T_{So}}\right)\left(\frac{L}{\delta}\right)\sim 1 \tag{B.23}$$

as $\delta/L\rightarrow 0$. The reduced energy equation — to first order — then reads:

$$U\frac{\partial T}{\partial x}+V\frac{\partial T}{\partial y}=\frac{\partial}{\partial y}\left(-\overline{vt}\right) \quad . \tag{B.24}$$

Equations (B.19) and (B.24) together with the continuity equation (3.1) are referred to as the "outer" set of equations.

B.2 The "Inner" Set of Equations

To include the wall effects (c.f. 3.2), we have to rescale the governing equations to retain at least one viscous and one conduction term. This is only possible, if the Reynolds and the Péclét number, based on "inner" scales, cannot become large. Therefore we require

$$Re_\eta = \frac{U_{Si}\eta}{\nu} \sim 1 \tag{B.25}$$

for the momentum equations (3.2, 3.3) and

$$Pe_{\eta_T} = \frac{U_{Si}\eta_T}{\alpha} \sim 1 \tag{B.26}$$

for the energy equation (3.4). This is always true for inner length scales η and η_T on the order of magnitude of:

$$\eta \sim \frac{\nu}{U_{Si}} \tag{B.27}$$

and

$$\eta_T \sim \frac{\alpha}{U_{Si}} \quad . \tag{B.28}$$

Since $\eta, \eta_T \ll \delta$, the boundary layer approximations (B.1) hold also for the inner layer, of course:

$$\frac{\partial}{\partial x} \sim \frac{1}{L} \ll \frac{\partial}{\partial y} \sim \frac{1}{\eta}, \frac{1}{\eta_T} \quad , \tag{B.29}$$

and scales for the mean streamwise velocity, the mean temperature, the fluctuating velocities and the fluctuating temperature are:

$$U \sim U_{Si} \quad , \tag{B.30}$$

$$T \sim T_{Si} \quad , \tag{B.31}$$

$$-\overline{u^2}, -\overline{v^2}, -\overline{uv} \sim {u_i}^2 \quad , \tag{B.32}$$

$$-\overline{ut}, -\overline{vt} \sim u_i t_i \quad , \tag{B.33}$$

respectively. The continuity equation (3.1) gives the cross-stream velocity scale

$$V \sim U_{Si} \frac{\eta}{L} \tag{B.34}$$

for the momentum equations and

$$V \sim U_{Si} \frac{\eta_T}{L} \tag{B.35}$$

for the energy equation.

Expressing the terms in the y-momentum equation (3.3, B.7) in the new "inner" scales and multiplying by $\eta/{U_{Si}}^2$ leads to a nondimensionalized representation with the following orders of magnitude:

$$\left(\frac{\eta}{L}\right)^2 + \left(\frac{\eta}{L}\right)^2 \quad \sim \quad ? + \left(\frac{\eta}{L}\right)^3 + \left(\frac{u_i}{U_{Si}}\right)^2 \left(\frac{\eta}{L}\right) + \left(\frac{\eta}{L}\right) + \left(\frac{u_i}{U_{Si}}\right)^2 \quad . \tag{B.36}$$

Proceeding along an analogous line of arguments as for the "outer" set of equations (c.f. B.1), we establish, that — again — the pressure term is the only term which can balance $\partial(-\overline{v^2})/\partial y$, the first and last terms on the right-hand side of equation (B.36). We obtain exactly the same reduced y-momentum equation:

$$0 = \frac{1}{\rho_\infty} \frac{\partial P_*}{\partial y} + \frac{\partial}{\partial y}\left(\overline{v^2}\right) \quad , \tag{B.37}$$

which is an approximation to first order and contains the condition

$$\left(\frac{\eta}{L}\right)\left(\frac{U_{Si}}{u_i}\right)^2 \to 0 \quad , \tag{B.38}$$

in the limit as $\eta/L \to 0$. The derivative of mean pressure with respect to x can again be written as in equation (B.15).

Substituting in the equation for the streamwise mean momentum, equation (3.2,

B.16), and multiplying by $\eta/{U_{Si}}^2$, we yield:

$$\left(\frac{\eta}{L}\right) + \left(\frac{\eta}{L}\right) \quad \sim \quad \left(\frac{\eta}{L}\right)^2 + \left(\frac{u_i}{U_{Si}}\right)^2 \left(\frac{\eta}{L}\right) + 1 + \left(\frac{u_i}{U_{Si}}\right)^2 + ? \quad . \tag{B.39}$$

Scaled this way, the mean convection terms on the left-hand side are small compared to the last three terms on the right-hand side, which are a viscous term, a Reynolds' stress term and the buoyancy term. The x-momentum equation — to first order — reduces to

$$0 = \frac{\partial}{\partial y}\left(\nu\frac{\partial U}{\partial y} - \overline{uv}\right) + g\beta(T - T_\infty) \quad , \tag{B.40}$$

with the requirement

$$\left(\frac{u_i}{U_{Si}}\right)^2 \sim 1 \quad . \tag{B.41}$$

Finally we examine the energy equation, equation (3.4, B.20). Expressing it in terms of the "inner" scaling quantities and nondimensionalizing it through multiplication by $\eta_T/U_{Si}T_{Si}$ we obtain the orders of magnitude as:

$$\left(\frac{\eta_T}{L}\right) + \left(\frac{\eta_T}{L}\right) \quad \sim \quad \left(\frac{\eta_T}{L}\right)^2 + \left(\frac{u_i}{U_{Si}}\right)\left(\frac{t_i}{T_{Si}}\right)\left(\frac{\eta_T}{L}\right) + 1 + \left(\frac{u_i}{U_{Si}}\right)\left(\frac{t_i}{T_{Si}}\right) \quad . \tag{B.42}$$

In this case, too, we can neglect the mean convection terms, which are one order of magnitude less than the second viscous term. A fluctuating term stays in the equation with the condition

$$\left(\frac{u_i}{U_{Si}}\right)\left(\frac{t_i}{T_{Si}}\right) \sim 1 \quad . \tag{B.43}$$

The energy equation — to first order — can then be written as:

$$0 = \frac{\partial}{\partial y}\left(\alpha\frac{\partial T}{\partial y} - \overline{vt}\right) \quad . \tag{B.44}$$

Equations (B.40) and (B.44) together with the continuity equation (3.1) are referred to as the "inner" set of equations.

References

[1] R. Aris. *Vectors, Tensors and the Basic Equations of Fluid Mechanics.* reprint by Dover, 1962.

[2] G. I. Barenblatt. *Dimensional Analysis.* Gordon and Breach, New York, 1987.

[3] G. K. Batchelor. *The Theory of Homogeneous Turbulence.* Cambridge University Press, Cambridge, UK, 1953.

[4] G. K. Batchelor. *An Introduction to Fluid Dynamics.* Cambridge University Press, Cambridge, UK, 1967.

[5] F. J. Bayley. An analysis of turbulent free convection heat transfer. *Proc. Inst. Mech. Engrs.*, 169:361–368, 1955.

[6] P. D. Beuther. *Experimental Investigation of the Axisymmetric Turbulent Buoyant Plume.* PhD thesis, University at Buffalo, 1980.

[7] H. Blasius. Grenzschichten in Flüssigkeiten mit kleiner Reibung. *Z. Math. u. Phys.*, 56:1–37, 1908.

[8] L. C. Burmeister. *Convective Heat Transfer.* John Wiley and Sons, New York, NY, 1983.

[9] V. P. Carey and J. C. Mollendorf. Variable viscosity effects in several natural convection flows. *Int. Journal of Heat Mass Transfer*, 23:95–109, 1980.

[10] T. Cebeci and A. Khattab. Prediction of turbulent free convective heat transfer from a vertical plate. *Journal of Heat Transfer*, 97:469–471, 1975.

[11] R. Cheesewright. Turbulent natural convection from a vertical plane surface. *Journal of Heat Transfer*, 90:1–8, 1968.

[12] R. Cheesewright and E. Ierokiopitis. Velocity measurements in a turbulent natural convection boundary layer. In *Proceedings of the Seventh International Heat Transfer Conference*, volume II, pages NC 31,305–309, Munich, 1982.

[13] A. M. Clausing. Natural convection correlations for vertical surfaces including influences of variable properties. *Journal of Heat Transfer*, 105:138–143, 1983.

[14] A. P. Colburn and O. A. Hougen. Studies in heat transmission—flow of fluids at low velocity. *Industrial and Engineering Chemistry*, 22:522–539, 1930.

[15] J. D. Cole. *Perturbation Methods in Applied Mathematics.* Blaisdell Publishing Company, 1968.

[16] J. Coutanceau. Convection naturelle turbulente sur une plaque verticale isotherme, transition, échange de chaleur et frottement pariétal, lois de répartition de vitesse et de température. *Int. Journal of Heat Mass Transfer*, 12:753–769, 1969.

[17] E. R. G. Eckert and Thomas W. Jackson. Analysis of turbulent free convection boundary layer on flat plate. Technical Report TN 2207, National Advisory Committee for Aeronautics, 1950.

[18] J. W. Elder. Turbulent free convection in a vertical slot. *Journal of Fluid Mechanics*, 23:99–111, 1965.

[19] D. A. Frank-Kamenickij. *Copt. Rend. Acad. Sci. SSSR*, 17:9, 1937.

[20] T. Fujii, M. Takeuchi, M. Fujii, K.Suzaki, and H.Uehara. Experiments on natural convection heat transfer from the outer surface of a vertical cylinder to liquids. *Int. Journal of Heat Mass Transfer*, 13:753–787, 1970.

[21] B. Gebhardt. Effects of viscous dissipation in natural convection. *Journal of Fluid Mechanics*, 14:225–232, 1962.

[22] B. Gebhardt. Instability, transition, and turbulence in buoyancy-induced flows. *Annual Review of Fluid Mechanics*, 5:213–246, 1973.

[23] W. K. George. The self-preservation of turbulent flows and its relation to initial conditions and coherent structures. In *Advances in Turbulence*, pages 39–73. Hemisphere, NY, 1989.

[24] W. K. George. The decay of homogeneous isotropic turbulence. *Physics of Fluids A*, 4(7):1492–1509, 1992.

[25] W. K. George. Some new ideas for similarity of turbulent shear flows. In *Proc. of Turbulence, Heat and Mass Transfer Symposium*, Lisbon, Portugal, 1994.

[26] W. K. George and S. P. Capp. A theory for natural convection turbulent boundary layers next to heated vertical surfaces. *Int. Journal of Heat Mass Transfer*, 22:813–826, 1979.

[27] W. K. George, L. Castillo, and P. Knecht. The zero pressure-gradient turbulent boundary layer, 1994. submitted for publication.

[28] E. Griffiths and A. H. Davis. The transmission of heat by radiation and convection. In *British Food Investigation Board Spec. Rept. 9*. D.S.I.R. London, 1922,1931.

[29] A. G. Hansen. *Similarity Analyses of Boundary Value Problems in Engineering.* Prentice-Hall, Englewood Cliffs, NJ, 1964.

[30] R. A. W. M. Henkes and C. J. Hoogendoorn. Comparison of turbulence models for the natural convection boundary layer along a heated vertical plate. *Int. Journal of Heat Mass Transfer*, 32:157–169, 1989.

[31] R. A. W. M. Henkes and C. J. Hoogendoorn. Numerical determination of wall functions for the turbulent natural convection boundary layer. *Int. Journal of Heat Mass Transfer*, 33:1087–1097, 1990.

[32] C. J. Hoogendoorn and H. Euser. Velocity profiles in the turbulent free convection boundary layer. In *Proceedings of the Sixth International Heat Transfer Conference*, volume 2, pages NC 2,193–198, Toronto, 1978.

[33] F. P. Incropera and D. P. de Witt. *Fundamentals of Heat and Mass Transfer.* John Wiley and Sons, New York, NY, 1985.

[34] M. Jakob and W.Linke. *Forsch. Arb. Ing. Wes.*, 4:75, 1933.

[35] W. P. Jones and B. E. Launder. The prediction of laminarization with a two-equation model of turbulence. *Int. Journal of Heat Mass Transfer*, 15:301, 1972.

[36] T. Von Kármán. *Z. Angew. Math. Mech.*, 1:233, 1921.

[37] H. Kato, N. Nishiwaki, and M. Hirata. On the turbulent heat transfer by free convection from a vertical flat plate. *Int. Journal of Heat Mass Transfer*, 11:1117–1125, 1968.

[38] A. N. Kolmogorov. Equations of turbulent motion in an incompressible fluid. *Izv. Akad. Nauk. USSR*, VI(1.2):56–58, 1942.

[39] A. K. Kulkarni and S. L. Chou. Turbulent natural convection flow on a heated vertical wall immersed in a stratified atmosphere. *Journal of Heat Transfer*, 111:378–384, 1989.

[40] S. S. Kutateladze, A. G. Kirdyashkin, and V. P. Ivakin. Turbulent natural convection on a vertical plate and in a vertical layer. *Int. Journal of Heat Mass Transfer*, 15:193–202, 1972.

[41] L. Lorenz. *Ann. Phys. Chem*, 13:582, 1881.

[42] H. B. Mason and R. A. Seban. Numerical predictions for turbulent free convection from vertical surfaces. *Int. Journal of Heat Mass Transfer*, 17:1329–1336, 1974.

[43] M. Miyamoto, H. Kajino, J. Kurima, and I. Takanami. Development of turbulence characteristics in a vertical free convection boundary layer. In *Proceedings of the Seventh International Heat Transfer Conference*, volume II, pages NC 34,323–328, Munich, 1982.

[44] A. S. Monin and A. M. Yaglom. *Statistical Fluid Mechanics*, volume I. MIT Press, Cambridge,MA, 1975.

[45] K. Noto and R. Matsumoto. Turbulent heat transfer by natural convection along an isothermal vertical flat plate. *Journal of Heat Transfer*, 97:621–624, 1975.

[46] A. Oberbeck. *Ann. Phys. Chem*, 7:271, 1879.

[47] S. Ostrach. An analysis of laminar free convection flow and heat transfer about a flat plate parallel to the direction of the generating bodyforce. Technical Report TN 2635, National Advisory Committee for Aeronautics, 1952.

[48] D. D. Papailiou and P. S. Lykoudis. Turbulent free convection flow. *Int. Journal of Heat Mass Transfer*, 17:161–172, 1974.

[49] T. W. J. Peeters and R. A. W. M. Henkes. The reynolds-stress model of turbulence applied to the natural-convection boundary layer along a heated vertical plate. *Int. Journal of Heat Mass Transfer*, 35:403–420, 1992.

[50] A. Pirovano, S. Viannay, and M. Jannot. Convection naturelle en régime turbulent le long d'une plaque plane verticale. In *Proceedings of the Fourth International Heat Transfer Conference*, volume IV, pages NC 1.8, 1–12, Paris-Versailles, 1970.

[51] O. A. Plumb and L. A. Kennedy. Application of a k–ϵ model to natural convection from a vertical isothermal surface. *Journal of Heat Transfer*, 99:79–85, 1977.

[52] L. Prandtl. *Gesammelte Abhandlungen*, volume 2. Springer-Verlag, Berlin, 1961.

[53] Z. H. Qureshi and B. Gebhardt. Transition and transport in a buoyancy driven flow in water adjacent to a vertical uniform flux surface. *Int. Journal of Heat Mass Transfer*, 21:1467–1479, 1978.

[54] E. Ruckenstein and J. D. Felske. Turbulent natural convection at high prandtl numbers. *Journal of Heat Transfer*, 102:773–775, 1980.

[55] O. A. Saunders. The effect of pressure upon natural convection in air. *Proc. Royal Society A*, 157:278–291, 1936.

[56] H. Schlichting. *Boundary-Layer Theory.* McGraw-Hill, New York, NY, 7th edition, 1979.

[57] L. I. Sedov. *Similarity and Dimensional Methods in Mechanics.* Academic Press, New York, NY, 1959.

[58] D. L. Siebers, R. F. Moffat, and R. G. Schwind. Experimental, variable properties natural convection from a large, vertical, flat surface. *Journal of Heat Transfer*, 107:124–132, 1985.

[59] R. R. Smith. *Characteristics of Turbulence in Free Convection Flow Past a Vertical Plate.* PhD thesis, University of London, 1972.

[60] J. H. Spurk. *Strömungslehre.* Springer-Verlag, Berlin, 1989.

[61] J. H. Spurk. *Dimensionsanalyse in der Strömungslehre.* Springer-Verlag, Berlin, 1992.

[62] H. Tennekes and J. L. Lumley. *A First Course in Turbulence.* MIT Press, Cambridge,MA, 1972.

[63] W. M. To and J. A. C. Humphrey. Numerical simulation of buoyant, turbulent flow: — 1. free convection along a heated, vertical, flat plate. *Int. Journal of Heat Mass Transfer*, 29:573–592, 1986.

[64] T. Tsuji and Y. Nagano. Characteristics of a turbulent natural convection boundary layer along a vertical flat plate. *Int. Journal of Heat Mass Transfer*, 31:1723–1734, 1988.

[65] T. Tsuji and Y. Nagano. Velocity and temperature measurements in a natural convection boundary layer along a vertical flat plate. *Experimental Thermal and Fluid Science*, pages 208–215, 1989.

[66] T. Tsuji, Y. Nagano, and M. Tagawa. Experiment on spatial and temporal turbulent structures of a natural convection boundary layer. In *Heat Transfer in Turbulent Flow, AIAA/ASME Thermophysics and Heat Transfer Conference*, volume 138, pages 19–26, 1990.

[67] T. Tsuji, Y. Nagano, and M. Tagawa. Experiment on spatio-temporal turbulent structures of a natural convection boundary layer. *Journal of Heat Transfer*, 114:901–908, 1992.

[68] G. C. Vliet and C. K. Liu. An experimental study of turbulent natural convection boundary layers. *Journal of Heat Transfer*, 91:517–531, 1969.

[69] C. Y. Warner. *Turbulent Natural Convection in Air along a Vertical Flat Plate.* PhD thesis, University of Michgan, Ann Arbor, 1966.

[70] C. Y. Warner and V. S. Arpaci. An experimental investigation of turbulent natural convection in air at low pressure along a vertical heated flat plate. *Int. Journal of Heat Mass Transfer*, 11:397–406, 1968.

[71] J. R. Welty and D. R. Peinecke. Velocity measurements for buoyancy induced flow in mercury adjacent to vertical single cylinders. *Journal of Heat Transfer*, 98:146–148, 1976.

[72] K. T. Yang and V. W. Nee. Structure of turbulent free convection boundary layers along a vertical plate. In *Proceedings of the Fourth International Heat Transfer Conference*, volume IV, pages NC 1.12, 1–11, Paris-Versailles, 1970.